RADIATION FROM CIRCULARLY SYMMETRIC E.M. SOURCES

A THESIS SUBMITTED IN PARTIAL FULFILMENT OF
THE REQUIREMENTS FOR THE DEGREE

OF

DOCTOR OF PHILOSOPHY

BY

LALIT KUMAR

PHYSICS GROUP
BIRLA INSTITUTE OF TECHNOLOGY & SCIENCE
PILANI RAJASTHAN INDIA
MAY 1979

Dedicated

to the loving memory

of

my beloved sisters

Pratibha and Neelam.

BIRLA INSTITUTE OF TECHNOLOGY AND SCIENCE

PILANI (RAJASTHAN)

C E R T I F I C A T E

This is to certify that the thesis entitled ' Radiation from plasma columns excited by circularly symmetric e.m. sources' and submitted by Shri Lalit Kumar, I.D.No. 74SB5501 for award of Ph.D. degree of the Institute, embodies original work done by him under my supervision.

J-S Verma

(J. S. VERMA)
Professor of Physics
Birla Institute of Technology and Science
Pilani, Rajasthan.

Dated: 15.5.79

A C K N O W L E D G E M E N T S

I wish to express my gratitude to my thesis supervisor Prof. J.S. Verma for encouraging and guiding me to pursue this work.

I am very much grateful to Dr. H.L. Kundu, M/s T.N.R.K. Kurup, S.C.Rastogi, B.K. Raghunath and K.C.Gupta for providing me various facilities and taking a personal interest in my work. I am very much thankful to Dr. V.K. Tewary and Prof. K.V.Ramanan for their kind help on various occasions.

I express my sincere thanks to Drs. S.S.S. Agarwala, G.S.Sidhu, H.S.Dewan and Mr. Devender Singh, all at Vacuum Tubes Division, CEERI, Pilani for various technical suggestions and for providing the facilities for fabrication of the thoriated Tungsten cathode and some discharge tubes used for this work.

The keen interest and skill shown by M/s Shiv Narain, Banwari Lal and G.D.Sharma in fabricating various components and the promptness and patience of M/s Ashok Tawathia, Banwari Lal, Shanker Sharma, B.P. Singh in running the lengthy computer programmes and Ganesh in typing the thesis is highly commendable.

I am very thankful for the timely help and moral support provided by my friends Drs.N.K.Joshi, G.R.Rao, P.K.Banerjee, Chandra Sekhar, M.C.Gupta, Animesh Jain, M/s Murli Dhar, C.P.Joshi and Miss Amita Agarwala, which have greatly contributed

towards the completion of this work. I am also indebted to Dr. R.K.Nahar, M/s Ashok Kaushik, Suresh C.Tiwari and R.P.Agarwal for their invaluable help in the preparation of the thesis.

I have no words to express my feelings for my parents and family members, my cousin Mr. S.K. Jain and Sister-in-law Mrs. Usha Jain, whose blessings and good wishes have always regenerated my strength and self-confidence.

Thanks are also due to Dr. C.R. Mitra, Director, B.I.T.S. for permitting me to use the facilities available at the Institute and to the National Oceanic and Atmospheric Administration, U.S.A. and the University Grants Commission for providing the financial assistance to carry out this work.

Lalit

(LALIT KUMAR)

LIST OF MAJOR SYMBOLS

A	surface area of the Langmuir probe.
a	radius of the electromagnetic source
a_n	coefficients in the power series expansions of $h(x)$ and $e(x)$
a_x, a_y a_z, a_ϕ	unit vectors in the x, y, z and ϕ directions respectively
b	radius of the plasma column; seperation between the plates of radial waveguide (ch.5)
$\bar{C}_e$	average random electron speed
c	outer radius of the dielectric tube
D	directivity of the antenna
D_a	ambipolar diffusion coefficient
d	thickness of the plasma slab
$\bar{E}$	electric field intensity
E_ρ, E_ϕ, E_z	components of $\bar{E}$ in cylindrical coordinate system
$\tilde{E}$	Fourier transform of E_ϕ with respect of z-coordinate
e	electronic charge
$e(x), e_1(x)$ $e_2(x)$	series solutions of wave equation for $\tilde{E}$ in inhomogeneous plasma
$F(\theta)$	pattern function of antenna system
f	signal frequency
$\bar{H}$	magnetic field intensity
H_ρ, H_ϕ, H_z	components of $\bar{H}$ in cylindrical coordinate system
$\tilde{H}$	Fourier transform of H_ϕ with respect to z-coordinate
H_n^1	Hankel function of first kind and n^{th} order
HPBW	half power beam width
h	$XY/2a$, 2
$h(x), h_1(x)$ $h_2(x)$	series solution of differential equation for $\tilde{H}$ in nonhomogeneous plasma
I	electric current
I_e	electron current collected by the Langmuir probe
I_i	ion current collected by the Langmuir probe
$\bar{J}$	electric current density
J_n	Bessel function of n^{th} order
JR_n	real part of the value of Bessel function J_n with complex argument

JI_n	imaginary part of the value of Bessel function J_n with complex argument
j	$\sqrt{-1}$; integer in the series $h_2(x)$ and $e_2(x)$
k	$\omega\sqrt{\mu\varepsilon}$: propagation constant of the electromagnetic wave
k_o	$\omega_o\sqrt{\mu_o\varepsilon_o}$: propagation constant of the electromagnetic wave in free space
$k(\rho)$	radially dependent propagation constant of the electromagnetic wave
k	Boltzman constant
k_ρ	radial propagation constant
$\bar{M}$	magnetic current density
$\bar{M}'_1, \bar{M}'_2$	magnetic radiation vector
M_ϕ	ϕ-component of $\bar{M}'$
m	mass of electron, integer in the series $h(x)$ and $e(x)$, etc
n	integer
$\bar{n}$	average plasma density
n_o	plasma density at the axis of the plasma column
n_ρ	radially dependent plasma density
P	gas pressure
R	radius of the discharge tube
R_{rad}	radiation resistance
T_e	electron temperature
t	$\alpha - \gamma_1^2/k_o^2$
u_{ir}	V_{ir}/k_o
u_{li}	V_{li}/k_o
V_p	probe potential
V_a	applied potential
$V_{1,2}$	electric radiation vectors
$\bar{V}_\theta$	θ-component of $\bar{V}$
v_o	$k_o\sqrt{1-\sin^2\theta}$
v_1	$k_o\sqrt{\varepsilon_\rho-\sin^2\theta}$
v_2	$k_o\sqrt{\varepsilon_d-\sin^2\theta}$
v_d	$k_o\sqrt{\varepsilon_d-\sin^2\theta}$
v_{1r}	real part of complex v_1
v_{1i}	imaginary part of complex v_1
W_R	radiated power

X	ω_p^2/ω^2
x	$2.405\ \rho/b$ (see 3.1), $(k_{o_1}\rho)^2$
Y	inhomogeneity profile index (ch.3); ω_c^2/ω^2 (ch.5)
Y_n	Neumann function of order n
Z	frequency of ionizing collisions
x, y, z	cartesian coordinates
ρ, ϕ, z	cylindrical coordinates
r, θ, ϕ	spherical polar coordinates
α	$1-\omega_{po}^2/\omega^2$ (ch.3), k_{o_1}'a sin θ (ch.5)
β	$\frac{\omega_{po}^2}{\omega^2}\ \frac{Y}{b^2}$
δ	Dirac's delta function
∇	del operator
Δ	small increment
$\Delta\phi$	phase shift
ε	permittivity of the medium
ε_o	permittivity of the free space
ε_d	relative permittivity of the dielectric
ε_p	relative permittivity of the plasma
ε_{pr}	real part of the complex ε_p
ε_{pi}	imaginary part of the complex ε_p
η_1	Fourier transform variable
η_1'	$1 - X$
λ	wavelength of the electromagnetic wave
μ	permeability of the medium
μ_o	permeability of free space
ν	electron collision frequency
σ	β/α
π	3.1415926
$\hat{\phi}$	unit vector in the ϕ - direction
$\mathcal{I}(\theta,\phi)$	radiation intensity
$\mathcal{I}_m$	maximum radiation intensity
ω	source (signal) frequency
ω_c	cyclotron frequency
ω_p	plasma frequency
ω_{po}	plasma frequency at the axis of inhomogeneous plasma column

TABLE OF CONTENTS

CHAPTER 1

INTRODUCTION

1.1 ANTENNAS IN PLASMA

The study of the behaviour of electromagnetic sources in plasma medium has been of immense interest among the research workers for the last two decades. This is mainly due to its relevance to space communication, re-entry problems, ionospheric physics and plasma diagnostics. The theory of sources in plasma and wave propagation through the plasma is now considered as a major branch of electromagnetics. Extensive reviews and bibliographies on antennas in plasma have been given by Felsen (1964), Wait et al (1964), Bachynski (1967), Balmain (1972) and Preis/etal (1975).

The behaviour of antennas in plasma is a very complicated phenomenon. It is characterised not only by the geometry and the current distribution of the antenna but also by the properties of the sheath region and the plasma surrounding the antenna. A plasma medium, unlike the free space, is dispersive, lossy, inhomogeneous and compressible. It is anisotropic in the presence of an external magnetic field. Moreover, a non-uniform region or sheath is also generated around an antenna when it is immersed in the plasma. Various effects like, the modification of antenna current distribution and radiation pattern, ionization enhanced voltage breakdown and transmission effects such as, reflection, attenuation and phase shift

drastically degrade the performance of the antenna surrounded by a plasma. The near fields of the antenna also subject the ambient plasma to very strong nonlinear electromagnetic fields which cause plasma heating, resonances and other complicated effects.

It can be realised that a rigorous analysis of the characteristics of an antenna in a plasma, taking into account all the pertinent effects and properties of the plasma is a formidable task. The analytical difficulties prompted the research workers to use various simple plasma models and various simplifying assumptions, to gain some insight into the various aspects of antenna behaviour in a plasma medium. The various approaches to the study of antenna characteristics in a plasma have been classified by Bachynski (1967) in the following categories.

i) theoretical analyses using highly idealised simple models,

ii) semi-rigorous theoretical analyses, and

iii) an intermediate approach to the theoretical analysis with as much experimental verification as is possible.

The first approach can be used to analyse almost an infinite number of idealised problems and a considerable insight can be gained about the various aspects of antenna behaviour in plasma. However, the results may not be directly

applicable to any physical situation, since the validity of the approximations is not known.

The semi-rigorous analysis involves considerable difficulties in physics and mathematics. And more often the obtained results are not in a usable form and require further simplifications. However, this approach provides a better understanding of the physics of the problem.

The last approach provides a gradual and better understanding of the physics of the situation. But the experiments on antennas in plasma are quite sophisticated, time consuming and have many limitations.

The studies on sources in plasma can be broadly divided into two groups, (i) study of sources in unbounded plasmas, concerning with the antennas aboard the satellites and space-vehicles moving through an unbounded media such as the ionosphere, and (ii) study of sources in bounded plasmas concerning with the sources aboard the space-vehicles surrounded by the re-entry plasma layer or the ionised rocket exhaust and the sources in laboratory plasmas.

Several simple geometries of unbounded plasmas such as, grounded or ungrounded plasma slabs, plasma cylinder, conical plasma layer and plasma sphere etc. have been considered for theoretical analyses. In the early theoretical studies of sources on space-vehicles the curved surfaces of the space vehicle and the surrounding plasma layer were

approximated by an infinite plane grounded plasma slab, for wavelengths which are small as compared to the size of the vehicle. In some cases an ungrounded plasma slab has also been considered by introducing a free space or dielectric layer between the plasma and the ground plane which accounts for the sheath region in the immediate vicinity of the space-vehicle. When the wavelength is comparable to the size of the space-vehicle, the curvature of the vehicle surface and the surrounding plasma layer must be taken into account. A plasma clad cylinder is generally considered as a mathematical model of the space-vehicle since it represents the aft-portion of many re-entry vehicles. The cylindrical geometry is also considered for most of the theories related to the laboratory plasmas. The conical and spherical plasma geometries have also been studied in some cases.

Various simple models of the plasma have been used in the theoretical analyses. The complexity of the analysis increases when a more realistic plasma model is considered. The simplest plasma model used in most of the theoretical work is the hydrodynamic or the continuous fluid model. In this model the properties of the plasma are given by the average behaviour of the particles constituting the plasma. A plasma may consist of three types of particles, the electrons, the ions and the neutrals. Consequently, three hydrodynamic models are possible namely, the single-fluid model (electrons), the double-fluid model (electrons and ions), and

the triple-fluid model (electrons, ions and neutrals). In most of the analyses concerning with the antennas in plasma, the single-fluid model is adopted.

A further classification of the plasma models can be made on the basis of whether the plasma is considered to be isotropic or anisotropic, homogeneous or inhomogeneous, lossless (collisionless) or lossy (collisional) and compressible (warm) or incompressible (cold). A plasma, when subjected to a magnetic field, becomes anisotropic and it is characterized by a tensor permittivity. It can support two types of electromagnetic wave modes known as the ordinary wave and the extra-ordinary wave. The isotropic plasma is characterized by a scaler permittivity and supports only one electromagnetic wave mode. Almost all the real plasmas have a spatial variation or inhomogeneity of plasma density. An exact solution of the problem for a realistic plasma density profile rarely exists and one usually resorts to the approximate solutions. The collisions among the charged particles and the neutrals make the permittivity of the plasma a complex quantity. The complex permittivity further complicates the analysis of a given problem and so the assumption of a collisionless plasma is generally made. A plasma is termed as compressible, if the thermal velocities of the particles are sufficiently high and a pressure gradient exists. In a compressible plasma the longitudinal acoustic wave modes are also possible in addition to the electromagnetic wave modes.

The number of the longitudinal wave modes is equal to the number of species of the particles constituting the plasma. A coupling between various acoustical wave modes and between the electromagnetic and the acoustical wave modes may further increase the complexity of the problem.

The characteristics of a variety of antennas in plasma have been studied in the literature. The majority of the work on antennas in plasma is devoted to the theoretical analysis and the experimental studies have been comparatively very few. The various simple types of antennas which have been extensively studied in the literature are: the short electric and magnetic dipoles, cylindrical dipoles, line sources, electric and magnetic ring sources, biconical antennas, slots, open-waveguide apertures, horns, axial and circumferential slots on the conducting cylinders and slotted sphere etc. The major emphasis of these studies has been on the radiation patterns and impedance characteristics with a view to understand the re-entry problems.

1.2 STUDIES ON PLASMA ANTENNAS

It has emerged from the studies on antennas in plasma that a plasma layer can support the complex waves of the surface and the leaky-wave types (Tamir and Oliner 1962, 1963). These authors have given a detailed discussion of the various types of complex waves which can be supported by an isotropic plasma layer and their influence on the radiation from the

source excited plasma layer. The surface waves are shown to exist for frequencies that are smaller than the plasma frequency whereas the leaky-waves are found to be dominant when the source frequency is higher than the plasma frequency. The radiation from a surface wave occurs when it encounters a discontinuity along the guiding structure, on the other hand, a leaky wave continuously radiates energy as it propagates along the guiding structure. The detailed treatments of the surface wave antennas have been given by Zucker (1961, 1969). The leaky wave antennas have been discussed by Zucker (1961), Tamir (1968) and others.

The leaky waves on a plasma slab are found to radiate at an oblique angle near the critical optical angle (Tamir 1962). Since the critical optical angle depends upon the permittivity of the plasma relative to that of the surrounding medium, the direction of the radiation peak can be changed by changing the permittivity of the plasma. Similar observations were made by Gupta (1970) for the case of an isotropic plasma column excited by a magnetic ring source and it was proposed that the plasma column itself can be used as an antenna.

Several other authors have also suggested that a plasma column can be used as an antenna. Samaddar (1963-1964) studied the scattering of obliquely incident plane waves from an anisotropic plasma column and predicted the feasibility of using the anisotropic plasma column as an electronically

scanning antenna.

Kaufman and Steier (1963) experimentally studied the radiation characteristics of a plasma column antenna. A gas discharge column was used as a tunable antenna at S-band. The plasma column was excited in the dipolar resonance ($\omega = \omega_p/\sqrt{2}$; ω = source frequency, ω_p = plasma frequency) by means of a parallel wire transmission line. The radiation characteristics were those of a line of parallel dipoles oriented perpendicular to the plasma column. The plasma-antenna could be electronically tuned by changing the discharge current. Contrary to the common belief that such a plasma antenna would be greatly lossy due to the presence of collisions in plasma, the radiations with negligible plasma losses were obtained. The radiations from the plasma column were also found at plasma densities other than that for the dipolar resonance. At the plasma densities higher than that for the dipolar resonance, enhanced radiation peaks were observed at an oblique angle. These radiations at the oblique angle were considered to be due to the excitation of surface waves on the plasma column. In a rather different situation, Ghose (1967) has proposed the use of a plasma column as a receiving antenna in a nuclear environment.

Recently, Levitskiy and Burykin (1973, 1974) have made a remarkable theoretical and experimental study of radiation due to surface waves on narrow plasma columns contained in straight and bent tubes. The bent tube offered a prominent

discontinuity to the surface waves and hence a higher radiation efficiency was obtained. Burykin et al (1975) have also presented the theoretical and experimental results of the radiation due to surface waves on a plasma column having non-uniform radius.

Now we return to the studies on radiation from leaky waves on the plasma surfaces and confine our attention to the cylindrical plasma geometries. The infinitely long cylindrical geometry is preferred over the infinite slab geometry because the former has only one of its dimensions, i.e. the length unbounded whereas the later has both of its sides unbounded. Moreover, a cylindrical plasma column is most readily produced in the laboratory.

Harris (1963) has studied the radiation from a magnetic line source axially oriented on a conducting cylinder surrounded by a multiple layered plasma. Large narrow radiation peaks were obtained in the radiation pattern, which were attributed to the presence of leaky waves. Samaddar and Yildis (1964) studied the coupled electroacoustical waves on a compressible plasma cylinder excited by a magnetic ring source and discussed the possibility of excitation of leaky waves. Cheng and Chen (1970) have obtained the radiation patterns of a magnetic ring source outside a compressible plasma column.

Gupta (1970) and Gupta and Garg (1971) carried out extensive studies on the radiation characteristics of infinitely long plasma columns excited by electric and magnetic ring sources and open-ended waveguides. The plasma was considered to be cold, isotropic, homogeneous and collisionless. Multiple narrow radiation peaks were obtained near and before the critical optical angle. Some empirical relations of the direction of the radiation peaks with the source radius, plasma column radius and plasma density were established. Although the leaky wave poles were not obtained but the radiation peaks were expected to be due to the presence of leaky waves. It was proposed that the plasma column can be used as a multiple narrow beam antenna.

Ram (1972) studied the radiation patterns for various plasma geometries like : a plasma column with a central conductor, annular plasma column with an air core and a central conductor and multiple-layered plasma column, and also proposed that a plasma column can be used as an electronically scanning antenna. Three different types of sources of excitation, the electric and magnetic ring source, open-ended coaxial cable and open-ended circular waveguide supporting the circularly symmetric modes were considered. The plasma model considered was the same as used by Gupta (1970). The surface wave and the radiation fields of a compressible plasma column with an axial conductor excited by a magnetic ring source were also analyzed (Ram 1972). Joshi and Verma (1974, 1975a) have

also analyzed similar problems as analyzed by Man (1972) for the case of an anisotrppic plasma column. Sharma (1977) has solved a number of idealised problems on radiation from source excited plasma columns consisting of varicus combination of the multiple layers of air, gaseous and semiconductor plasmas.

The major conclusions of the above studies are that a plasma column suitably excited by an electromagnetic source gives enhanced multiple narrow radiation peaks, the direction of which can be controlled by changing the plasma frequency, the cyclotron frequency or the source frequency; the number of radiation peaks, the peak amplitude and the half power beamwidth etc. can be controlled by a proper choice of the geometrical parameters of the plasma antenna system.

In order to decide upon the practical feasibility of such a plasma-antenna system, one would require to examine the validity of the various assumptions used in the above theoretical analyses, in a practical laboratory situation. In the following paragraphs we discuss the validity of these assumptions.

i) The first assumption common to all the above analyses is that of an infinite length of the plasma column. The infinite geometries are generally approximated in practice by taking a structure much longer as compared to a wavelength. In the laboratory, it is not easy to generate a very long plasma

column. Moreover, a long plasma column is not homogeneous along its length. One may suggest the use of some sort of a matched termination at the end of the plasma column. But the impedance matching will not be very easy since the parameters will have to vary for achieving the scanning. An interesting solution is obtained if one looks into the mechanism of radiation from the plasma column. It has been mentioned above that a leaky wave continuously radiates energy as it propagates along the plasma column. Thus one may calculate the amount of power radiated by the wave per unit length and find out the length of the plasma column after which the wave is left with a negligible power. Even if this power is reflected, it will not cause any serious effect. Thus an infinitely long plasma column assumed in the theory can be conveniently approximated byafinitely long laboratory plasma column of a suitable length.

ii) Another assumption is that of a homogeneous plasma column. The laboratory plasmas, in general, have a spatial inhomogeneity of plasma density. The positive column of a discharge is considered to be sufficiently homogeneous along its length but it has a radial inhomogeneity of plasma density. The density profile in a positive column is generally approximated by a parabolic function. Thus it is essential to know the influence of the density profile of the plasma on the radiation characteristics.

iii) The plasma has been assumed to be cold in most of the above theoretical analyses. This assumption sounds reasonable, since for most of the plasmas the electron thermal velocity is much smaller than the phase velocity of the wave and it can be easily neglected.

iv) It has also been assumed that the plasma is collisionless. But in practice the plasmas are collisional. The effect of the losses is to attenuate the wave which results into a loss of radiated power. Therefore, it is essential to make a quantitative estimate of the influence of collisions on the radiated power and other antenna characteristics.

v) The assumption of isotropic plasma is perfectly valid if no external magnetic field is applied to the plasma. But it is rather difficult to generate an anisotropic plasma column assumed in the theory by Joshi et al (op.cit.), Since it is difficult to generate a homogeneous axial magnetic field without covering a larger portion of the plasma column with the magnetic coils which will obstruct the radiation.

vi) All the analyses mentioned above are based upon the assumption that the plasma column is bounded by the free space around it. Except for the cases of a flame plasma and charged particle beams etc. most of the laboratory plasmas are created in a container made of a dielectric which is usually the glass. Thus a knowledge of the radiation pattern distortion and other effects due to the presence of the dielectric tube is essential.

We may conclude that the theoretical studies on the influence of plasma collision frequency, inhomogeneity of plasma density and the dielectric tube surrounding the plasma are very much essential for choosing the proper plasma-antenna parameters and for comparison with the experimental results.

The method of solution of the problem of radiation from an inhomogeneous anisotropic plasma column excited by a magnetic ring source, has been discussed by Joshi and Verma (1975b). However, they did not obtain the solution in an explicit form. Recently Wong and Cheng (1977) have also studied the radiation from an electric currentloop in an inhomogeneous plasma column, but their final results are not available.

1.3 OUTLINE OF THE PRESENT WORK

The above limitations of the theoretical analyses of the plasma-antennas motivated the author to pursue a detailed study of the effects of the collision frequency, the inhomogeneity of plasma density and the dielectric tube containing the plasma on some of the major antenna characteristics. The theoretical predictions of the feasibility of a leaky-wave plasma-antenna also encouraged the author to take up an experimental study of the plasma-antenna system. A simple model consisting of a long cylindrical plasma column generated by a d.c. discharge in a glass tube and a suitable electromagnetic source was chosen for the theoretical and

experimental study. The electromagnetic sources were chosen to be the circularly symmetric and electric and magnetic ring sources and open-ended circular waveguide supporting the TM_{01}- or TE_{01}-mode. The major antenna characteristics which have been theoretically studied are: the radiation pattern, the radiation resistance and the directivity. The chapter-wise organisation of the present work is given in the following paragraphs.

The second chapter deals with the theoretical study of the radiation characteristics of a plasma-antenna system consisting of an infinitely long column of isotropic, homogeneous, collisional and incompressible plasma contained in a dielectric tube. The electric and magnetic ring sources and the open-ended circular waveguide carrying the circularly symmetric TM_{01}- or TE_{01}-mode are used as the source of excitation. The effects of collision frequency and the dielectric tube on the antenna characteristics mentioned above have been studied. The plasma column has been assumed to be homogeneous for the sake of mathematical simplicity. The assumption of isotropic plasma is valid since we have not considered any external magnetic field in the laboratory model described above. The infinite length of the plasma column assumed in the theoretical analyses can be approximated in the laboratory by a sufficiently long plasma column as explained in the preceding section. The assumption of incompressible plasma is generally valid for low density laboratory plasmas.

In the third chapter we take into account the inhomogeneity of the plasma density. The plasma column is assumed to be infinitely long, isotropic, inhomogeneous, collisionless incompressible and contained in a dielectric tube. The electric and magnetic ring sources have been considered for the excitation of the plasma column. A parabolic density profile which resembles with the actual plasma density profile in a discharge tube is considered for theoretical analysis. The electron collision frequency has been neglected for the sake of mathematical simplicity. The other assumptions have been shown to be valid for the laboratory model, in the above paragraph. The influence of the shape of the plasma density profile on the antenna characteristics has been discussed.

The fourth chapter describes the experimental plan for the study of plasma-antenna system. The experimental facility consists of the following major parts:(i) discharge tubes with cold or hot cathodes for generating the plasma column, (ii) the Langmuir probe and microwave interferometer set-up for plasma diagnostics, (iii) electromagnetic sources for the excitation of the plasma column, (iv) set-up for measuring the radiation pattern and input impedance of the antenna system.

The fifth chapter deals with a rather different problem, concerning with the radiation from an open-ended

radial waveguide in an anisotropic plasma medium. It is proposed that a radial waveguide can be used as a spacecraft antenna, since it has suitable radiation characteristics and can be easily flush-mounted on the spacecraft.

The last chapter summarises the significant findings of the present work. A brief account of the scope for future work in this direction is also included.

REFERENCES

Balmain, K.G.(1972) Antennas in plasma: Characteristics as a function of frequency, Radio Science, Vol 7, No 8,9, p 671

Bachynski, M.P. (1967) Sources in Plasma, RCA Review, Vol 28, No 1, p 111

Burykin, Y.I., Levitsky, S.M. and Martyenko, W.G. (1975) The radiation of electromagnetic waves by a variable cross-section cylindrical plasma waveguide, Rad.Eng. Electron.Phys., Vol.20, No 11, p 86

Cheng, D.K. and Chen, H.C.(1970) Radiation from a ring source around a compressible plasma column, App. Sci. Res., Vol 22, p 259

Felsen, L.B. (1964) Radiation from plasmas, J.Res. Nat.Bur. Stand., Vol 68D, No 4, p 480

Ghose, R.N. (1967) Plasma antenna in a nuclear environment IEEE Trans., Vol AP-15, No 5, p 713

Gupta, K.C. (1970) A multiple narrow beam antenna using a column of isotropic plasma, Int.J.Electron., Vol 29 No 1, p 45

Gupta, K.C. and Garg, R.K.(1971) Antennas using cylindrical columns of isotropic plasma, Res.Rep., I.I.T.K./E.E./ 71

Harris, J.H.(1963) Radiation through cylindrical plasma sheaths, J.Res.Nat.Bur.Stand., Vol 67D, No 6, p 717

Joshi, N.K. and Verma, J.S.(1974) Electronically scannable narrow beam plasma antenna system, Nachrichtentechn.Z., Vol 27, No 3, p 118

_____ (1975a) A narrow beam antenna system using an air column having a central conductor and surrounded by an anisotropic plasma column, Radio-Science, Vol 10, No 2, p 197

_____ (1975b) Radiation field of magnetic ring source surrounded by an inhomogeneous axially magnetised plasma column, J.Inst.Elec.Telecom.Engrs., Vol 21, No 10, p 538

Kaufman, I. and Steier, W.H.(1963) A plasma antenna and wave filter, Electromagnetic theory and antennas Pt 2 ed. by E.C.Jordan, (Pergamon Press)

Levitskiy, S.M. and Burykin, Y.P. (1973) Radiation of electromagnetic waves by plasma waveguides, Rad.Eng.Electron. Phys., Vol 18, No 12, p 1938

Levitskiy, S.M. and Burykin, Y.I.(1974) Radiation of electromagnetic waves from a regular plasma waveguide using surface waves, Rad.Eng. and Electron.Phys., Vol 19, No 9, p 57

Preis, D.H., Ward, M.A.V. and King, R.W.P. (1975) Experimental aspects of antennas in plasma, Int.Conf. Plasma Sci., Ann Arbor, Mich., USA

Ram, D.(1972) Electronically scannable narrow beam plasma antenna system, Ph.D. thesis, Birla Institute of Tech. & Science, Pilani, Rajasthan, India

Samaddar, S.N. (1963-64) Scattering of plane waves from an infinitely long cylinder of anisotropic materials at oblique incidence with an application to an electronic scanning antenna, App.Sci. Res. B, Vol 10, p 385

Samaddar, S.N. and Yildiz, M.(1964) Excitation of coupled electro-acoustical waves by a ring source in a compressible plasma cylinder, Can.J.Phys., Vol 42, No 4, p 638

Sharma, S.C.(1977) Electromagnetic excited radiations from plasma columns and optical waveguides, Ph.D.Thesis, Birla Institute of Tech. & Science, Pilani,Rajasthan,India

Tamir, T.(1969) Leaky-wave antennas, Antenna theory Pt 2, ed by R.E. Collin and F.J.Zucker (McGraw Hill)

Tamir, T. and Oliner, A.A.(1962) The influence of complex waves on the radiation field of a slot-excited plasma layer, IRE Trans., Vol AP-10, No 1, p 55

_____ (1963) The spectrum of electromagnetic waves guided by a plasma layer, Proc. IEEE, Vol 51 No 2, p 317

Wait, J.R. and Brackett, E.A.(1967) Bibliography on waves in plasma, ESSA Tech.Rep. IERSI-ITSA 39

Wong, W.C. and Cheng, D.K. (1977) Radiation from a current loop in an inhomogeneous plasma column, IEEE AP-S International Symposium, Stanford Univ. Stanford, California.

Zucker, F.J.(1961) Surface and leaky-wave antennas, Antenna engineering handbook, ed by H.Jasik, (McGraw Hill)

_____ (1969) Surface-wave antennas, Antenna theory Pt 2, ed by R.E. Collin and F.J.Zucker,(McGraw Hill)

CHAPTER 2

RADIATION FROM A HOMOGENEOUS, ISOTROPIC AND COLLISIONAL PLASMA COLUMN CONTAINED IN A DIELECTRIC TUBE

2.5 EXCITATION BY OPEN-ENDED CIRCULAR WAVEGUIDE (TM_{01}- AND TE_{01}- MODES)

2.6 CONCLUSIONS

2.1 INTRODUCTION

The excitation of leaky waves on plasma structures has been investigated by several authors. It was first established by Tamir and Oliner (1962), using an infinitely long magnetic line source, that leaky waves are strongly excited on a plasma slab when the signal frequency is higher than the plasma frequency. Under different conditions these leaky waves may produce either a relatively sharp radiation peak near the critical optical angle alongwith some minor peaks, or a single broad peak at the broadside. Samaddar and Yildiz (1964) analysed the excitation of coupled electro-acoustical waves by a magnetic ring source on a compressible plasma cylinder and discussed the possibility of excitation of leaky waves. However, they did not obtain any radiation pattern. Seshadri (1965) investigated the excitation of surface waves and space waves on a simple isotropic plasma cylinder by means of an axially oriented dipole. He evaluated the radiation fields for $\omega/\omega_p = 1.05$ (where ω = signal frequency and ω_p = electron plasma frequency) and obtained a broad peak at the broadside for thin plasma column and sharp peaks together with some minor peaks near broadside for thicker plasma columns. Samaddar (1966) studied the radiation fields of a dielectric coated cylindrical core loop antenna surrounded by a lossy plasma sheath. He plotted the amplitude and phase patterns for various values of ω_p/ω and ν/ω (ν = collision frequency). He obtained sharp radiation peaks and observed that the direction and amplitude

of the radiation peaks depend upon the ω_p/ω and ν/ω . The change in direction with ν/ω, of course, is very small. The last two authors, however, did not appreciate the existence of leaky waves. More recently, a detailed study of radiation from various configurations of cold, isotropic and homogeneous plasma columns excited by a variety of circularly symmetric sources, Such as electric and magnetic ring sources, open-ended waveguides and open-onded coaxial cable, has been made by Gupta (1970), Gupta and Garg (1971) and Ram and Verma (1972, 1973 a, 1973 b and 1974). These authors carried out an extensive study of the effects of plasma density, plasma column radius and source dimensions etc. on the radiation patterns, and proposed that a plasma-antenna system may be used as an electronically scanning antenna system.

It has been felt that the feasibility of the above proposal cannot be ascertained unless a thorough theoretical study is made, in order to understand the influence of the plasma collisions, the glass tube which will be used to contain a laboratory plasma and the inhomogeneity of the laboratory plasma on the important antenna characteristics. In the present chapter, we attempt to study the effects of collisions and the dielectric tube on the radiation patterns, directivity and radiation resistance of plasma-antenna systems. Isotropic, homogeneous, incompressible and lossy plasma cylinders contained in a dielectric tube and excited by electric and magnetic ring sources and open-ended circular waveguide are considered for analysis.

2.2 EXCITATION BY RING SOURCES

In this section we study the excitation of plasma columns by idealized ring sources carrying uniform magnetic or electric current. Only the lowest order circular symmetric modes of excitation are considered. A loop carries a uniform current when its circumference is smaller than the wavelength. In a situation where the circumference of the ring becomes several wavelengths, the higher order modes will also be excited, but the present analysis will represent only the lowest order mode. Further, it is worthwhile to note that an electric dipole oriented along the z-axis will excite the same types of mode as excited by the magnetic ring source. And similarly, the modes excited by an electric ring source will be the same as those excited by an axially oriented magnetic dipole.

To study the radiation characteristics of the plasma-antenna system the ring source is placed inside an infinitely long cylinder of isotropic, homogeneous, incompressible and lossy plasma. The relative permittivity (ϵ_p) of the lossy plasma, in the absence of any magnetic field and neglecting the motion of ions, is given by

$$\epsilon_p = 1 - \omega_p^2/\omega\,(\omega + j\nu) < \xi \qquad (2.1)$$

where

ω_p = electron plasma frequency (radians)
ω = signal frequency
ν = collision frequency

The radiation field is obtained by setting up the source form of the Maxwell's equations and solving the wave equation by Fourier transform technique and the method of steepest descents. The technique is fairly standard and a detailed description is given by Duncan (1959) and Tyras (1969). The radiation patterns, radiation resistance and directivity are numerically evaluated for typical values of collision frequency and dielectric tube thickness and their effect on the above characteristics is discussed. The results are also compared with the lossless case and the no dielectric tube case.

2.3 EXCITATION BY A MAGNETIC RING SOURCE

2.3.1 Introduction

In this section we analyze the radiation characteristics of a system consisting of a magnetic ring source placed inside a plasma column filled in a dielectric tube and having properties described in the prece-ding section. A magnetic current ring source carrying a uniform current excites the lowest order circularly symmetric E-type mode, having field components E_ρ, E_z and H_ϕ. Due to the circular symmetry of the source, the component E_ρ will be zero at $z = 0$. Thus, in the plane of the source the tangential electric field vanishes and a conducting screen may be placed at the location of the source without disturbing the fields.

Now the magnetic ring source can be simulated by a very narrow annular slot in a large conducting sheet at z = 0. The annular slot will be a good approximation of the magnetic ring source if the slot width is small compared to the wavelength, and the electric field in the slot is radial and uniform.

As mentioned in the introduction, similar problems have been analyzed by several authors using different plasma models or plasma geometries (Samaddar and Yildis, 1964, Gupta, 1970, Gupta and Garg, 1971, Ram and Verma, 1972). In the present analysis, we will emphasize upon the influence of collision frequency and the dielectric tube used to contain a laboratory plasma, upon the radiation pattern, directivity and the radiation resistance of the plasma-antenna system. The results will be useful to choose the proper plasma parameters and geometrical configuration for experimental realisation of the plasma-antenna system.

2.3.2 Formulation of the Problem

Consider an infinitely long cylindrical plasma column of radius b and relative permittivity ϵ_p surrounded by a dielectric tube of inner radius b, outer radius c and relative permittivity ϵ_d. The entire region outside the dielectric tube is free space. A magnetic ring source of radius a, carrying a uniform circumferential magnetic current M, is

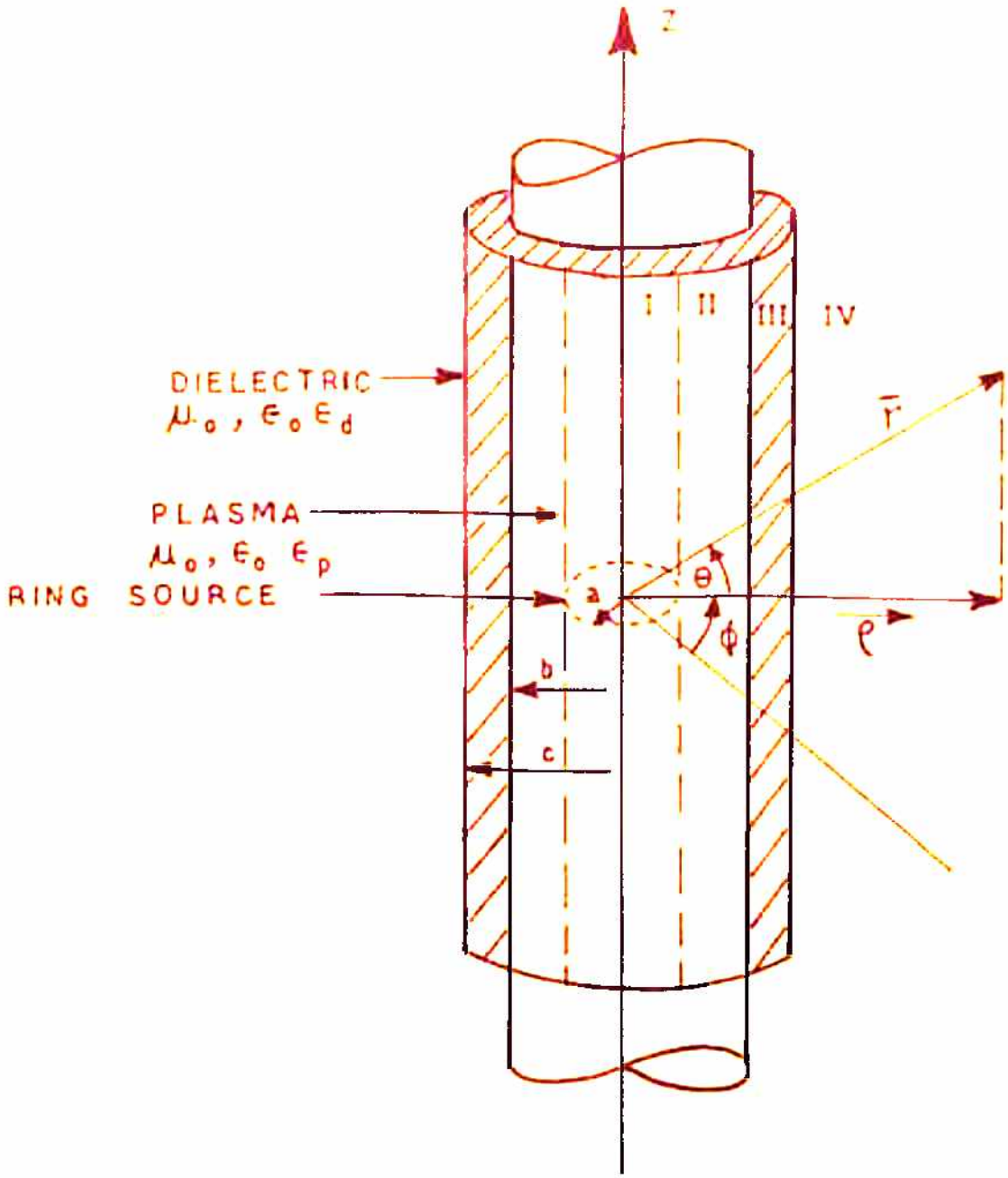

FIG. 2.1 INFINITELY LONG PLASMA COLUMN SURROUNDED BY DIELECTRIC TUBE EXCITED BY RING SOURCE

placed coaxial to the plasma column (Fig. 2.1). Since the geometry has a circular cylinder symmetry, the circular cylindrical coordinate system (ρ, ϕ, z) is used. For the sake of convenience the ring source is placed at the origin (z = 0) and it is represented in terms of Dirac delta functions as follows:

$$\bar{M} = \hat{\phi}\, M\, \delta(\rho - a)\, \delta(z) \qquad (2.2)$$

where $\hat{\phi}$ is a unit vector in the ϕ-direction and M is the strength of the ring source having the dimensions of volts per square meter.

Assuming a harmonic time-dependence of the form $e^{-j\omega t}$ for the source and all the field components, the Maxwell's equations for the electromagnetic fields can be written as

$$\nabla \times \bar{E} = j\omega \mu_0 \vec{H} - \vec{M} \qquad (2.3)$$

$$\nabla \times \bar{H} = -j\omega \epsilon_0 \epsilon(\rho)\, \bar{E} + J_e \qquad (2.4)$$

where

$$\epsilon(\rho) = \epsilon_p \qquad 0 \leq \rho < b$$
$$= \epsilon_d \qquad b < \rho < c$$
$$= 1 \qquad \rho > c \qquad (2.5)$$

and the time-dependence $\exp(-j\omega t)$ has been suppressed throughout. On eliminating $\bar{E}$ from the above Maxwell's equations, we get

$$\nabla \times \nabla \times \bar{H} - \omega^2 \mu_o \varepsilon_o \varepsilon(\rho)\, \bar{H} = j\omega \varepsilon_o\, \varepsilon(\rho)\, \bar{M} \qquad (2.6)$$

Since the source of excitation is axially symmetric and the media involved are homogeneous in the polar angle ϕ, all the field quantities will also be independent of ϕ, i.e. $\partial/\partial\phi \equiv 0$. Moreover, the magnetic ring source excites only the E_ρ, E_z and H_ϕ field components. Thus the above eqn. (2.6) gives the following nonhomogeneous partial differential equation for H_ϕ.

$$\frac{\partial^2 H_\phi}{\partial \rho^2} + \frac{1}{\rho}\frac{\partial H_\phi}{\partial \rho} + (k^2(\rho) - 1/\rho^2) H_\phi + \frac{\partial^2 H_\phi}{\partial z^2} = -j\omega \varepsilon_o \varepsilon(\rho) M\, \delta(\rho - a)\, \delta(z) \qquad (2.7)$$

where,

$$k^2(\rho) = \omega^2 \mu_o \varepsilon_o \varepsilon(\rho) \qquad (2.8)$$

The other non-zero field components E_ρ and E_z can be obtained in terms of H_ϕ using equation (2.4).

In order to solve equation (2.7) we take its Fourier transform with respect to z, which reduces it to an ordinary differential equation. The Fourier transform of H_ϕ is defined as

$$\tilde{H}(\rho, \eta) = \int_{-\infty}^{+\infty} H_\phi(\rho, z) \exp(-j\eta z)\, dz \qquad (2.9)$$

and the inverse transform is given by

$$H_\phi(\rho, z) = 1/2\pi \int_{-\infty}^{+\infty} \tilde{H}(\rho, \eta) \exp(+j\eta z)\, d\eta \qquad (2.10)$$

Now, after operating the Fourier transform the following ordinary differential equation is obtained.

$$\frac{d^2\tilde{H}}{d\rho^2} + \frac{1}{\rho}\frac{d\tilde{H}}{d\rho} + (k^2(\rho) - \eta^2 - 1/\rho^2)\,\tilde{H} = j\omega\epsilon_o\epsilon(\rho)M\delta(\rho-a) \quad (2.11)$$

2.3.3 Solution of the Problem

It is easily recognized that except for $\rho = a$ the equation (2.11) is of the form of Bessel equation. The appropriate solutions to this equation in the various regions of space, denoted I-IV in Fig.(2.1), must satisfy the conditions that the fields be finite at $\rho = 0$, and at $\rho = \infty$ they must be regular and satisfy the radiation condition. The solutions in various regions satisfying these conditions are found to be

$$\tilde{H}_I(\rho,\eta) = A_1 J_1(v_1\rho) \qquad 0 \leq \rho \leq a \qquad (2.12\ a)$$

$$\tilde{H}_{II}(\rho,\eta) = A_2 J_1(v_1\rho) + B_2 Y_1(v_1\rho) \qquad a \leq \rho \leq b \qquad (2.12\ b)$$

$$\tilde{H}_{III}(\rho,\eta) = A_3 J_1(v_2\rho) + B_3 Y_1(v_2\rho) \qquad b \leq \rho \leq c \qquad (2.12\ c)$$

$$\tilde{H}_{IV}(\rho,\eta) = A_4 H_1^{(1)}(v_o\rho) \qquad \rho \geq c \qquad (2.12\ d)$$

where, $v_o = (k_o^2 - \eta^2)^{1/2}$ $v_1 = (k_o^2\,\epsilon_p - \eta^2)^{1/2}$,

$v_2 = (k_o^2\,\epsilon_d - \eta^2)^{1/2}$ (2.13)

and J_n and Y_n and $H_n^{(1)}$ are the nth order Bessel function, Neumann function and Hankel function of the first kind

respectively. A_1, A_2, B_2 ----, A_4 are the arbitrary coefficients to be determined by applying the boundary conditions on $\tilde{H}(\rho,\eta)$.

The delta function $\delta(\rho-a)$ implies a boundary condition on $\tilde{H}(\rho,\eta)$ at $\rho = a$ which can be obtained by integrating equation (2.11) with respect to ρ over an interval 2Δ, from $a-\Delta$ to $a+\Delta$, resulting into

$$\left.\frac{d\tilde{H}_{II}}{d\rho}\right|_{a+\Delta} - \left.\frac{d\tilde{H}_{I}}{d\rho}\right|_{a-\Delta} = -j\omega\varepsilon_0\varepsilon_p H \qquad (2.14)$$

$\Delta \to 0$

The other boundary conditions on $\tilde{H}(\rho,\eta)$ are furnished by the continuity of the tangential components of electric and magnetic fields, E_z and H_ϕ at the boundaries $\rho = a$ and $\rho = c$ and by the continuity of H_ϕ at $\rho = a$. Thus we have six unknowns A_1, A_2, B_2 ...., A_4 and six boundary conditions. The application of these boundary conditions on $\tilde{H}(\rho,\eta)$ will give a set of six algebraic equations, which can be solved by matrix methods to obtain the coefficients A_1 ...., A_4. Since we are interested in the radiation fields ($\rho > c$) we take the inverse Fourier transform of $\tilde{H}_{IV}(\rho,\eta)$ to obtain the field component $H_\phi(\rho,z)$ for $\rho > c$,

$$H_\phi(\rho,z) = 1/2\pi \int_{-\infty}^{+\infty} A_4 \cdot H_1^{(1)}(V_0\rho)\exp(j\eta z)\, d\eta \qquad ..(2.15)$$

This integral is evaluated by considering it as a contour integral in the complex η-plane. To give effect to the contour integration the pole and branch point singularities of the integrand are obtained. A suitable contour is then chosen, the contribution at the poles is obtained by the Cauchy residue theorem and gives the surface wave fields and the line integral along the branch cut at the branch points $\eta = \pm k_o$ gives the radiation field. Since the integrand involves complicated expressions of Bessel functions etc., we do not attempt to find out the location of the leaky wave poles. To obtain the asymptotic value of the radiation fields we evaluate the integral along the branch cut by the method of steepest-descents. Since the procedure of asymptotic evaluation of the integral for $k_o\rho \gg 1$ is fairly standard, we omit the details and write down the resulting expression for H_ϕ the far-zone radiation field. Since the radiation fields are measured in spherical polar coordinate system, before integration, we make a transformation of coordinates from cylindrical to spherical polar coordinate system ($\rho = r\,\mathrm{Cos}\theta$, $z = r\,\mathrm{Sin}\theta$). The far-zone radiation field in spherical polar coordinate system is then written as

$$H_\phi(r,\theta) = j\frac{k}{\pi}\sqrt{\epsilon_o/\mu_o}\;F(\theta)\;\frac{e^{j(k_o r - \pi/4)}}{r} \qquad (2.16)$$

where $F(\theta)$ is the pattern function, given by

$$F(\theta) = 2\varepsilon_p \varepsilon_d (k_o a)\, J_1(v_1 b)/\pi(P.R + Q.S) \qquad (2.17)$$

where

$$P = \varepsilon_d (v_1 b)\, J_o(v_1 b)\, J_1(v_2 b) - \varepsilon_p (v_2 b) J_1(v_1 b) J_o(v_2 b) \qquad (2.18a)$$

$$Q = -\varepsilon_d (v_1 b) J_o(v_1 b) Y_1(v_2 b) + \varepsilon_p (v_2 b) J_1(v_1 b) Y_o(v_2 b) \qquad (2.18b)$$

$$R = (v_2 c) Y_o(v_2 c) H_1^{(1)}(v_o c) - \varepsilon_d (v_o c) Y_1(v_2 c) H_o^{(1)}(v_o c) \qquad (2.19a)$$

$$S = (v_2 c) J_o(v_2 c) H_1^{(1)}(v_o c) - \varepsilon_d (v_o c) J_1(v_2 c) H_o^{(1)}(v_o c) \qquad (2.19b)$$

Here v_o, v_1 and v_2 are the same as defined by equation (2.13) but with $\eta = k_o \sin\theta$.

The above expression for the pattern function reduces to equation (2) of Gupta (1970) for $\varepsilon_d = 1$ and $c = b$ and to the expression for ring source in free space for $\varepsilon_d = \varepsilon_p = 1$.

At this stage we realise that the complex permittivity of the plasma also appears in the arguments of the Bessel functions through v_1, it means that we are dealing with Bessel functions with complex arguments. To obtain the value of complex argument Bessel functions, a Fortran subroutine subprogram was written which separates the real and imaginary parts of the series expansion of the Bessel

function and gives the real and imaginary values separately. The program was tested for purely real, purely imaginary and complex arguments and found to work satisfactorily.

We now proceed to separate out real and imaginary parts of $F(\theta)$ and write it in a form suitable for numerical computation.

$$\text{Since } \varepsilon_p = \left\{ 1 - \frac{\omega_p^2}{\omega^2 + \nu^2} \right\} + j \left\{ \frac{\omega_p^2 \nu}{\omega(\omega^2 + \nu^2)} \right\}$$

$$\text{or, } \varepsilon_p = \varepsilon_{pr} + j\varepsilon_{pi} \qquad (2.20)$$

Therefore, $v_1 = v_{1r} + j\, v_{1i}$

where,

$$v_{1r} = k_o \left[\left\{ (\varepsilon_{pr} - \sin^2\theta)^2 + \varepsilon_{pi}^2 \right\}^{1/2} + (\varepsilon_{pr} - \sin^2\theta) \right]^{1/2} / \sqrt{2} \qquad (2.20a)$$

$$v_{1i} = k_o \left[\left\{ (\varepsilon_{pr} - \sin^2\theta)^2 + \varepsilon_{pi}^2 \right\}^{1/2} - (\varepsilon_{pr} - \sin^2\theta) \right]^{1/2} / \sqrt{2} \qquad (2.20b)$$

and $J_n(v_1 \rho) = JR_n(v_1 \rho) + j\, JI_n(v_1 \rho)$ (2.21)

Making the above substitutions in equations (2.17) and (2.18) yields

$$F(\theta) = \frac{X_r + jX_i}{Y_r + jY_i} \qquad (2.22)$$

Where,

$$X_r = 2\varepsilon_d(k_o a) \left\{ \varepsilon_{pr} JR_1(v_1 a) - \varepsilon_{pi} JI_1(v_1 a) \right\} \qquad (2.23a)$$

$$X_i = 2\varepsilon_d(k_o a) \left\{ \varepsilon_{pi} JR_1(v_1 a) + \varepsilon_{pr} JI_1(v_1 a) \right\} \qquad (2.23b)$$

$$Y_r = \pi (P_r R_r - P_i R_i + Q_r S_r - Q_i S_i) \quad (2.24a)$$

$$Y_i = \pi (P_r R_i + P_i R_r + Q_r S_i + Q_i S_r) \quad (2.24b)$$

$$P_r = -(v_2 b)\, J_o(v_2 b)\, X_1 + \varepsilon_d J_1(v_2 b)\, X_3 \quad (2.25a)$$

$$P_i = -(v_2 b)\, J_o(v_2 b)\, X_2 + \varepsilon_d J_1(v_2 b)\, X_4 \quad (2.25b)$$

$$Q_r = (v_2 b)\, Y_o(v_2 b)\, X_1 - \varepsilon_d Y_1(v_2 b)\, X_3 \quad (2.26a)$$

$$Q_i = (v_2 b)\, Y_o(v_2 b)\, X_2 - \varepsilon_d Y_1(v_2 b)\, X_4 \quad (2.26b)$$

$$R_r = (v_2 c) Y_o(v_2 c)\, J_1(v_o c) - \varepsilon_d (v_o c) Y_1(v_2 c) J_o(v_o c) \quad (2.27a)$$

$$R_i = (v_2 c) Y_o(v_2 c)\, Y_1(v_o c) - \varepsilon_d (v_o c) Y_1(v_2 c) Y_o(v_o c) \quad (2.27b)$$

$$S_r = (v_2 c) J_o(v_2 c) J_1(v_o c) - \varepsilon_d (v_o c) J_1(v_2 c) J_o(v_o c) \quad (2.28a)$$

$$S_i = (v_2 c) J_o(v_2 c) Y_1(v_o c) - \varepsilon_d (v_o c) J_1(v_2 c) Y_o(v_o c) \quad (2.28b)$$

$$X_1 = \varepsilon_{pr} JR_1(v_1 b) - \varepsilon_{pi} JI_1(v_1 b) \quad (2.29a)$$

$$X_2 = \varepsilon_{pi} JR_1(v_1 b) + \varepsilon_{pr} JI_1(v_1 b) \quad (2.29b)$$

$$X_3 = (v_{1r} b) JR_o(v_1 b) - (v_{1i} b) JI_o(v_1 b) \quad (2.30a)$$

$$X_4 = (v_{1i} b) JR_o(v_1 b) + (v_{1r} b) JI_o(v_1 b) \quad (2.30b)$$

2.3.4 Antenna System Characteristics

The important characteristics of an antenna system are the radiation pattern, gain , directivity, radiation resistance, impedance, bandwidth and polarisation etc. In the present study, we have considered only the first few characteristics.

The Radiation Pattern :

The radiation pattern of an antenna system is the most basic requirement since it specifies the spatial distribution of the energy radiated by the antenna system. The radiation patterns are generally described in spherical polar coordinate system, in two principal planes : the horizontal plane or ϕ-plane and the vertical plane or θ-plane. In the present case, due to the circular symmetry of the source, the fields are independent of ϕ and we have an isotropic radiation pattern (a circle) in the ϕ-plane. In θ-plane , $|F(\theta)|$ is evaluated for various values of parameters, for θ-values at 0.5° interval. Only half of the radiation pattern is obtained, since symmetry exists about $\theta = 0$. Each pattern is then normalised to its maximum value to facilitate the comparison of relative pattern shapes for different parameters. The amplitudes of the maximum of the patterns are separately tabulated for comparison.

Radiation Resistance :

The radiation resistance of an antenna is equal to the total radiated power by the antenna, carrying a unit current. To evaluate the total radiated power, we assume that the antenna impedance remains constant. The radiated power is then calculated by integrating the radial Poynting vector over a spherical surface centered at the center of

the antenna system. The total radiated power is then given by

$$W_R = \frac{2N^2}{\pi}\sqrt{\varepsilon_o/\mu_o}\int_o^{\pi/2}|F(\theta)|^2 \cos\theta \, d\theta \qquad (2.31)$$

Now, assuming that a unit current flows through the ring source, i.e. N = 1, the radiation resistance is given by

$$R_{rad} = W_R \qquad (2.32)$$

The integral in equation (2.31) has been numerically evaluated on a computer using the Simpson's method.

The Directivity :

The directivity of an antenna signifies its ability to concentrate the radiated power in a given direction or to absorb effectively the incident power from that direction. It is defined as the ratio of power per unit solid angle radiated in the direction of maximum radiation to the average radiated power.

The power radiated per unit solid angle, known as the radiation intensity, is defined by

$$\phi(\theta, \phi) = \frac{N^2}{\pi^2}\sqrt{\varepsilon_o/\mu_o}\,|F(\theta)|^2 \quad \text{watts/sterradian} \qquad (2.33)$$

and the average power per unit solid angle is $W_R/4\pi$. The directivity, D, expressed in dB, is given by

$$D = 10 \log_{10} (4\pi \phi_m/W_R) \text{ dB} \qquad (2.34)$$

where, ϕ_m is the maximum radiation intensity. One may write

$$D = 10 \log_{10} \left[\frac{2|F(\theta_m)|^2}{\int_0^{\pi/2} |F(\theta)|^2 \cos\theta \, d\theta} \right] dB \qquad (2.36)$$

where θ_m is the direction of maximum radiation.

The directivity is thus readily obtained using the equation (2.35) and the value of the integral as obtained above.

2.3.5 Effect of Geometrical and Plasma Parameters on the Antenna Characteristics

The expressions for the pattern function (2.17) and (2.18) involve the geometrical parameters like, the radius of the ring source a, the radius of plasma column, b, the radius of dielectric tube, c, the relative permittivity of the dielectric, ε_d, and the plasma parameters ω_p and ν which enter through ε_p. All these parameters have been kept in the dimensionless form such as $k_o a$, $k_o b$, $k_o c$, ω_p/ω and ν/ω in order to make the analysis of numerical results more general. The influence of many of these parameters like the ring source radius, plasma column thickness and plasma density, on the radiation pattern has been studied by several authors and their general results are summarized below. In the present section we study the influence of

dielectric tube thickness and the collision frequency on some more physical and quantifiable antenna characteristics like radiation resistance, directivity, half power beam-width (HPBW) etc., in addition to the shape of radiation patterns. The numerical results of antenna characteristics for $\omega_p/\omega = 0.5$, $\varepsilon_d = 5.0$, $k_o a = 5.0$, $k_o b = 10.0$ and various values of ν/ω and $k_o c$ are presented below.

(a) Effect of Ring Source Radius :

The effect of ring source radius on the radiation from a plasma column has been studied by Gupta and Garg (1971) and Ram and Verma (1972). The ring source radius appears only in the numerat-or of the pattern function. It was noted by Gupta et al that for low plasma density case a null appears in the radiation pattern at an angle given by the first zero of $J_1(v_1 a)$ or $v_1 a = 3.8318$. We have also observed similar nulls near $\theta = 24^\circ$ for $\omega_p/\omega = 0.5$. They further noticed that a peak occurs near the maxima of $J_1(v_1 a)$ for the low plasma density case. A similar observation can be made in the patterns obtained for the present case for $\omega_p/\omega = 0.5$. For higher plasma densities, however, the radiation pattern is not governed by the ring source radius and it influences the peak amplitude only (Gupta et al 1971; Ram et al 1972).

(b) Effect of Plasma Column Radius :

It was predicted by Tamir et al (1962) for a plasma slab geometry that the direction of the major peak shifts only slightly with increasing plasma slab thickness. A number of minor peaks also appear for thick plasma slabs and their number increases with the slab thickness due to the excitation of higher order leaky waves. Similar observations have been made by Seshadri (1965) for the electric dipole in a cylindrical plasma column and by Gupta (1970) and Ram and Verma (1972) for magnetic ring sources in cylindrical plasma columns. Ram et al (1972) and Gupta (1970) also reported an enhancement of radiation peaks with plasma column thickness.

(c) Effect of Plasma Frequency :

It has been established by several authors (Tamir et al, 1962 ; Gupta, 1970; Ram et al, 1972 etc.) that the radiation peak appears near the critical optical angle and so the direction of major peak shifts as one changes the plasma frequency. The direction of the major peak shifts towards the broadside as the plasma frequency is increased for a fixed signal frequency, i.e. the permittivity is decreased. The opposite effect will be observed by increasing the signal frequency, while keeping the plasma frequency constant. The above authors also observed that for thick plasma columns some minor peaks also appear at angles

smaller than that for the major peak and their number is more for the smaller values of ω_p/ω than for the larger values of ω_p/ω.

(d) Effect of Collision Frequency :

A typical set of values of the collision frequency ν/ω = 0.0 (lossless case), 0.01, 0.1 and 1.0 has been chosen to estimate the influence of collisions on the antenna characteristics. The dielectric tube has been chosen to be made of glass with dielectric constant ε_d = 5.0 and normalised outer radius $k_o e$ = 11.5. The other parameters are $k_o a$ = 5.0, $k_o b$ = 10.0 and ω_p/ω = 0.5. The normalised radiation patterns for these values are shown in Fig.(2.2) for comparison. The numerical results for radiation resistance, directivity, the peak position, HPBW and peak amplitudes are given in the table (2.1). For small value of ν/ω = 0.01 there is a negligible change in the pattern shape. The peak amplitude, radiation resistance and directivity are, of course, slightly decreased. As ν/ω is increased upto 1.0, the major peak becomes broader and weaker. The minor lobe at the broadside rises relative to the major lobe, but its actual amplitude decreases with increasing ν/ω. The radiation resistance and directivity continuously fall with increasing ν/ω. This behaviour is in agreement with the results of Harris et al (1966). A deep null appears at 0=2k° for all values

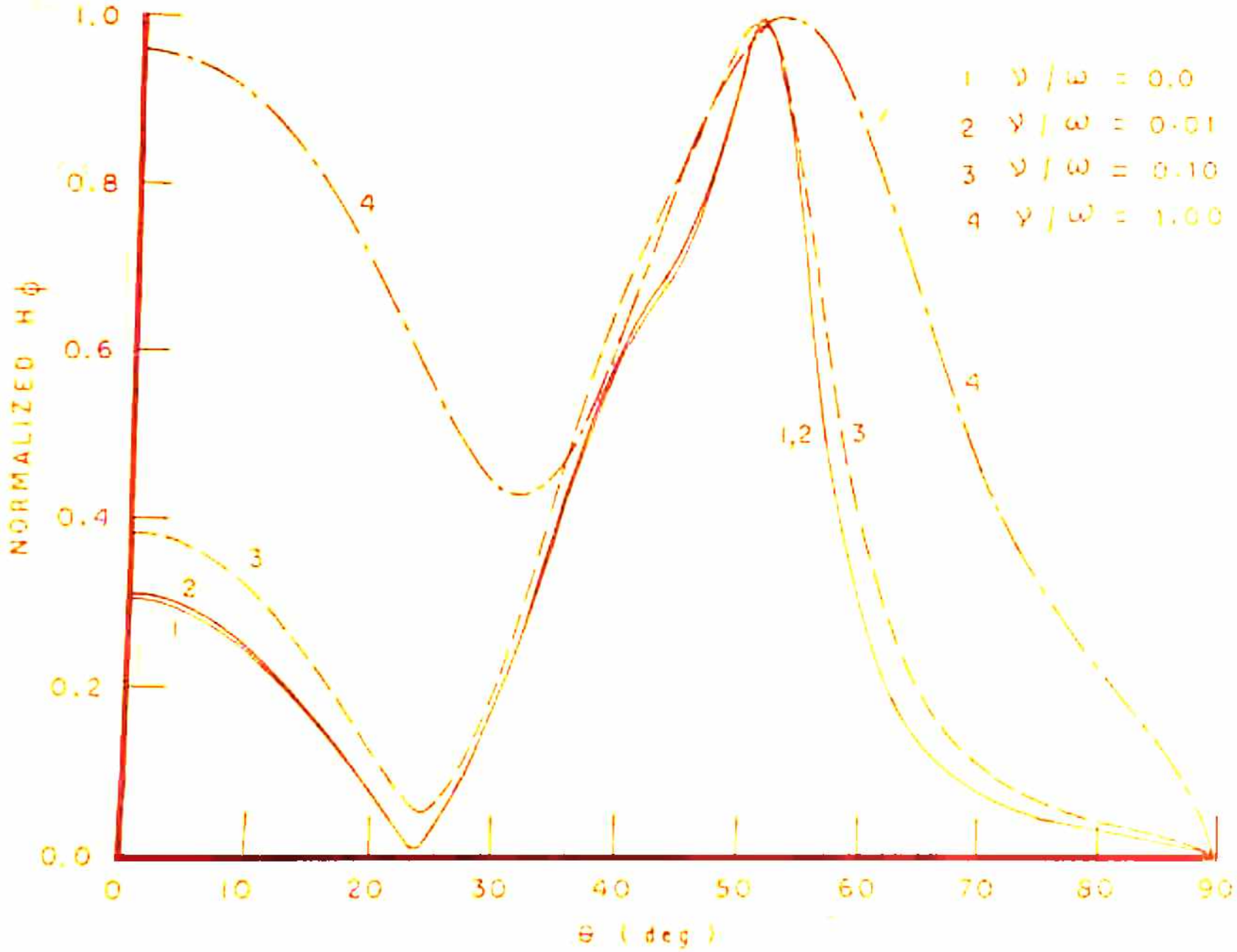

FIG. 2.2 EFFECT OF COLLISION FREQUENCY ON THE RADIATION PATTERN (MAGNETIC RING SOURCE)

$K_0 a = 5.0$, $K_0 b = 10.0$, $K_0 C = 11.5$, $\epsilon_d = 5.0$, $\omega_p / \omega = 0.5$

TABLE 2.1 EFFECT OF COLLISION FREQUENCY ON THE RADIATION CHARACTERISTICS OF HOMOGENEOUS PLASMA COLUMN EXCITED BY MAGNETIC RING SOURCE

ν/ω	Peak Position θ°	HPBW	Peak Amplitude (rel. units)	Radiation Resistance (rel. units)	Directivity (dB)
0.00 (Collisionless)	51.5	11.0	7.0354	8.4060	10.7101
0.01	51.5	11.0	6.7433	7.9483	10.5849
0.10	51.0	14.5	4.8333	5.0803	9.6350
1.00	54.0	21.5	1.9713	2.1843	5.5123

$k_o a = 5.0$, $k_o b = 10.0$, $k_o c = 11.5$, $\varepsilon_d = 5.0$ and $\omega_p/\omega = 0.5$

TABLE 2.2 EFFECT OF DIELECTRIC TUBE ON THE RADIATION CHARACTERISTICS OF HOMOGENEOUS PLASMA COLUMN EXCITED BY MAGNETIC RING SOURCE

$k_o c$	Peak Position θ°	HPBW	Peak Amplitude (rel. units)	Radiation Resistance (rel. units)	Directivity (dB)
10.0 (no dielectric tube)	51.0	14.5	4.8316	5.0907	9.6243
10.5	53.5 41.0	18.7	4.4490 4.3181	5.0050	8.9816
11.0	44.5	16.5	4.8791	5.3333	9.5071
11.5	51.0	14.5	4.8333	5.0803	9.6350
13.1415	52.0	17.0	4.7880	5.0706	9.5628
14.7123	52.5	17.5	4.7365	5.1738	9.3813

$k_o a = 5.0$, $k_o b = 10.0$, $\varepsilon_d = 5.0$, $\omega_p/\omega = 0.5$ and $\nu/\omega = 0.1$

of ν/ω. This value of θ corresponds to a value of $v_1 a \simeq 3.83$, the first zero of $J_1(X)$.

(e) Effect of Dielectric Tube Thickness :

To represent an actual laboratory situation, the dielectric tube is considered to be made of glass. The dielectric constant ϵ_d is taken to be 5.0, to represent the dielectric constant of the borosilicate glasses at microwave frequencies. The typical set of values of the glass tube thickness parameter, chosen for calculation is $k_o(c-b) = 0.0,\ 0.5,\ 1.0,\ 1.5,\ 3.1415$ and 4.7123. The last three values correspond to a thickness equal to $\lambda/4$, $\lambda/2$ and $3\lambda/4$. The normalized radiation patterns are shown in Figs. (2.3) and (2.4). The numerical results for peak amplitude, HPBW, radiation resistance and directivity are summarized in table (2.2). A very interesting feature of these results is that for the glass tube thickness $(c-b) \simeq \lambda/4$ the radiation pattern almost overlaps the one for the no glass tube case fig. (2.3). The pattern for the thickness equal to the other multiples of $\lambda/4$, i.e. $\lambda/2$ and $3\lambda/4$, differs only slightly near the peak from that of no glass tube case. The peak amplitude, radiation resistance and directivity are more or less of the same order for these cases. For other thicknesses, i.e., for $k_o(c-b) = 0.5$ and 1.0, the direction of the peak and the shape of the pattern near the peak significantly differ from those of the no glass tube case.

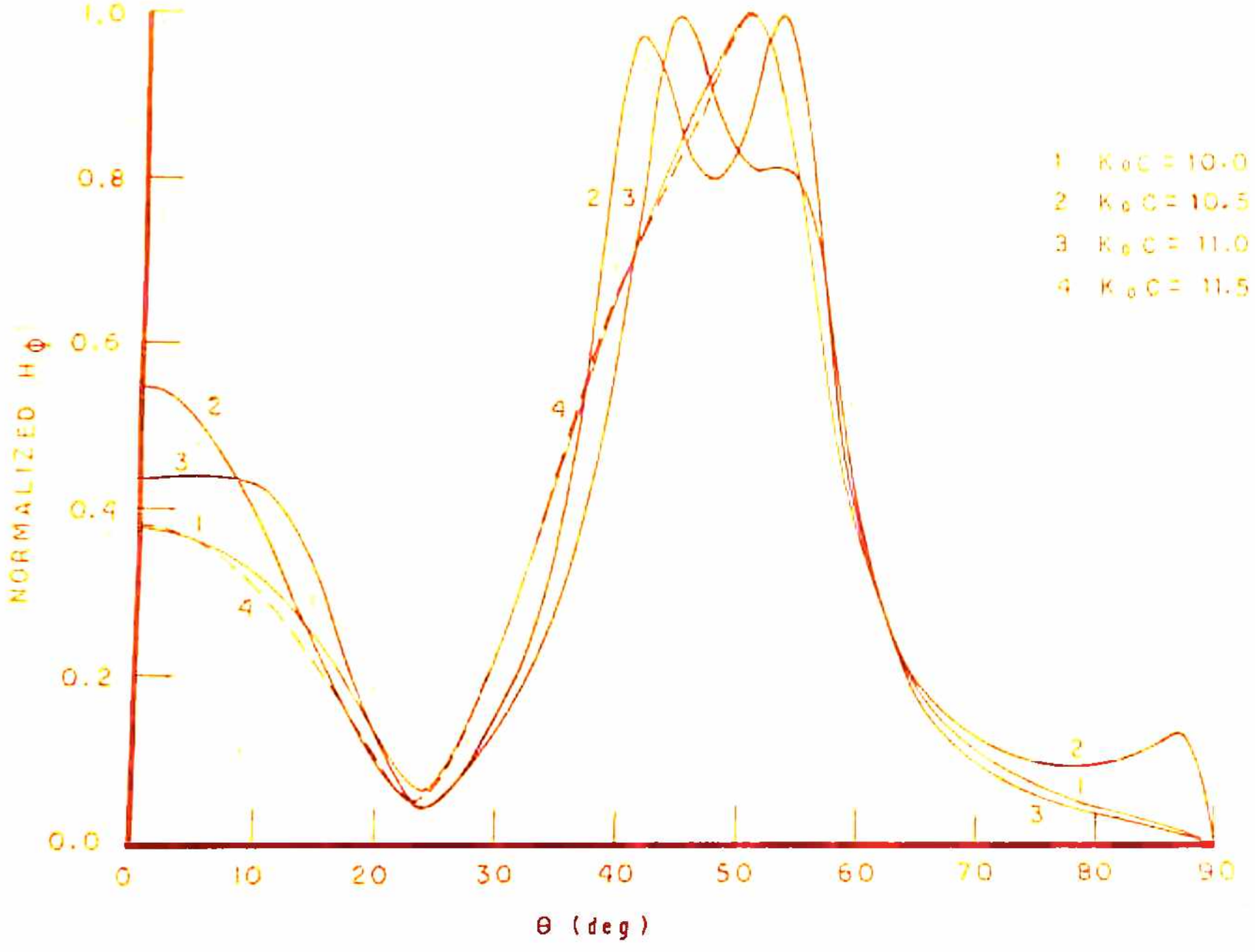

FIG. 2.3 EFFECT OF DIELECTRIC TUBE ON RADIATION PATTERN (MAGNETIC RING SOURCE)

$K_0a = 5.0$, $K_0b = 10.0$, $\epsilon_d = 5.0$, $\omega_p/\omega = 0.5$, $\nu/\omega = 0.1$

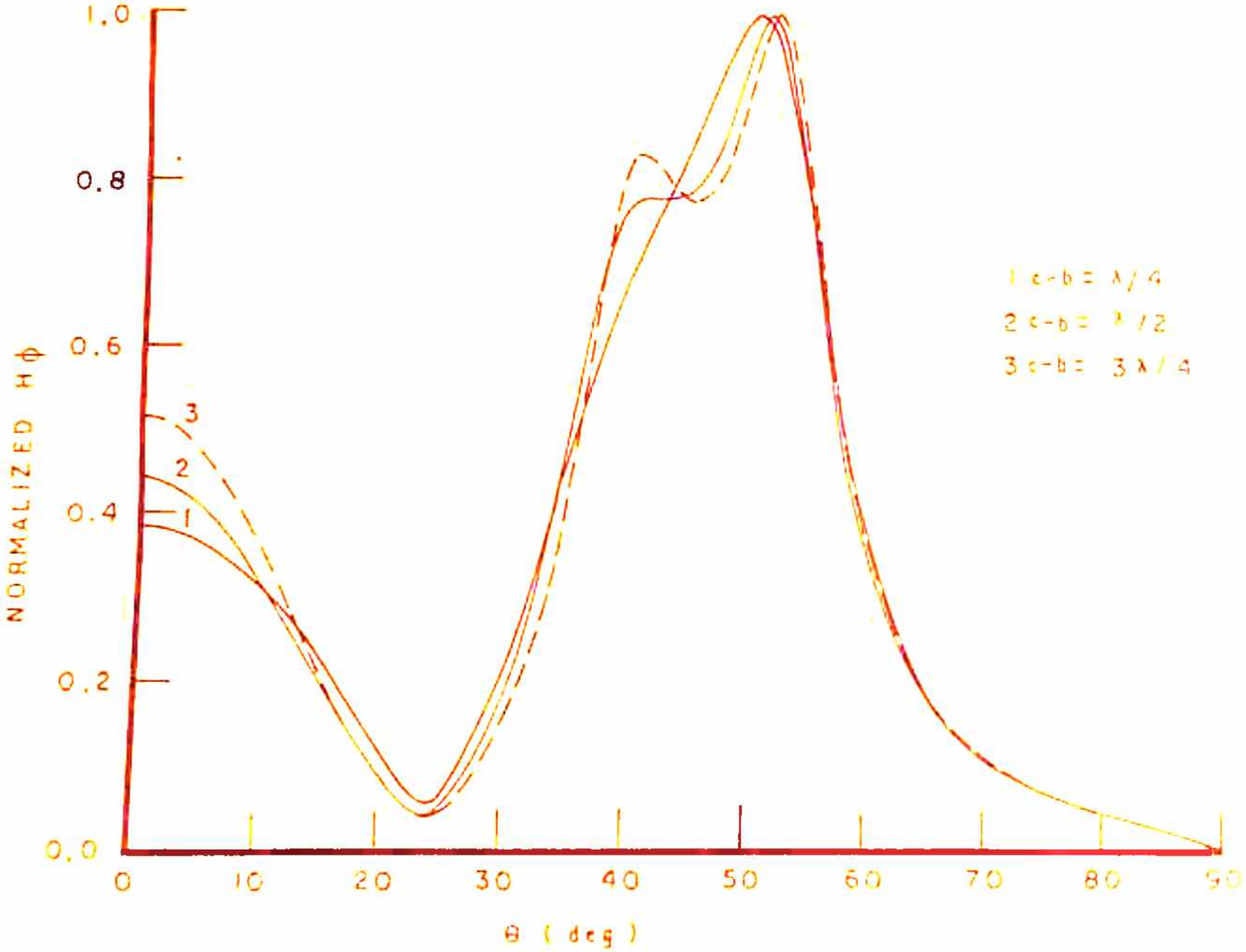

FIG. 2.4 EFFECT OF nλ/4-THICK DIELECTRIC TUBE ON RADIATION PATTERN (MAGNETIC RING SOURCE)

$K_0 a = 5.0$, $K_0 b = 10.0$ $\epsilon_d = 5.0$, $\omega_p / \omega = 0.5$ and $\nu / \omega = 0.1$

2.4 EXCITATION BY AN ELECTRIC RING SOURCE

In this section we analyze the problem of radiation from a cylindrical plasma column excited by an electric ring source. The plasma is assumed to be isotropic, homogeneous and lossy, and is contained in a dielectric tube. We assume that a uniform, harmonic electric current flows through the ring source which excites the lowest order circularly symmetric H-type mode. The H-type mode has the field components E_ρ, E_ϕ and H_z. The electric ring source is complementary to the magnetic ring source which has been considered in the previous section. The radiation fields for the electric ring source can be directly obtained from the field components of the magnetic ring source by using the Babinet's principle. But for the sake of completeness we would prefer to write down the important steps in the analysis of the electric ring source problem.

The radiation pattern is obtained by numerically evaluating the pattern function for various typical values of the relative collision frequency and glass tube thickness. The radiation resistance and directivity are then calculated by using the equations (2.32) and (2.35).

Similar problems of radiations from plasma columns excited by electric ring source have been analyzed by Samaddar (1966), Gupta and Garg (1971), Ram and Verma (1974) and others.

2.4.1 Formulation of the Problem

The geometry of the problem to be analysed is similar to the one discussed in the preceding section and shown in fig.(2.1). In the present case the ring source in fig.(2.1) is a ring of electric current expressed in terms of the Dirac delta functions as :

$$\bar{J} = \hat{\phi}\, I\, \delta(\rho - a)\, \delta(z) \qquad (2.36)$$

where I is the strength of the current source expressed in Amperes.

The Maxwell's equations for the electromagnetic fields in the presence of source are

$$\nabla \times \bar{E} = j\omega\mu_0 \bar{H} \qquad (2.37)$$

and

$$\nabla \times \bar{H} = -j\omega\varepsilon_0\varepsilon(\rho)\, \bar{E} + \bar{J} \qquad (2.38)$$

where $\varepsilon_{(\rho)}$ is the relative permittivity in different regions of space and defined by eqn. (2.5). In the above equations a harmonic time dependence of the form exp $(-j\omega t)$ is assumed for all the source and field quantities and suppressed throughout.

On eliminating $\bar{H}$ from the above equations we obtain a vector-wave equation. The ϕ-component of this equation is written in the cylindrical coordinate system as :

$$\frac{\partial^2 E_\phi}{\partial \rho^2} + \frac{1}{\rho}\frac{\partial E_\phi}{\partial \rho} + (k^2(\rho) - 1/\rho^2) E_\phi + \frac{\partial^2 E_\phi}{\partial z^2}$$

$$= -j\omega\mu_0 I\, \delta(\rho - a)\, \delta(z) \qquad (2.39)$$

where $k^2(\rho) = \omega^2 \mu_o \varepsilon_o \varepsilon(\rho)$

2.4.2 Solution of the Problem

To obtain the solution of equation (2.39), it is first reduced to an ordinary differential equation by taking its Fourier transform with respect to z. The resulting equation takes a form of the Bessel equation except at $\rho = a$. We now proceed to obtain the appropriate solutions for $\tilde{E}(\rho, \eta)$ the Fourier transform of $E_\phi(\rho, z)$, in the regions of space I - IV (fig.2.1). The solutions must satisfy the conditions that the fields should be finite at $\rho = 0$, should be regular at $\rho = \infty$ and satisfy the radiation condition. The solutions $\tilde{E}_I$ to $\tilde{E}_{IV}$ are the same as given by equations (2.12) and (2.13) except that H is replaced by $\tilde{E}$.

The unknown coefficients in the solutions are obtained by applying boundary conditions on the field components. The source at $\rho = a$ imposes the boundary condition :

$$\left.\frac{d\tilde{E}_{II}}{d\rho}\right|_{a+\Delta} - \left.\frac{d\tilde{E}_{I}}{d\rho}\right|_{a-\Delta} = -j\omega\mu_o I \qquad (2.40)$$

where $\Delta \to 0$.

To obtain the radiation fields the inverse Fourier transform of $\tilde{E}_{IV}$ is taken. The resulting integral is solved by contour integration using the Cauchy residue theorem and

the method of steepest descents. The resulting asymptotic solution for the radiation field E_ϕ in spherical polar coordinate system is given by

$$E_\phi = j \frac{I}{\pi} \sqrt{\mu_o/\epsilon_o} \; F(\theta) \frac{e^{j(k_o r - \pi/4)}}{r} \qquad (2.41)$$

where

$$F(\theta) = (x_r + jx_i)/(Y_r + jY_i) \qquad (2.42a)$$

$$x_r = 2(k_o a) J R_1(v_1 a) \qquad (2.42b)$$

$$x_i = 2(k_o a) J I_1(v_1 a) \qquad (2.42c)$$

and, Y_r and Y_i are the same as defined by eqn.(2.24) with

$$P_r = -(v_2 b) J_o(v_2 b) J R_1(v_1 b) + J_1(v_2 b)\, x_3 \qquad (2.43a)$$

$$P_i = -(v_2 b) J_o(v_2 b) J I_1(v_1 b) + J_1(v_2 b)\, x_4 \qquad (2.43b)$$

$$Q_r = (v_2 b) Y_o(v_2 b) J R_1(v_1 b) - Y_1(v_2 b)\, x_3 \qquad (2.44a)$$

$$Q_i = (v_2 b) Y_o(v_2 b) J I_1(v_1 b) - Y_1(v_2 b)\, x_4 \qquad (2.44b)$$

$$R_r = (v_2 c) Y_o(v_2 c) J_1(v_o c) - (v_o c) Y_1(v_2 c) J_o(v_o c) \qquad (2.45a)$$

$$R_i = (v_2 c) Y_o(v_2 c) Y_1(v_o c) - (v_o c) Y_1(v_2 c) Y_o(v_o c) \qquad (2.45b)$$

$$S_r = (v_2 c) J_o(v_2 c) J_1(v_o c) - (v_o c) J_1(v_2 c) J_o(v_o c) \qquad (2.46a)$$

$$S_i = (v_2 c) J_o(v_2 c) Y_1(v_o c) - (v_o c) J_1(v_2 c) Y_o(v_o c) \qquad (2.46b)$$

and x_3 and x_4 are given by eqn.(2.30) and v_1, v_2 and v_o are given by eqns.(2.13) and (2.20) with $\eta = k_o \sin\theta$.

2.4.3 Numerical evaluation of Antenna System Characteristics

Some of the major radiation characteristics of the antenna system: the radiation pattern, radiation resistance and directivity are numerically evaluated for various values of the dielectric tube thickness and the relative collision frequency. As mentioned in the previous section, the dielectric tube is chosen to be made of glass with $\epsilon_d = 5.0$. The influence of plasma frequency, plasma column thickness and ring source radius on the radiation pattern has already been discussed by Gupta et al (1971) and Ram et al (1972), for similar plasma geometries. Thus, we keep these parameters constant at $\omega_p/\omega = 0.5$, $k_o a = 5.0$ and $k_o b = 10.0$. The numerical results for typical values of the glass tube thickness and collision frequency are discussed below.

(a) Effect of Collision Frequency:

To study the influence of collision frequency on antenna system characteristics, a typical set of values of $\nu/\omega = 0.0$ (collisionless case), 0.01, 0.1 and 1.0 is chosen. These values correspond to cold laboratory plasmas and microwave signal frequencies. The glass tube outer radius is kept constant at $k_o c = 11.5$ which corresponds to approximately a quarter wavelength tube thickness. The normalised radiation patterns are illustrated in fig.(2.5)

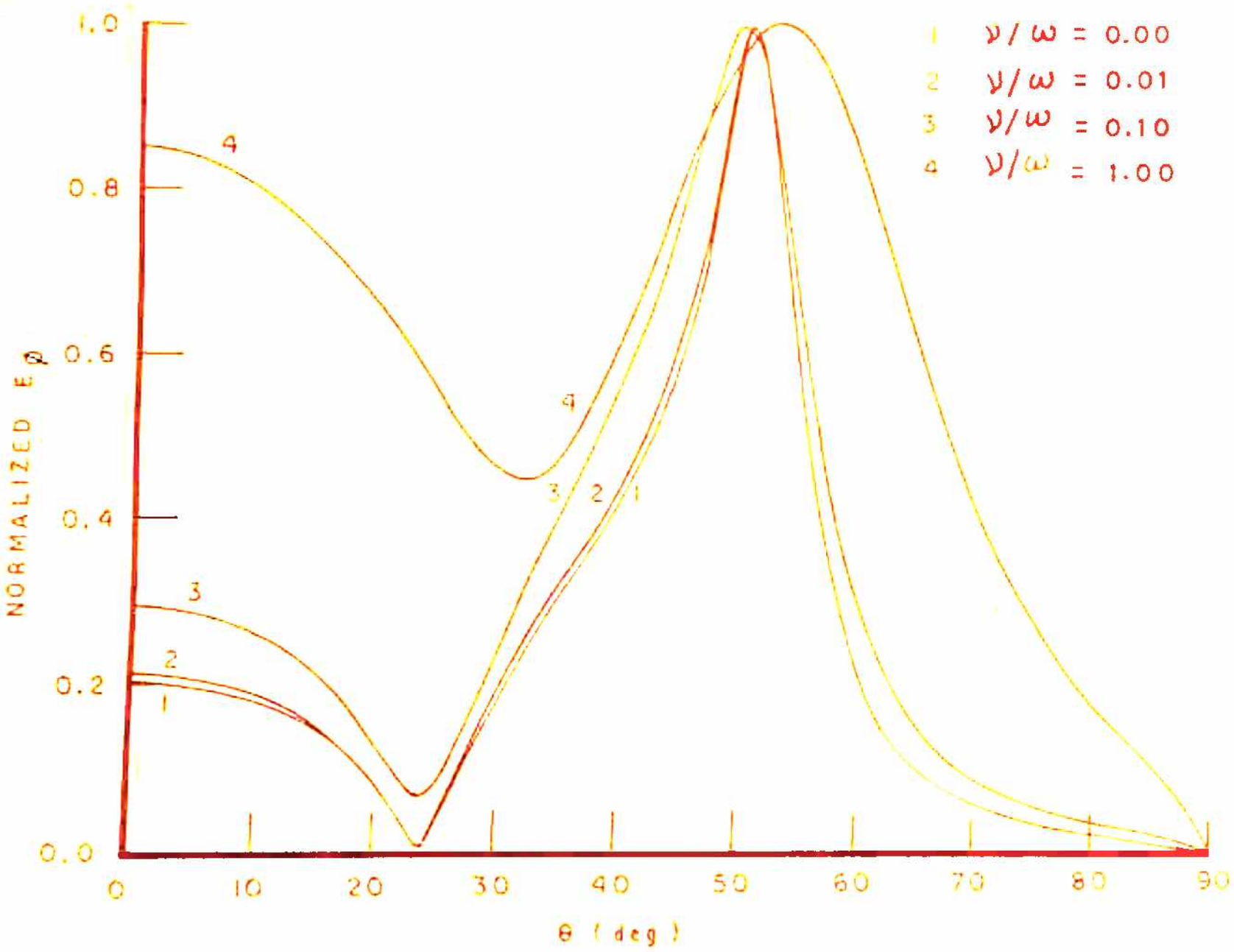

FIG. 2.5 EFFECT OF COLLISION FREQUENCY ON RADIATION PATTERN (ELECTRIC RING SOURCE)
$K_0 a = 5.0$, $K_0 b = 10.0$, $K_0 C = 11.5$, $\epsilon_d = 5.0$ and $\omega_p/\omega = 0.5$

TABLE 2.3 EFFECT OF COLLISION FREQUENCY ON THE RADIATION CHARACTERISTICS OF HOMOGENEOUS PLASMA COLUMN EXCITED BY ELECTRIC RING SOURCE

ν/ω	Peak Position θ°	HPBW	Peak Amplitude (rel. units)	Radiation Resistance (rel. units)	Directivity (dB)
0.00 (Collisionless)	51.0	7.0	9.2710	10.6960	12.0606
0.01	51.0	7.5	8.7953	10.0577	11.8715
0.10	50.5	10.5	5.9298	6.2712	10.4976
1.00	53.5	21.0	2.1138	2.2538	5.9823

$k_o a = 5.0$, $k_o b = 10.0$, $k_o c = 11.5$, $\epsilon_d = 5.0$ and $\omega_p/\omega = 0.5$

TABLE 2.4 EFFECT OF DIELECTRIC TUBE ON THE RADIATION CHARACTERISTICS OF HOMOGENEOUS PLASMA COLUMN EXCITED BY ELECTRIC RING SOURCE

$k_o c$	Peak Position θ°	HPBW	Peak Amplitude (rel. units)	Radiation Resistance (rel. units)	Directivity (dB)
10.0 (no dielectric tube)	50.5	10.5	5.9194	6.4155	10.3836
10.5	50.5	3.5	5.0862	2.3124	13.4975
11.0	51.5	3.5	4.6133	2.3695	12.5440
11.5	50.5	10.5	5.9298	6.2712	10.4976

$k_o a = 5.0$, $k_o b = 10.0$, $\epsilon_d = 5.0$, $\omega_p/\omega = 0.5$ and $\nu/\omega = 0.1$

and the numerical results for other characteristics are presented in table(2.3). Just a glance at fig.(2.5) reveals that the radiation pattern for low collision frequency ($\nu/\omega = 0.01$) almost overlaps the pattern for the lossless case ($\nu/\omega = 0$). The radiation peak becomes broader for the higher values of ν/ω. Moreover, the level of broadside radiation rises relative to the major peak and the direction of the major peak changes slightly with increasing collision frequency. A study of table (2.3) indicates that the peak amplitude, radiation resistance and the directivity, all decrease with the increasing collision frequency. This behaviour is in agreement with the theoretical predictions. The above results are found to be in agreement with the results of Samaddar (1966). We may conclude that a relative collision frequency of the order of 10^{-2} or less does not cause a very large loss of power and may be tolerated.

(b) Effect of Glass Tube Thickness:

As the diameter of the plasma column is increased a thicker and stronger container is required, and so typical values of the glass tube thickness equal to 5%, 10%and 15 %of the plasma column radius are chosen. The results are also obtained for the no glass tube case. The collision frequency is fixed at $\nu/\omega = 0.1$. The normalised radiation patterns are shown in fig.(2.6) and the numerical

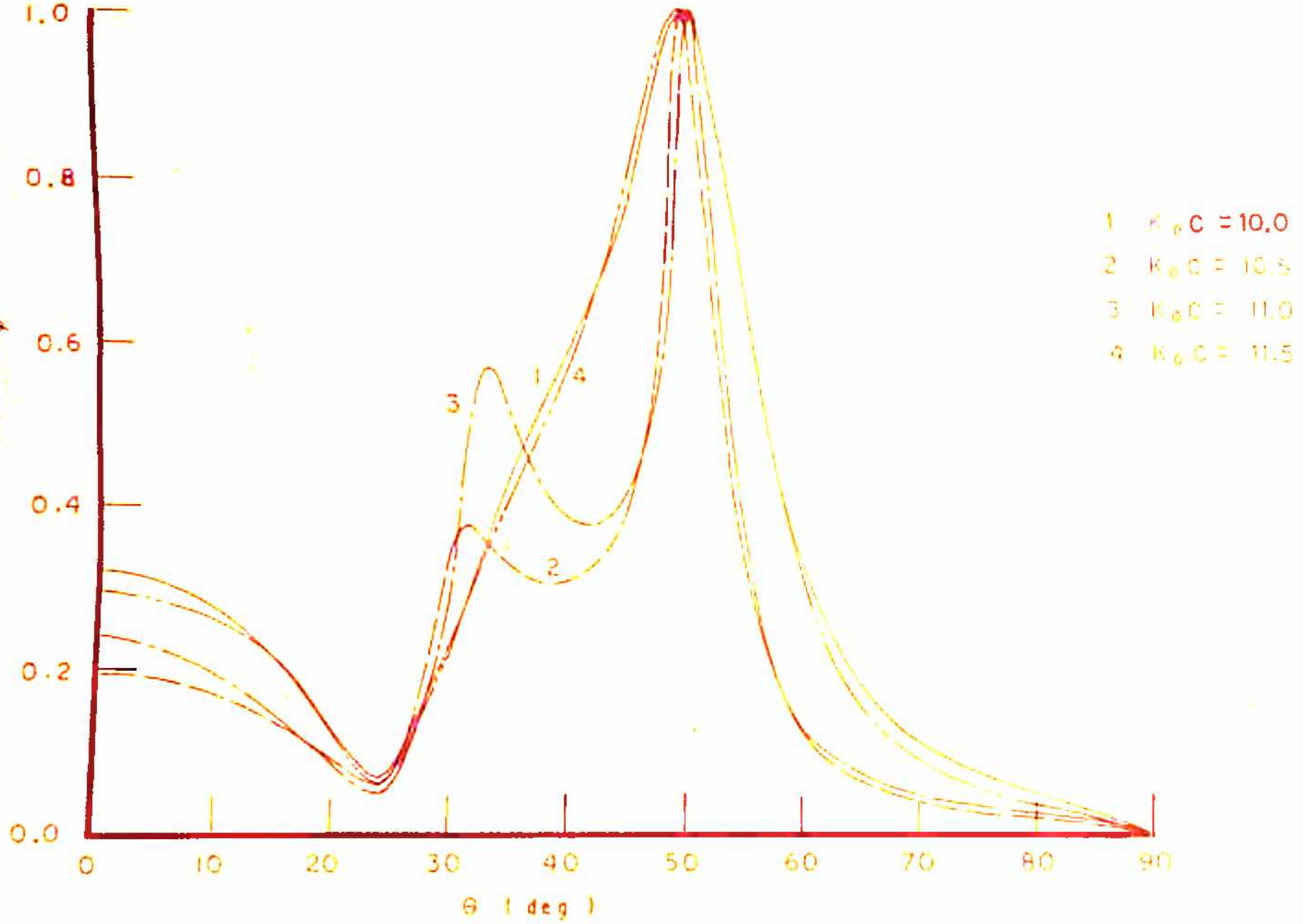

FIG. 2.6 EFFECT OF DIELECTRIC TUBE ON RADIATION PATTERN (ELECTRIC RING SOURCE)

$K_0 a = 5.0$, $K_0 b = 10.0$, $\epsilon_d = 5.0$, $\omega_p / \omega = 0.5$, $\nu / \omega = 0.1$

results for other characteristics are given in table (2.4). It is clear from the fig. (2.6) that the direction of the major peak does not change significantly with the increasing glass tube thickness, which is in agreement with the geometrical optics; the major peak becomes narrow and new sidelobes appear in the radiation pattern. Similar to the case of magnetic ring source, in this case also we find that the radiation pattern for $k_o(c-b) = 1.5$, i.e. $(c-b) = \lambda/4$, overlaps the pattern for the no glass tube case. Furthermore, the peak amplitude, radiation resistance and the directivity are more or less of the same order for both the no glass tube and $\lambda/4$-thick glass tube cases. It was shown in the preceding section that the radiation characteristics for the glass tube thickness equal to integral multiples of $\lambda/4$ also does not differ significantly from those for the no glass tube case. The same results are expected for the present case, being a complementary of the preceding case. Thus a quarter wavelength thick glass tube will not distort the pattern of the plasma-antenna system.

2.5 EXCITATION BY OPEN-ENDED CIRCULAR WAVEGUIDE

2.5.1 Introduction

In the present section we explore the radiation characteristics of a plasma-antenna system consisting of a lossy plasma column surrounded by a dielectric tube and

excited by an open-ended circular waveguide. The plasma is assumed to be homogeneous, isotropic, collisional and incompressible.

The open-ended waveguide and slot radiators have been widely used on space-vehicles since they can be easily flush-mounted on the space-vehicle body. Consequently, there has been a great deal of interest in radiation properties of open waveguides radiating into plasma medium. The admittance of the open waveguide radiating through plasma layers has been studied by Villeneuve (1965), Crosswell et al (1967), Galejs and Mentzoni (1967) and more recently by El-Khamy et al (1970). Theoretical and experimental studies of radiation from open waveguides covered with plasma layers have been made by Cloutier and Bachynski (1963), Jacavanco (1964), Kusab (1969) and others. More recently, Gupta and Garg (1971) and Ram and Verma (1974) have investigated the radiation patterns of plasma cylinders excited by open-ended circular waveguides. They studied the effect of plasma density, plasma column thickness and waveguide radius on the radiation pattern. In the following paragraphs, we proceed to study the influence of plasma collision frequency and dielectric tube thickness on the radiation pattern, radiation resistance and directivity.

The circularly symmetric modes of the circular waveguide, the TM_{01} - and TE_{01}- modes are considered. The fields at the excitation aperture are assumed to be the same as they would be if the waveguide did not terminate there. We further assume that the currents on the outer wall of the open-ended waveguide have a negligible effect on the radiation. Now the field distribution at the open aperture is replaced by an equivalent surface current density. This surface current can be divided into a large number of filamentary current rings with different radii ranging from zero to the inner radius of the waveguide. The radiation fields due to such filamentary current rings in a plasma column have already been obtained in the preceding sections. The radiation field due to the surface current distribution at the aperture can now be obtained by taking a vector sum of the radiation fields due to all the filamentary current rings having their radii between zero and the waveguide radius.

2.5.2 Formulation of the Problem:

The geometry of the problem to be analyzed is shown in fig.(2.7). It consists of an infinitely long plasma column of radius b contained in a dielectric tube having inner radius b, outer radius c. The relative permittivity of the plasma, ϵ_p, is given by eqn.(2.1) and that of the dielectric is denoted by ϵ_d. The source of

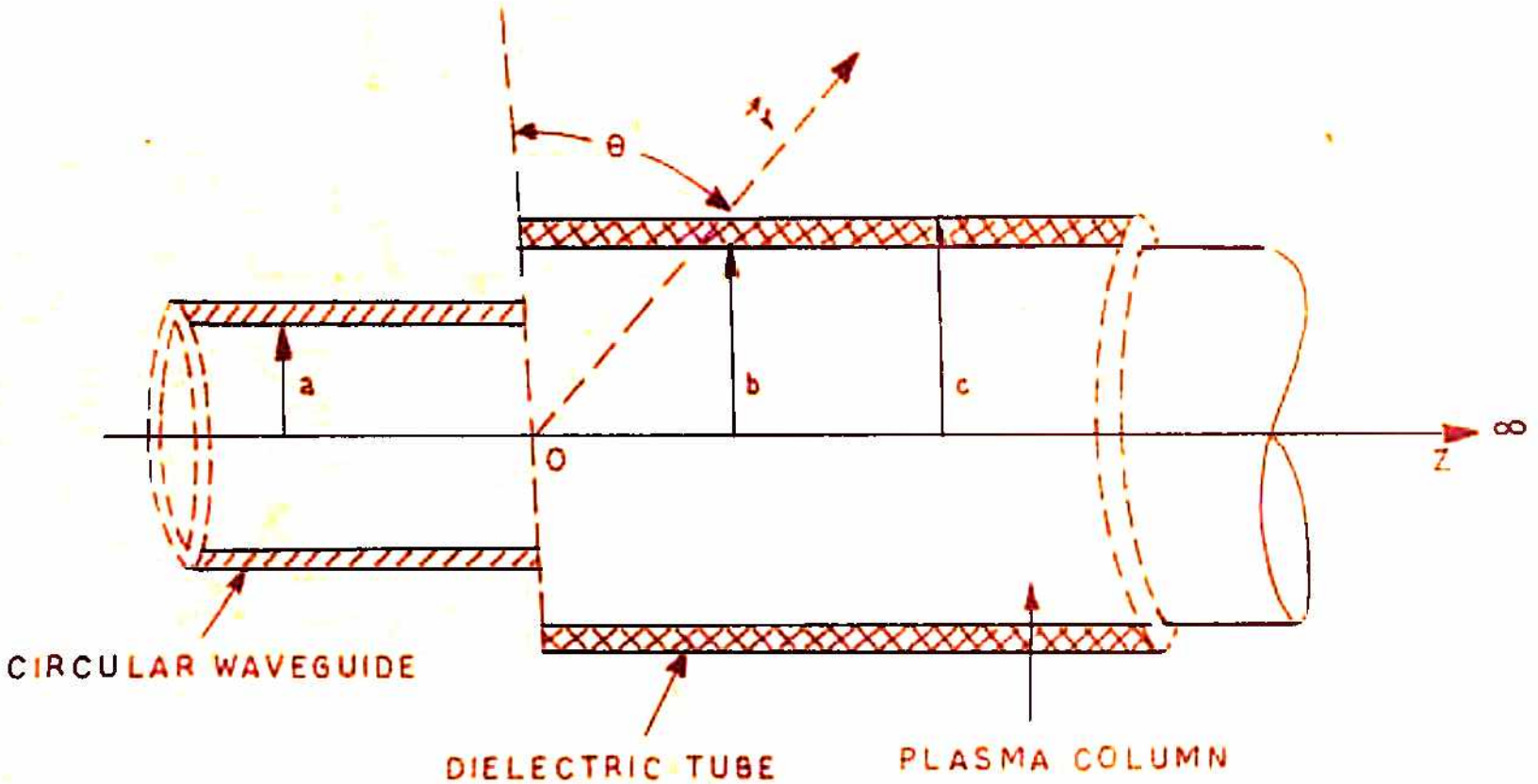

FIG. 2.7 THE INFINITELY LONG PLASMA COLUMN SURROUNDED BY DIELECTRIC TUBE AND EXCITED BY CIRCULAR WAVEGUIDE.

excitation is an open-ended circular waveguide having inner radius a and placed at z = 0. The circularly symmetric modes of excitation, the TM_{01} and TE_{01} modes are considered. The solution of the problem for the two modes are obtained below.

2.5.3 Solution of the Problem for TM_{01}-Mode

For the TM_{01}-mode the strength of a filamentary current ring of radius $\rho \propto J_1(h\rho)$, the field at its location. Thus by dropping the constant of proportionality we can write the current distribution for an elementary magnetic current ring of radius ρ as :

$$\bar{M} = \hat{\rho}\, J_1(h\rho)\, \delta(\varphi)\, \delta(z) \qquad (2.47)$$

where h is given by the first root of the Bessel function $J_0(ha)$.

The radiation field for the magnetic ring source of radius ρ, as obtained in section (2.3) can be written as

$$H_\phi = j\sqrt{\varepsilon_0/\mu_0}\; k_0/\pi\; f(\theta)\, \frac{e^{j(k_0 r - \pi/4)}}{\gamma} \qquad (2.48a)$$

where $f(\theta) = f_1(\theta).f_2(\theta)$ (2.48b)

$f_1(\theta) = 2\varepsilon_p \varepsilon_\phi/(P.R + Q.S)$ (2.48c)

and $f_2(\theta) = M\rho\, J_1(\gamma_1\rho)$ (2.48d)

$= \rho\, J_1(h\rho) J_1(\gamma_1\rho)$

Now to obtain the pattern function for the waveguide excitation we integrate $f(\theta)$ over ρ from 0 to a.

Then,

$$F(\theta) = f_1(\theta) \int_0^a \rho\, J_1(h\rho) J_1(v_1\rho)\, d\rho \qquad (2.49)$$

Now using the following Lommel integrals

$$(\alpha^2-\beta^2) \int_0^x x\, J_n(\alpha x) J_n(\beta x)\, dx = x\left\{\beta\, J_n(\alpha x) J_n'(\beta x) - \alpha J_n'(\alpha x) J_n(\beta x)\right\}$$

$$(\text{for } \alpha \neq \beta) \qquad (2.50a)$$

$$\text{and} \quad \int_0^x x J_n^2(\alpha x)\, dx = \frac{1}{2} x^2 \left[1 - \frac{n^2}{\alpha^2 x^2} J_n^2(\alpha x) + J_n'^2(\alpha x)\right] \qquad (2.50b)$$

we get the pattern function for $v_1 \neq h$

$$F(\theta) = \frac{(v_1 a)\, J_0(v_1 a)\, J_1(ha)}{h^2 - v_1^2} \cdot f_1(\theta) \qquad (2.51a)$$

and for $v_1 = h$

$$F(\theta) = \frac{a^2 J_1^2(ha)}{2} f_1(\theta) \qquad (2.51b)$$

Now for a collisional plasma ϵ_p is a complex quantity and hence v_1 is also a complex quantity. As mentioned in section (2.3.3) the Bessel functions involving complex quantity v_1 in their arguments are evaluated by a subroutine programme, which gives the real and imaginary parts of the value of Bessel function separately. Moreover, to facilitate the numerical evaluation of the pattern function on a computer which cannot handle complex numbers, the real and imaginary parts of the pattern function are separated and it is written as

$$F(\theta) = (X_r + jX_i)/(Z_r + jZ_i) \qquad (2.52)$$

where, for $h \neq v_1$

$$X_r = 2\mathcal{E}_d(k_o a)J_1(ha)\left\{(\varepsilon_{pr}u_{1r}-\varepsilon_{pi}u_{1i})JR_o(v_1 a)-(\varepsilon_{pr}u_{1i}+\varepsilon_{pi}u_{1r})JI_o(v_1 a)\right\} \quad (2.53a)$$

$$X_i = 2\mathcal{E}_d(k_o a)J_1(ha)\left\{(\varepsilon_{pr}u_{1i}+\varepsilon_{pi}u_{1r})JR_o(v_1 a)+(\varepsilon_{pr}u_{1r}-\varepsilon_{pi}u_{1i})JI_o(v_1 a)\right\} \quad (2.53b)$$

$$Z_r = Y_r\left\{h^2-k_o^2(\varepsilon_{pr}-\sin^2\theta)\right\}+k_o^2\varepsilon_{pi}Y_i \quad (2.54a)$$

$$Z_i = Y_i\left\{h^2-k_o^2(\varepsilon_{pr}-\sin^2\theta)\right\}-k_o^2\varepsilon_{pi}Y_r \quad (2.54b)$$

$$u_{1r} = v_{1r}/k_o \quad \text{and} \quad u_{1i} = v_{1i}/k_o \quad (2.55)$$

and for $h = v_1$

$$X_r = a^2\mathcal{E}_d\varepsilon_{pr}J_1(ha) \quad (2.56a)$$

$$X_i = a^2\mathcal{E}_d\varepsilon_{pi}J_1(ha) \quad (2.56b)$$

$$Z_r = Y_r \quad (2.57a)$$

$$Z_i = Y_i \quad (2.57b)$$

and Y_r and Y_i are the same as for the magnetic ring source given by eqns. (2.24) to (2.30).

Now since the radiation field is symmetric about $\theta = 0^\circ$, it is sufficient to calculate the pattern function $|F(\theta)|$ from $\theta = 0^\circ$ to 90° only, using eqns.(2.52) to (2.57). The radiation resistance can be obtained by evaluating the integral in eqn.(2.31). The directivity is calculated by using the eqn.(2.35). The numerical results for some typical values of dielectric tube thickness and collision

frequency are discussed below.

2.5.4 Numerical Evaluation of Antenna System Characteristics for TM_{01}- Mode

The pattern function (eqn 2.52) depends upon the waveguide radius a which appears only in its numerator, plasma column radius b and dielectric tube radius c, both of which appear in the denominator only. Moreover, it also depends upon the relative permittivity of the dielectric ε_d and the relative permittivity of plasma ε_p. Similar problems have been analyzed by Gupta et al (1971) and Ram et al (1974) for the case of a lossless plasma without any dielectric tube. Ram et al included an additional central conductor in the geometry. These authors have reported the influence of plasma density, plasma column thickness and waveguide radius on the radiation patterns. Here we will study the influence of collision frequency and dielectric tube thickness on the radiation pattern, radiation resistance and directivity. A typical set of values of the parameters $\omega_p/\omega = 0.5$, $\varepsilon_d = 5.0$ and $k_o a = k_o b = 2.405$ is chosen for computations.

(i) Effect of Collision Frequency

To estimate the influence of plasma collision frequency on the antenna characteristics we choose a typical set of values of the relative collision frequency $\nu/\omega = 0.0$ (collisionless), 0.01, 0.1 and 1.0. The outer

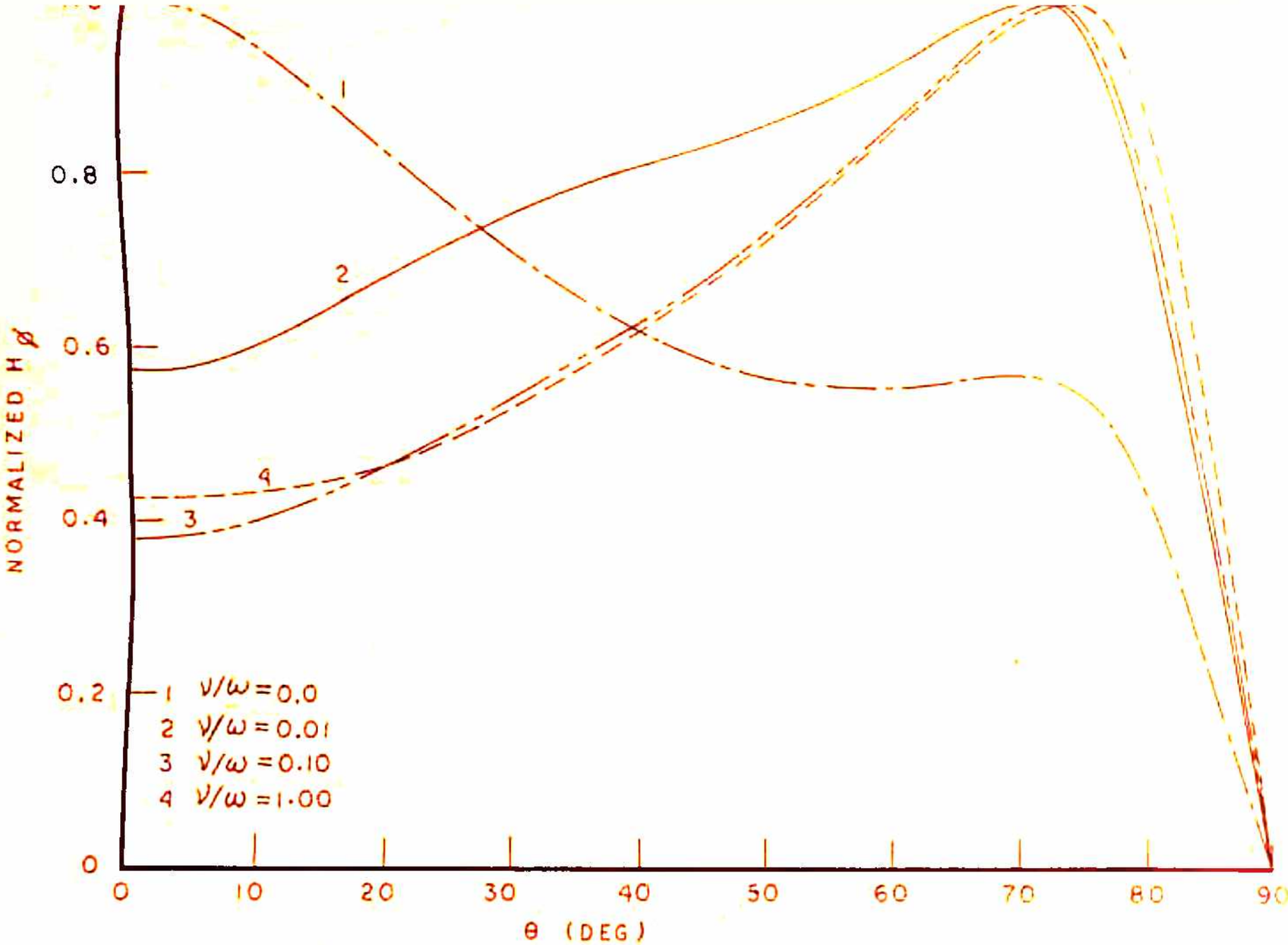

. 2.8 EFFECT OF COLLISION FREQUENCY ON THE RADIATION PATTERN (WAVEGUIDE TM_{01}-MODE)
$K_0 a = K_0 b = 2.405$, $K_0 C = 2.765$, $\varepsilon_d = 5.0$ and $\omega_p/\omega = 0.5$

radius of the dielectric tube is fixed by $k_0 c = 2.765$. The normalized radiation patterns are shown in fig. (2.8) and the other antenna characteristics are summarized in table (2.5). We notice that the inclusion of collision frequency drastically influences the antenna characteristics. The radiation at the broadside direction is suppressed and the radiation at the end-fire direction is enhanced by the inclusion of losses. A similar effect has been observed by Harris et al (1965) for a magnetic dipole on a plasma enclosed conducting cylinder. The HPBW decreases with increasing collision frequency. This result is also in agreement with the results of Hodara et al (1962). The directivity first increases with ν/ω but then slightly decreases as ν tends to ∞. The radiation resistance or the total radiated power is drastically reduced due to the collision frequency. Thus the antenna system becomes more directive at the expense of total radiated power.

(ii)Effect of Dielectric Tube

In order to estimate the influence of the dielectric tube which contains the plasma we choose the dielectric to be glass to correspond to an actual laboratory situation. The dielectric constant of the glass is taken to be $\varepsilon_d = 5.0$, which represents the value for the borosilicate glasses at microwave frequencies. The numerical results are obtained for the normalized glass tube thickness

Contd

TABLE 2.5 EFFECT OF COLLISION FREQUENCY ON THE RADIATION CHARACTERISTICS OF HOMOGENEOUS PLASMA COLUMN EXCITED BY CIRCULAR WAVEGUIDE (TM_{01}-MODE)

ν/ω	Peak Position θ°	HPBW	Peak Amplitude (rel. units)	Radiation Resistance (rel. units)	Directivity (dB)
0.00 (Collision-less)	0.0	62.0	15.4313	136.6430	5.4320
0.01	71.5	58.0	6.7321	25.8783	5.4560
0.10	73.0	33.5	1.0191	0.3909	8.2605
1.00	74.5	34.5	0.2044	0.0158	7.2580

$k_o a = k_o b = 2.405$, $k_o c = 2.765$, $\varepsilon_d = 5.0$ and $\omega_p/\omega = 0.5$

TABLE 2.6 EFFECT OF DIELECTRIC TUBE ON THE RADIATION CHARACTERISTICS OF HOMOGENEOUS PLASMA COLUMN EXCITED BY CIRCULAR WAVEGUIDE (TM_{01}-MODE)

$k_o c$	Peak Position θ°	HPBW	Peak Amplitude (rel. units)	Radiation Resistance (rel. units)	Directivity (dB)
2.405 (no dielectric tube)	49.5	49.0	0.9635	0.5494	5.2744
2.525	58.0	48.0	0.9297	0.4692	5.3830
2.645	66.0	43.5	0.9370	0.4157	6.2445
2.765	73.0	33.5	1.0191	0.3909	8.2605
3.906	51.5	46.5	0.9518	0.4989	5.6010

$k_o a = k_o b = 2.405$, $\varepsilon_d = 5.0$, $\omega_p/\omega = 0.5$ and $\nu/\omega = 0.1$

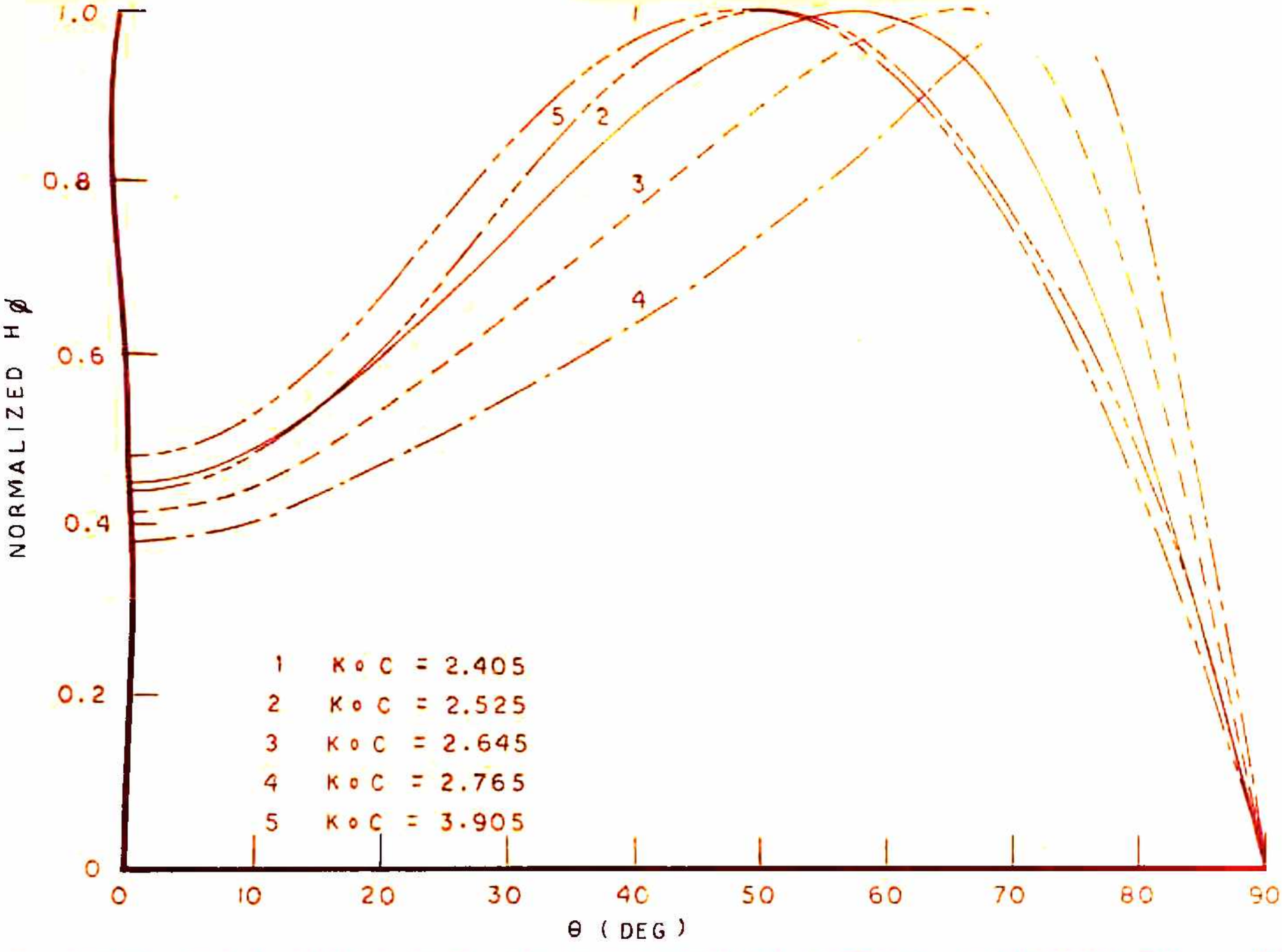

FIG. 2.9 EFFECT OF DIELECTRIC TUBE ON THE RADIATION PATTERN (WAVEGUIDE TM_{01} — MODE)

$K_0 a = K_0 b = 2.405$, $\epsilon_d = 5.0$, $\omega_p / \omega = 0.5$ and $\nu/\omega = 0.1$

$k_o(c-b)$ = 0.0, 0.12, 0.24, 0.36 and 1.6 which correspond to no glass tube 5%, 10%, 15% of the plasma column thickness, and approximately a quarter wavelength thickness respectively. The normalized radiation patterns are shown in fig.(2.9) and the numerical results for other characteristics are given in table (2.6). It is found that as the glass tube thickness is increased, the radiation peak first shifts towards the end-fire direction and then retreats for a thickness approximately equal to $\lambda/4$ to lie very close to the no glass tube case. Similarly all the other parameters, the HPBW, peak amplitude, radiation resistance and directivity also show an oscillatory behaviour. As for the magnetic ring source, in this case also the radiation pattern nearly retraces itself for the quarter wavelength increments in glass tube thickness.

2.5.5 Solution of the Problem for TE_{01}-Mode

For the TE_{01} mode also the strength of the elementary current ring source of radius ρ will be proportional to $J_1(h\rho)$, but, with h given by $J_o'(h\rho) = -J_1(h\rho) = 0$, thus by dropping the constant of proportionality we can write the elementary electric current distribution as :

$$\bar{J} = \hat{\phi}\, J_1(h\rho)\, \delta(\rho)\, \delta(s) \qquad (2.58)$$

The radiation field due to the TE_{01}-waveguide are now obtained by integrating the pattern function for the

electric ring source which has been obtained in section (2.4), over ρ from 0 to a. The source strength I is substituted by $J_1(h\rho)$. Then using the Lommel integrals (eqns 2.50) we can obtain the pattern function for the waveguide excitation. The pattern function for TE_{01} mode may also be obtained directly from the pattern function for the TM_{01} mode by applying the Babinet's principle. After separating the real and imaginary parts of the pattern function, we get

$$F(\theta) = (X_r + j X_i)/(Z_r + jZ_i) \qquad (2.59)$$

where, for $v_1 \neq h$

$$X_r = 2(k_o a) J_1(ha)(u_{1r} JR_o(v_1 a) - u_{1i} JI_o(v_1 a)) \qquad (2.60a)$$

$$X_i = 2(k_o a) J_1(ha)(u_{1r} JI_o(v_1 a) - u_{1i} JR_o(v_1 a)) \qquad (2.60b)$$

and for $v_1 = h$

$$X_r = a^2 J_1(ha) \qquad (2.61a)$$

$$X_i = 0 \qquad (2.61b)$$

and Z_r and Z_i are given by the eqns.(2.54) for $v_1 \neq h$ and eqns(2.57) for $v_1 = h$. But in this case Y_r and Y_i used in eqns.(2.54) and (2.57) are given by (eqns.(2.24) and eqns.(2.43) to (2.46).

2.5.6 Numerical Evaluation of Antenna System Characteristics for TE_{01}-Mode

As mentioned in the case of TM_{01}-mode the influence of plasma density, plasma column thickness and waveguide

radius has already been studied (Gupta et al, 1971, Ram et al, 1974) for somewhat similar geometries. Here we present the results for typical sets of values of ν/ω and $k_o c$ for the fixed values of $\omega_p/\omega = 0.5$, $\epsilon_d = 5.0$ and $k_o a = k_o b = 3.83$.

i) Effect of collision frequency

To estimate the influence of losses on the radiation pattern etc. we kept the dielectric tube thickness constant at $k_o c = 4.021$ and evaluated the antenna characteristics for $\nu/\omega = 0.0$ (collisionless), 0.01, 0.10 and 1.0. The results are illustrated in fig.(2.10) and table (2.7). We find that contrary to the TM_{01}-mode the major peak appears at the broadside for all values of ν/ω. The small value of $\nu/\omega = 0.01$ has a negligible effect on the characteristics. The radiation pattern for this value of ν/ω overlaps the pattern for the collisionless case. For higher values of ν/ω the radiation at the end-fire is suppressed. The HPBW undergoes a very small change with increasing collision frequency.

ii) Effect of Dielectric tube

As mentioned earlier, the dielectric tube is assumed to be a glass tube having dielectric constant $\epsilon_d = 5.0$. The collision frequency is fixed at $\nu/\omega = 0.1$ and the glasstube thickness is taken to be 0 , 5%, 10% and 15%

TABLE 2.7 EFFECT OF COLLISION FREQUENCY ON THE RADIATION CHARACTERISTICS OF HOMOGENEOUS PLASMA COLUMN EXCITED BY CIRCULAR WAVEGUIDE (TE_{01}-MODE)

ν/ω	Peak Position θ^o	HPBW	Peak Amplitude (rel. units)	Radiation Resistance (rel. units)	Directivity (dB)
0.00 (collisionless)	0.0	25.5	0.2674	0.1812	8.972
0.01	0.0	25.5	0.2655	0.1786	8.973
0.10	0.0	26.0	0.2551	0.1662	8.939
1.00	0.0	23.0	0.5668	0.7319	9.436

$k_o a = k_o b = 3.83$, $k_o c = 4.021$, $\epsilon_d = 5.0$ and $\omega_p/\omega = 0.5$

TABLE 2.8 EFFECT OF DIELECTRIC TUBE ON THE RADIATION CHARACTERISTICS OF HOMOGENEOUS PLASMA COLUMN EXCITED BY CIRCULAR WAVEGUIDE (TE_{01}-MODE)

$k_o c$	Peak Position θ^o	HPBW	Peak Amplitude (rel. units)	Radiation Resistance (Rel. units)	Directivity (dB)
3.83 (no dielectric tube)	0.0	26.5	0.3190	0.2616	9.907
4.021	0.0	25.5	0.2551	0.1662	8.939
4.213	0.0	24.0	0.2306	0.1209	9.442
4.404	0.0	23.0	0.2372	0.1211	9.681

$k_o a = k_o b = 3.83$, $\epsilon_d = 5.0$, $\omega_p/\omega = 0.5$ and $\nu/\omega = 0.1$

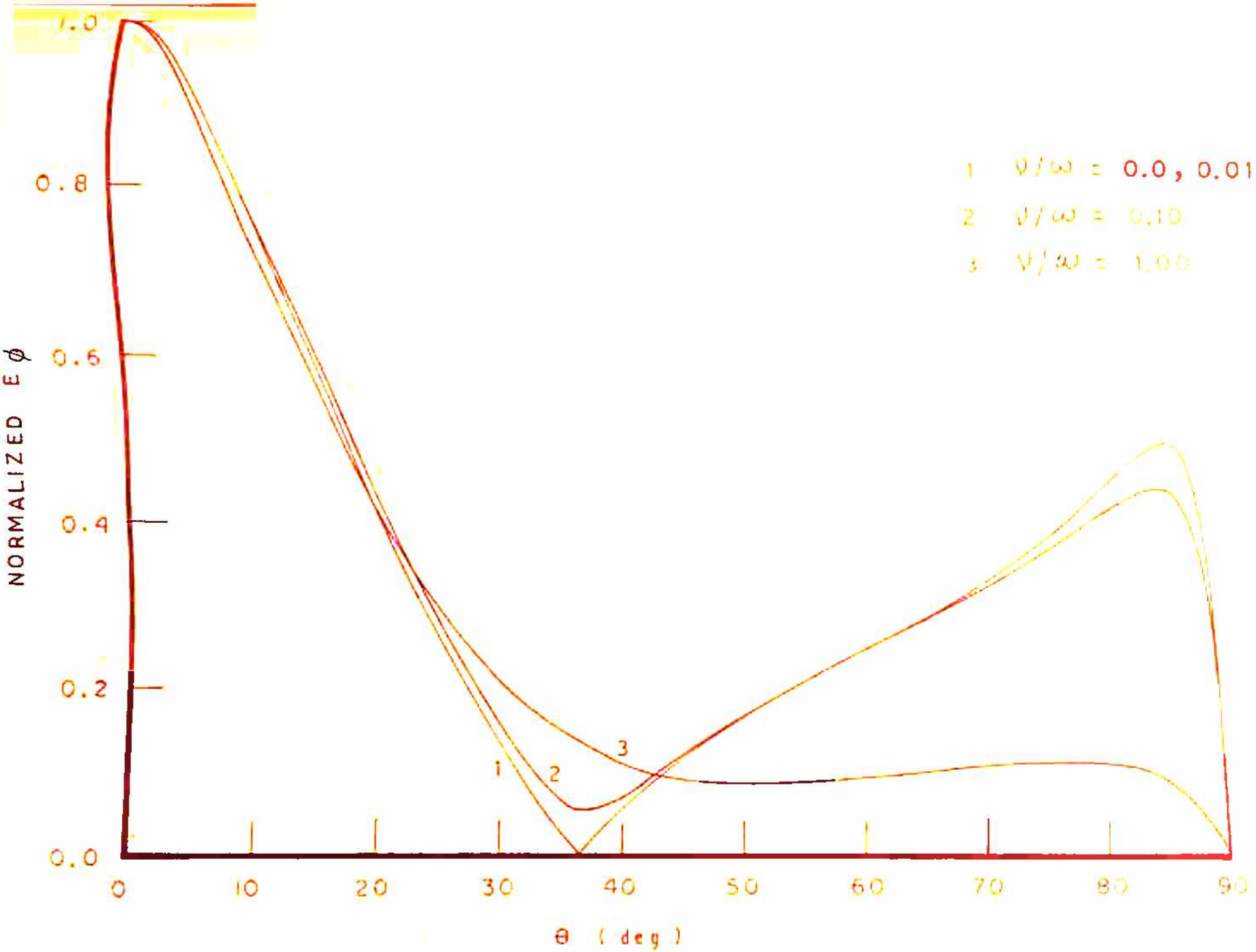

FIG. 2.10 EFFECT OF COLLISION FREQUENCY ON THE RADIATION PATTERN (WAVEGUIDE, TE_{01} — MODE) $K_o a = K_o b = 3.83$, $K_o C = 4.021$, $\epsilon_d = 5.0$ and $\omega_p/\omega = 0.5$

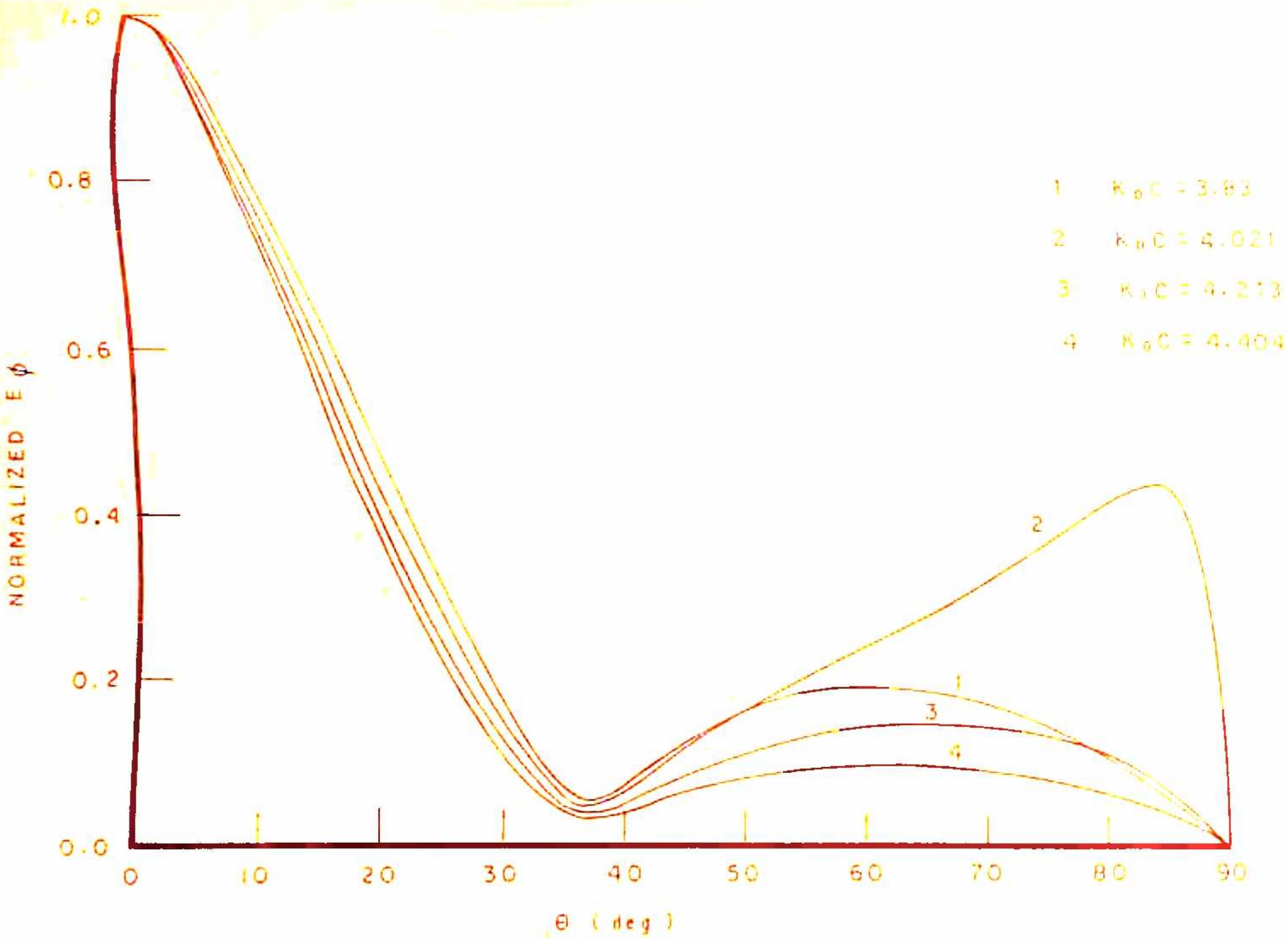

FIG. 2.11 EFFECT OF DIELECTRIC TUBE ON RADIATION PATTERN (WAVEGUIDE TE_{01} — MODE)
$K_0 a = K_0 b = 3.83$, $\epsilon_d = 5.0$, $\omega_p / \omega = 0.5$, $\nu / \omega = 0.1$

of the plasma column thickness. The results are shown in fig.(2.11) and table (2.8). The major peak appears at the broadside for all values. The peak amplitude , radiation resistance and directivity first decrease with increasing thickness and then increase. Similarly the side lobe level near the end-fire direction oscillates with increasing dielectric tube thickness. Similar to the case of TM_{01}-mode we expect that the radiation pattern for a quarter wavelength thick glass plate will coincide with that for the no glass tube case.

2.6 CONCLUSIONS

In this chapter the effect of plasma collision frequency and the dielectric tube thickness on the radiation characteristics of a plasma antenna system has been studied. The cylindrical plasma columns excited by circularly symmetric sources such as electric and magnetic ring sources and open-ended circular waveguide supporting the TE_{01}-and TM_{01}-modes, have been considered.

The most important feature which has emerged from a study of the effects of dielectric tube thickness on the radiation pattern is that the radiation pattern for a quarter wavelength thick glass tube almost overlaps the pattern for the no glass tube case. This result is consistent for both the ring sources and the open-ended circular waveguide. A glass tube thickness equal to the integral multiples of $\lambda/4$ also gives a radiation pattern which differs very slightly from the one in the absence of a glass tube. The peak ampli-

tude, radiation resistance and directivity are very slightly affected by the quarter-wave or multiple quarter-wave thick glass tubes as compared to no glass tube case.

The radiation patterns for the electric and magnetic sources are very much similar but not exactly the same as they would have been for the ring sources in free space. For the typical values of the parameters used for computations the direction of the major peak differs by about 0.5° only. The beamwidth is somewhat larger for the magnetic ring excitation than for the electric ring excitation. The directivity for the electric ring source is higher as compared to the magnetic ring case. The radiation patterns for the TM_{01}- and TE_{01}-mode circular waveguide excitation are markedly different from each other. The radiation peak appears on the broadside for the TE_{01}-mode whereas for the TM_{01}-mode it appears near the end-fire direction except in the lossless case where it appears on the broadside for the TM_{01}-mode also. It can be noticed that the HPBW is smaller and the directivity is larger for the TE_{01}-mode as compared to the TM_{01}-mode. This is because the excitation aperture is larger in the former case.

The general influence of increasing the collision frequency is a decrease in the radiated power. For the case of ring sources the radiation peaks become broader and weaker with the increasing collision frequency. The direc-

tion of the radiation peaks is shifted by a very small angle at high collision frequencies. For the waveguide excitation in the TM-mode the broadside radiation is suppressed and the radiation towards the end-fire is enhanced. But, for the TE-mode this effect is not observed rather the end-fire radiation is suppressed at a sufficiently high relative collision frequency. For both the TM_{01}- and TE_{01}-modes the radiation peak becomes narrower as the collision frequency is increased. For a sufficiently small relative collision frequency ($\nu/\omega = 0.01$) the radiation characteristics are very slightly affected except for the case of TM_{01}-mode waveguide excitation where the changes are rather drastic.

We may thus conclude that either a very thin or a quarter-wavelength thick glass tube causes a very little distortion of the antenna radiation pattern and very mildly affects the other antenna characteristics. A relative collision frequency of the order of 10^{-2} has a little effect on the antenna system characteristics except for the TM_{01}-mode waveguide excitation. Thus, in general, a relative collision frequency of this order may be tolerated without very seriously affecting the antenna system characteristics.

REFERENCES

Cloutier, G.G. and Bachynski, M.P. (1963) Antenna characteristics in the presence of a plasma sheath, Electromagnetic theory and antennas, ed. by E.C. Jordan (Pergamon Press) p 537

Crosswell, W.F., Rudduck, R.C. and Hatcher, D.M.(1967) The admittance of a rectangular waveguide radiating into a dielectric slab, IEEE Trans., Vol AP-15, No 5, p 627

Duncan, J.W.(1959) The efficiency of excitation of a surface wave on a dielectric cylinder, IRE Trans., Vol MTT-7, No 2, p 257

El-Khamy, S.E., El-Kamchouchi, H.A. and Hashist, B.M.(1976) The admittance of a rectangular waveguide radiating in an experimental plasma layer, Int.J.Electron., Vol 40, No 4, p 351

Galejs, J. and Mentzoni, M.H.(1967) Waveguide admittance for radiation into plasma layers - theory and experiment, IEEE Trans., Vol AP-15, No 3, p 465

Gupta, K.C.(1970) A multiple narrow beam antenna system using a column of isotropic plasma, Int.J.Electron. Vol 42, No 1, p 45

Gupta, K.C. and Garg, R.K.(1971) Antennas using cylindrical column of isotropic plasma, Res.Rep. I.I.T.K./E.E./71

Harris, J.H., Villenuve, A.T. and Broca, L.A.(1965) Radiation patterns from plasma enclosed cylindrical hypersonic vehicles, J.Res.Nat.Bur. Stand, Vol 69 D, No 10, p 1335

Hodara, H. and Cohn, G.I.(1962) Radiation from a gyroplasma coated magnetic line source, IRE Trans., Vol AP-10, No 5, p 581

Jacavanco, D.J.(1964) An experimental investigation of antenna pattern distortion due to a plasma layer, IEEE Trans., Vol AP-12, No 3, p 365

Ram, D and Verma, J.S.(1972) Electronically scannable narrow beam antenna system using isotropic plasma column having central conductor along the axis and excited by magnetic ring source, Ind.J.Pure.App.Phys. Vol 10, No 10, p 716

_____(1973a) Electronically scannable narrow beam plasma antenna system, Int.J.Electron., Vol 34, No 6, p 831

Ram, D. and Verma,J.S. (1973b) An antenna system using a plasma column having a central conductor and excited by a coaxial line, Int.J.Electron., Vol 35, No 5, p 665

_____(1974) Antenna system using a plasma column having a central conductor and excited by a waveguide, Radio Science, Vol 9, No 4, p 476

Russo, A.J.(1969) Radiation pattern of an open-ended waveguide covered by plasma layers, IEEE Trans., Vol AP-17 No 5, p 672

Samaddar, S.N.(1976) Radiation from a dielectric coated cylindrical core loop antenna surrounded by a lossy plasma sheath, Int.J.Electron., Vol 20, No 1, p 65

Samaddar, S.N. and Yildiz, M.(1964) Excitation of coupled electro-acoustical waves by a ring source in a compressible plasma cylinder, Can.J.Phys. Vol 42, No 4, p 638

Tamir, T. and Oliner, A.A.(1962) The influence of complex waves on the radiation field of a slot-excited plasma layer, IRE Trans., Vol AP-10, No 1, p 55

Tyras, G.(1969) Radiation and propagationof electromagnetic waves, (Academic Press) Ch 5

Villenuve, A.T.(1965) Admittance of a waveguide radiating into a plasma environment, IEEE Trans., Vol AP-13, No 1, p 115

CHAPTER 3

RADIATION FROM INHOMOGENEOUS COLLISIONLESS PLASMA COLUMN CONTAINED IN A DIELECTRIC TUBE

3.1 INTRODUCTION

It is well known that almost all the forms of real life plasma namely the laboratory plasma, the ionosphere and the plasma sheath generated around a space-vehicle etc. exhibit a spatial inhomogeneity of plasma density. In most of the early theoretical studies on radiation from plasma-enclosed electromagnetic sources the plasma was assumed to be homogeneous, to simplify the mathematical analysis (refs. given in Ch.2). Then it was realized that the radiation properties of a source enclosed by an inhomogeneous plasma may be markedly different than those when it is surrounded by a homogeneous plasma. Several studies were then conducted using some idealized as well as realistic plasma density profiles. Various methods are used to solve the wave equation in an inhomogeneous medium, (i) the equation can be exactly solved for idealised density profiles such as linear and exponential (Stratton 1941, Barrar 1955, and Casey 1971 etc.) for which the closed form solution exist, (ii) an exact solution for more general cases can be obtained in the form of an infinite power series expansion (Samaddar 1963, Rusch 1964, Yeh and Rusch, 1967 and Joshi and Verma 1975 etc.), (iii) the medium can be stratified into a large number of thin homogenous plasma layers of varying plasma density. The fields are then obtained by solving the wave equation in each layer and using the matrix methods (Harris 1963 etc.), (iv) the wave equation can be

directly integrated by using the numerical methods (Swift 1964, Fante 1971 etc.), (v) for the cases where the plasma density gradient is small the WKB method can be used to obtain an approximate solution (Unz 1967, Tyras 1969) and (vi) at high frequencies in the geometrical optical limit, a geometrical optical analysis can give an approximate solution (Tyras 1969, Woo and Ishimaru 1971).

Most of the authors referred above (Rusch 1964, Swift 1964, Tyras 1967, Yeh and Rusch 1967, Harris 1963 and Fante 1971) have studied the problem of a slotted cylinder covered with an inhomogeneous plasma layer using different plasma density profiles and techniques of solution to understand the re-entry problem. Woo and Ishimaru (1971) studied an arbitrarily oriented dipole in a cylindrical inhomogeneous plasma. Daniele and Zich (1973) studied the radiation from arbitrary sources in an isotropic stratified plasma. Joshi and Verma (1975) discussed the method of solution of radiation fields of a magnetic ring source in a magnetized inhomogeneous plasma column. El-Khamy et al (1976) studied the admittance of a waveguide radiating into an inhomogeneous plasma layer. More recently, Wong and Cheng (1977) studied the radiation from a circular loop in an inhomogeneous plasma column. In the present chapter, we make an attempt to study the effects of inhomogeneity of plasma density on the radiation characteristics of a

system consisting of a ring source in an infinite column of inhomogeneous plasma contained in a homogeneous dielectric tube. Both the electric and magnetic ring sources carrying a uniform harmonic current are considered. These sources excite the lowest order circularly symmetric H- and E-type modes respectively. A plasma density profile representing the positive column of a discharge tube is considered for analysis. The plasma density profile in the positive column is theoretically represented by a zeroth order Bessel function of first kind. For the sake of mathematical simplicity the Bessel function profile is approximated by a parabolic function profile. The wave equation in the inhomogeneous plasma region is solved by the infinite power series method (Whitteker and Watson 1952). The radiation field is obtained by the asymptatic evaluation of the inverse Fourier transform integral by the method of steepest descents. This study will be helpful to understand the behaviour of a laboratory plasma-antenna system using the positive column of an electrical discharge as the plasma column.

3.2 THE INHOMOGENEOUS PLASMA DENSITY PROFILE

The plasma column is assumed to be isotropic, lossless, incompressible and inhomogeneous. For the case of positive column the plasma density is generally taken as a parabolic function of the radial distance which is

most probably assumed on the basis of experimental evidence. For the case of a positive column of a glow discharge Cobine (1958) has described the work of Engel and Steenbeck (1932-34), for gas pressures such that the mean free path of the electrons is very short in comparison with the diameter of the tube containing the discharge. In their analysis the plasma electron density is shown to have the following radial dependence:

$$n(\rho) = n_o J_o(\rho\sqrt{Z/D_a}) \qquad (3.1)$$

where n_o = the plasma density at the axis ($\rho = 0$)

Z = frequency of the ionizing collisions.

D_a = the ambipolar diffusion coefficient.

Since the electron density can not be negative, $\rho\sqrt{Z/D_a}$ cannot exceed a value 2.405 which is the first zero of the Bessel function J_o. Furthermore, the value of $\rho\sqrt{Z/D_a}$ will be maximum at $\rho = b$, the radius of the plasma column. This implies that

$$b\sqrt{Z/D_a} \leq 2.405 \qquad (3.2)$$

If the production of ions and the diffusion coefficient at any pressure are such that at the inner wall of the dielectric tube containing the plasma (i.e. at $\rho = b$) the electron density is zero, then $b\sqrt{Z/D_a} = 2.405$. Hence eqn.(3.1) can be written as :

$$n(\rho) = n_o J_o(2.405\ \rho/b) \qquad (3.3)$$

Now if we define the plasma frequency

$$\omega_p = \sqrt{n(\rho)\ e^2/m\varepsilon_o} \qquad (3.4)$$

where e is the electronic charge and m is the mass of the electron then the relative permittivity is given by

$$\varepsilon_p = 1 - \omega_p^2/\omega^2$$

$$= 1 - \frac{n(\rho)\ e^2}{m\varepsilon_o\ \omega^2} \qquad (3.5)$$

The relative permittivity of the plasma ε_p and hence $n(\rho)$ will appear in the Maxwell's equations and then in the wave equation. To simplify the mathematical difficulty involved in solving the second order differential equation containing the function $n(\rho)$ (eqn.3.1) we make the following approximation. We approximate the Bessel function in the interval $0 \leqslant \rho \leqslant 2.405\sqrt{D_a/Z}$ by a parabolic function of the following form.

$$J_o(\rho\sqrt{Z/D_a}) \cong 1 - Y(\rho/b)^2 \qquad 0 \leqslant \rho \leqslant b \qquad (3.6)$$

where Y is a (constant) such that $0 \leqslant Y \leqslant 1$.

Then $$n(\rho) = n_o\ (\ 1 - Y(\rho/b)^2) \qquad (3.7)$$

The curves for the function $1-Y(x/2.405)^2$ and $J_o(x)$, where $x = (2.405\ \rho/b)$ are plotted in fig.(3.1) for comparison.

By combining the eqns.(3.5) and(3.7) the relative permittivity of the plasma can be written as

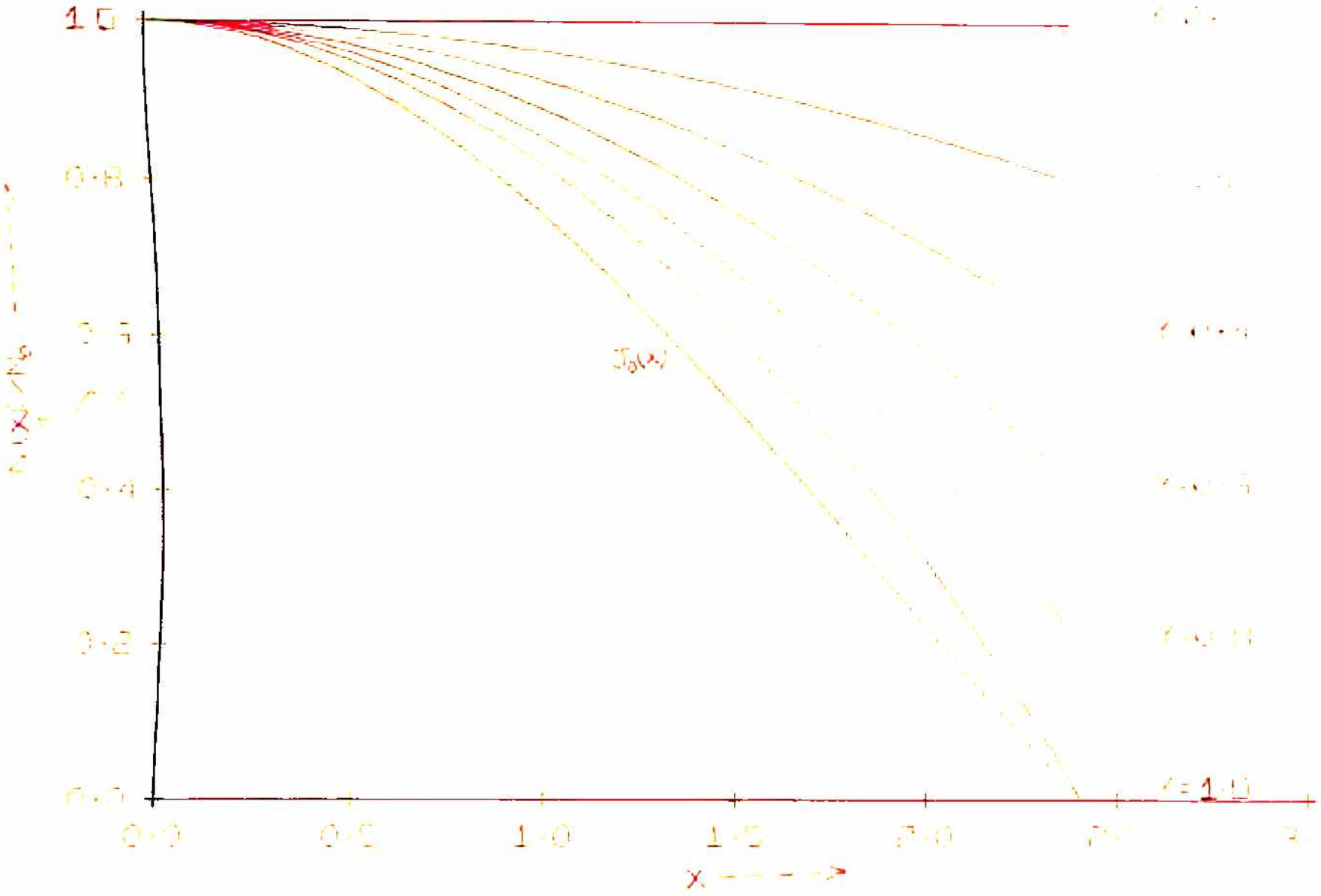

FIG. 3.1 INHOMOGENEOUS PLASMA DENSITY PROFILES

$$\epsilon_p = 1 - \frac{\omega_{po}^2}{\omega^2} + \frac{\omega_{po}^2}{\omega^2} Y (\rho/b)^2 \qquad (3.8)$$

where $\omega_{po} = \sqrt{n_o e^2/m\epsilon_o}$ is the plasma frequency at the axis of the plasma column.

3.3 EXCITATION BY MAGNETIC RING SOURCE

3.3.1 Introduction

In this section we study the radiation characteristics of a plasma-antenna system consisting of a magnetic current ring source placed inside an infinitely long cylindrical column of plasma surrounded by a dielectric tube. The plasma is assumed to be isotrppic, inhomogeneous, lossless and incompressible. The equivalent relative permittivity of the plasma is given in the preceding section by eqn.(3.8). The dielectric tube may represent a glass tube in an actual laboratory experiment. A magnetic current ring source carrying a uniform current will excite the lowest order circularly symmetric E-type mode having the field components E_ρ, E_z and H_ϕ. As mentioned in the chapter 2 (sec.2.3), the magnetic current ring source may be simulated by a very narrow annular slot in a large conducting screen. The requirement for the annular slot to be a good approximation of the ring source is that the slot width should be small compared to the wave-length and the electric field in the slot should be radial and uniform. It is also important to note that an electric

dipole oriented along the axis of the system will also excite the same types of modes as excited by the magnetic current ring source being considered here.

3.3.2 Formulation of the Problem

The geometry of the problem to be analyzed is the same as considered in the previous chapter and shown in fig.(2.1). An infinitely long inhomogeneous plasma column having a radius b is enclosed by a coaxial dielectric cylinder having an inner radius b and an outer radius c. The relative permittivity of the plasma denoted by ϵ_p is given by eqn.(3.8) and that of the dielectric is denoted by ϵ_d. The relative permeabilities of the dielectric and the plasma are taken to be equal to unity. The region outside the dielectric tube is free space. Due to the circular cylindrical symmetry of the problem the cylindrical coordinate system (ρ, ϕ, z) is used. The axis of the plasma cylinder is aligned with the Z-axis of the coordinate system. A magnetic current ring source of radius a and carrying a uniform harmonic magnetic current M is placed at the origin in the Z = 0 plane. The source current distribution is represented by the Dirac delta function in the following form

$$\bar{M} = \hat{\phi}\, M\, \delta(\rho - a)\, \delta(z) \qquad (3.9)$$

where $\hat{\phi}$ is a unit vector in the ϕ-direction and M is the strength of the magnetic ring source expressed in volts/sq. meter.

Assuming a harmonic time dependence of the form $\exp(-j\omega t)$ and suppressing it throughout, the source form of the Maxwell's equations are written as

$$\nabla \times \bar{E} = j\omega \mu_o \bar{H} - \bar{M} \tag{3.10}$$

$$\nabla \times \bar{H} = -j\omega \varepsilon_o \varepsilon(\rho)\, \bar{E} \tag{3.11}$$

where

$$\varepsilon(\rho) = \varepsilon_p = 1 - \frac{\omega_{p\rho}^2}{\omega^2} + \frac{\omega_{p\rho}^2}{\omega^2} Y (\rho/b)^2 \qquad 0 \leq \rho < b$$

$$= \varepsilon_d \qquad b < \rho < c$$

$$= 1 \qquad \rho > c \tag{3.12}$$

Now on eliminating $\bar{E}$ from the above Maxwell's equations we get a vector wave equation for $\bar{H}$, the ϕ - component of this equation is written as

$$(\nabla \times \nabla \times \bar{H})_\phi - \omega^2 \mu_o \varepsilon_o \varepsilon(\rho) H_\phi = j\omega \varepsilon_o \varepsilon(\rho) M\, \delta(\rho - a)\, \delta(z) \tag{3.13}$$

The magnetic ring source produces a field having the components E_ρ, E_z and H_ϕ and all the other components vanish. Further, due to the circular symmetry of the source and the fact that the media involved are homogeneous in the polar angle ϕ, all the field quantities will also be independent of ϕ and $\partial/\partial\phi \equiv 0$. Now on expanding the above equation in cylindrical coordinates we get the following partial differential equation for H_ϕ.

$$\frac{\partial^2 H_\phi}{\partial z^2} + \frac{\partial^2 H_\phi}{\partial \rho^2} + \left\{ \frac{1}{\rho} - \frac{1}{\varepsilon(\rho)} \frac{\partial \varepsilon(\rho)}{\partial \rho} \right\} \frac{\partial H_\phi}{\partial \rho}$$

$$- \left\{ \frac{1}{\rho^2} + \frac{1}{\rho \varepsilon(\rho)} \frac{\partial \varepsilon(\rho)}{\partial \rho} - k_o^2 \varepsilon(\rho) \right\} H_\phi$$

$$= -j\omega\varepsilon_o\varepsilon(\rho)\, M\, \delta(\rho-a)\, \delta(z) \qquad (3.14)$$

where $k_o^2 = \omega^2\mu_o\varepsilon_o$

The other field components can be obtained in terms of H_ϕ by using the Maxwell's equations.

The above partial differential equation is reduced to an ordinary differential equation by taking its Fourier transform with respect to z. The resulting equation takes the form :

$$\frac{d^2\tilde{H}}{d\rho^2} + \left\{\frac{1}{\rho} - \frac{1}{\varepsilon(\rho)}\frac{d\varepsilon(\rho)}{d\rho}\right\}\frac{d\tilde{H}}{d\rho} + \left\{k_o^2\varepsilon(\rho) - \eta^2 - \frac{1}{\rho^2} - \frac{1}{\rho\varepsilon(\rho)}\cdot\frac{d\varepsilon(\rho)}{d\rho}\right\}\tilde{H} = -j\omega\varepsilon_o\varepsilon(\rho)\, M\, \delta(\rho-a) \qquad (3.15)$$

where $\tilde{H}$ is the Fourier transform of H_ϕ by the Kernel $\exp(-j\eta z)$ as defined by eqn.(2.9) in chapter 2. The functional form of $\tilde{H}$ is $\tilde{H}(\rho,\eta)$.

In the various regions of space denoted I-IV the above equation takes the forms:

$$\frac{d^2\tilde{H}}{d\rho^2} + \left\{\frac{1}{\rho} - \frac{1}{\varepsilon_p}\frac{d\varepsilon_p}{d\rho}\right\}\frac{d\tilde{H}}{d\rho} + \left\{k_o^2\varepsilon_p - \eta^2 - \frac{1}{\rho^2} - \frac{1}{\rho\varepsilon_p}\frac{d\varepsilon_p}{d\rho}\right\}\tilde{H} = -j\omega\varepsilon_o\varepsilon_p M\,\delta(\rho-a) \quad 0 \le \rho < b \qquad (3.16)$$

$$\frac{d^2\tilde{H}}{d\rho^2} + \frac{1}{\rho}\frac{d\tilde{H}}{d\rho} + \left(k_o^2\varepsilon_d - \eta^2 - \frac{1}{\rho^2}\right)\tilde{H} = 0 \quad b < \rho < c \qquad (3.17)$$

$$\frac{d^2\tilde{H}}{d\rho^2} + \frac{1}{\rho}\frac{d\tilde{H}}{d\rho} + \left(k_o^2 - \eta^2 - \frac{1}{\rho^2}\right)\tilde{H} = 0 \quad \rho > c \qquad (3.18)$$

3.3.3 Solution of the Problem

We now proceed to solve the present problem to obtain the far zone radiation field. First of all we proceed to solve the eqns. (3.16) to (3.18) in the regions of space denoted as I - IV in fig. (2.1). It can be easily recognised that the eqns. (3.17) and (3.18) are of the form of the Bessel equation and will have the Bessel functions as their solutions. The equation (3.16) is found to have no closed form solution and it is solved by a series solution method. The appropriate solutions to these equations must satisfy the conditions that the field be finite at $\rho = 0$, the fields satisfy the electromagnetic boundary conditions at the boundaries $\rho = a$, $\rho = b$ and $\rho = c$, the field be regular at $\rho = \infty$ and that it satisfies the radiation condition. The unknown coefficients in the solutions are obtained by the application of these boundary conditions. Then the inverse Fourier transform of the solution in region IV is taken. The resulting integral is solved by considering it as a contour integral in the complex η-plane and using the method of steepest descents (Tyras 1969) to obtain the asymptotic value of the radiation field.

In the following paragraphs we proceed to execute the procedure outlined above.

Before we proceed to obtain the solutions of the wave equation we make the following substitutions :

$$\varepsilon_p = \alpha + \beta (k_o\rho)^2 \qquad (3.19)$$

with

$$\alpha = 1 - \omega_{po}^2/\omega^2 \qquad (3.20a)$$

$$\beta = \frac{\omega_{po}^2}{\omega^2} \cdot \frac{Y}{(k_o b)^2} \qquad (3.20b)$$

$$\sigma = \beta/\alpha \qquad (3.20c)$$

$$\bar{H}(\rho,\eta) = \frac{1}{\rho^{\frac{1}{2}}} h(x,\eta) \qquad (3.21)$$

$$x = (k_o\rho) \qquad (3.22a)$$

and

$$t = \alpha - \eta^2/k_o^2 \qquad (3.22b)$$

On making these substitutions in the eqn.(3.16), it takes the following form:

$$4x(1+\sigma x)\frac{d^2h}{dx^2} - 4\sigma x \frac{dh}{dx} + (1+\sigma x)(\alpha\sigma x + t)h = -j\omega\varepsilon_o\varepsilon_p M \delta(\rho-a) \quad 0 \leqslant \rho < b \qquad (3.23)$$

For all values of ρ ($0 \leqslant \rho < b$) except $\rho = a$, the above equation reduces to a homogeneous differential equation. The resulting homegeneous equation has regular singularities at $x = 0$ and $x = -1/\sigma$. If we assume that ε_p does not vanish on $0 \leqslant \rho < b$ then $x = -1/\sigma$ will not be a singular point of the equation.

Now we proceed to obtain the solutions of the following homogeneous differential equation which is valid in the region $0 \leqslant \rho < b$.

$$4\sigma(1+\sigma x)\frac{d^2h}{dx^2} - 4\sigma x \frac{dh}{dx} + (1+\sigma x)(\alpha\sigma x + t)h = 0 \qquad (3.24)$$

We expand the function h(x) (the arguement η is dropped for the sake of brevity) as an infinite power series of the form:

$$h(x) = \sum_{m=0}^{\infty} a_m x^{m+n} \qquad (3.25)$$

The substitution of this solution in eqn.(3.24) yields the following indicial equation:

$$a_0 n(n-1) = 0 \qquad (3.26)$$

The roots of this indicial equation are n = 0 and 1. Since the two roots differ by an integer, the larger of the two, i.e. n = 1 gives a solution and the root n = 0 does not give any solution. Thus the first solution to eqn.(3.24) may be written as :

$$h_1(x) = \sum_{m=0}^{\infty} a_m x^{m+1} \qquad (3.27)$$

The coefficients a_m's are evaluated by substituting the series (3.27) into the eqn.(3.24) and equating the coefficients of various powers of x to zero. This gives

$$a_0 = 1 \quad \text{(arbitrary)} \qquad (3.28a)$$

$$a_1 = (4\sigma - t)/8 \qquad (3.28b)$$

$$a_2 = (ta_1 + (\alpha+t)\,\sigma\, a_0)/24 \qquad (3.28c)$$

and for $m \geq 3$ $a_m = -\{(4\sigma m(m-2)+t)a_{m-1} + (\alpha+t)\sigma\, a_{m-2} + \alpha\,\sigma^2 a_{m-3}\}/4m(m+1)$ (3.28d)

A second independent series soultion can be written in the form (Whitteker and Watson 1952):

$$h_2(x) = h_1(x)\ln(x) + \sum_{j=0}^{\infty} b_j x^j \qquad (3.29)$$

with the coefficients

$$b_o = -a_o/t \qquad (3.30a)$$

$$b_1 = 0 \qquad (3.30b)$$

$$b_2 = -\{12a_1+(\alpha+t)\sigma\, b_o\}/8 \qquad (3.30\ c)$$

and for $j \geq 3$

$$b_j = -\big[4(2j-1)a_{j-1}+8(j-2)\sigma\, a_{j-2} + \{4\sigma(j-1)(j-3)+t\}\, b_{j-1} + (\alpha+t)\sigma b_{j-2}+\alpha\sigma^2 b_{j-3}\big]/4j(j-1) \qquad (3.30d)$$

The circle of convergence of the above series solutions (eqns. 3.27 and 3.29) for $\varepsilon_p \neq 0$, in the region $0 \leq \rho < b$ is defined by $\sigma x \ll 1$ or $Y \ll |(\omega^2-\omega_{p\sigma}^2)/\omega_{po}^2|$ (Whitteker and Watson 1952). It can be shown that for $Y = 0$, i.e. the homogeneous case, the series $h_1(x)$ is related to the Bessel function $J_1(v_1\rho)$ where v_1 is defined by eqn. (2.13) in chapter 2.

Now, the appropriate solutions in all the regions of space (I-IV) can be written as :

$$\tilde{H}_I(\varphi,\eta) = A_1 \sum_{m=0}^{\infty} a_m (k_\sigma \rho)^{2m+1} \qquad 0 \leq \rho < a \qquad (3.31a)$$

$$\tilde{H}_{II}(\varphi,\eta) = A_2 \sum_{m=0}^{\infty} a_m (k_\sigma \rho)^{2m+1} + B_2\Big\{\sum_{m=0}^{\infty} a_m (k_\sigma \rho)^{2m+1} \cdot \ln(k_\sigma \rho)^2 + \sum_{j=0}^{\infty} b_j (k_\sigma \rho)^{2j-1}\Big\} \quad a < \rho < b \qquad (3.31b)$$

$$\tilde{H}_{III}(\rho,\eta) = A_3 J_1(v_d\rho) + B_3 Y_1(v_d\rho) \quad b<\rho<c \qquad (3.31c)$$

$$\tilde{H}_{IV}(\rho,\eta) = A_4 H_1^{(1)}(v_o\rho) \quad \rho > c \qquad (3.31d)$$

where, $v_o = \sqrt{k_o^2 - \eta^2}$ and $v_d = \sqrt{k_o^2 \varepsilon_d - \eta^2}$ (3.32)

Where J_1, Y_1 and $H_1^{(1)}$ are the first order Bessel function, Neumann function and Hankel function of the first kind. A_1, A_2, B_2 ... A_4 are the unknown coefficients to be determined by applying the boundary conditions. The source at $\rho = a$ introduces a discontinuity in the tangetial component of the electric field E_z equal to the magnetic current density at $\rho = a$. The other boundary conditions are provided by the continuity of the tangential components of electric and magnetic fields E_z and H_ϕ across the boundaries. The coefficients A_1, A_2, B_2, ... A_4 are obtained by applying these boundary conditions and solving the resulting set of equations by matrix methods. The expressions for the coefficients are simplified by using the recurrence relations between the Bessel functions and the following Wronskian relation between $h_1(x,\eta)$ and $h_2(x,\eta)$

$$h_1' h_2 - h_2' h_1 = - \frac{4(1+\sigma x)}{\eta - t} \qquad (3.33)$$

Since we are interested in the radiation field ($\rho > c$), we calculate A_4 and take the inverse Fourier transform of $\tilde{H}_{IV}(\rho,\eta)$ to obtain the field component $H_\phi(\rho,z)$

$$H_\phi(\rho,z) = 1/2\pi \int_{-\infty}^{\infty} A_4 H_1^{(1)}(v_o\rho)\, e^{j\eta z}\, d\eta \qquad (3.34)$$

This integral is evaluated by contour integration and using the method of steepest descents, as outlined in the sec.(2.3.3). The far zone radiation field in the spherical coordinate system is found to be :

$$H_{\phi}(r,\theta) = j \frac{N}{\pi} \sqrt{\varepsilon_o/\mu_o} \cdot F(\theta) \cdot \frac{e^{j(k_o r - \pi/4)}}{r} \qquad (3.35)$$

Where $F(\theta)$, called the pattern function is given by

$$F(\theta) = \frac{2\,\varepsilon_d \cdot \varepsilon(b) \cdot (k_o a) \sum a_m (k_o a)^{2m+1}}{\pi\,(P \cdot R + Q \cdot S)} \qquad (3.36)$$

with

$$P = \varepsilon(b)(v_d b) J_o(v_d b) \Sigma a_m (k_o b)^{2m+1} - 2\varepsilon_d J_1(v_d b) \Sigma a_m (m+1)(k_o b)^{2m+1} \qquad (3.37a)$$

$$Q = -\varepsilon(b)(v_d b) Y_o(v_d b) \Sigma a_m (k_o b)^{2m+1} + 2\varepsilon_d Y_1(v_d b) \Sigma a_m (m+1)(k_o b)^{2m+1} \qquad (3.37b)$$

$$R = \varepsilon_d (v_o c) Y_1(v_d c)\, H_o^{(1)}(v_o c) - (v_d c) Y_o(v_d c) H_1^{(1)}(v_o c) \qquad (3.37c)$$

$$S = \varepsilon_d (v_o c) J_1(v_d c) H_o^{(1)}(v_o c) - (v_d c) J_o(v_d c) H_1^{(1)}(v_o c) \qquad (3.37d)$$

where, v_o, v_d and a_m's are the same as defined by equation (3.32) and (3.28) but with $\psi = k_o \sin\theta$, which is the saddle point. The summation runs over m = 0 to ∞.

For the special case of homogeneous plasma (Y=0) it can be found that the series involved in eqns.(3.37) are related to the Bessel functions by the following equations.

$$\sum_{m=0}^{\infty} a_m (k_o b)^{2m} = \frac{2}{(v_1 b)} \cdot J_1(v_1 b) \qquad (3.38)$$

and $$\sum_{m=0}^{\infty} a_m (m+1)\ (k_o b)^{2m} = J_o(v_1 \rho) \qquad (3.39)$$

where $$v_1 = k_o \sqrt{\epsilon_p - \sin^2\theta} \qquad (3.40)$$

Using these relations the above pattern function can be reduced to that for the homogeneous column obtained in the previous chapter (eqns. 2.17 and 2.18).

3.3.4 Numerical Evaluation of the Antenna System Characteristics

A brief general discussion of some important antenna system characteristics has been made in chapter 2. In this section we discuss the results of numerical evaluation of the radiation pattern, radiation resistance and directivity of the inhomogeneous plasma-antenna system. The effects of the shape of the plasma density profile for a fixed axial plasma density and for a fixed average plasma density on the above antenna system characteristics are discussed.

The azimuthal plane (ϕ-plane) radiation pattern is isotropic due to the circular symmetry of the source. The vertical plane (θ-plane) radiation pattern is evaluated by computing the pattern function (eqns. 3.36 and 3.37) for values of θ at 0.5° interval. Since symmetry exists about the $\theta = 0$ plane only half of the pattern from $\theta = 0^\circ$ to 90° is sufficient. Each pattern is normalised to its maximum value to facilitate the comparison of relative pattern shapes for different plasma density profiles.

The radiation resistance and directivity are calculated by using the eqns.(2.31), (2.32) and (2.35).

The expression for the pattern function involves sum of the infinite series so we first discuss the convergence and evaluation of the infinite series. Next, we discuss the effect of the shape of the density profile on the antenna system characteristics.

i) Convergence of the Series Solutions

The criterion for convergence of the series solution has already been mentioned above. The convergence of the series $h_1(x)$ was numerically tested for the values of Y = 0 and 1 and for θ = 0 to 90° at 5° intervals. For the case Y = 0 the results were compared with the corresponding Bessel function (eqn.3.38). The summation was found to agree upto seventh decimal place for the arguments $k_o\rho < 8.0$ for $m \leq 14$. For arguments $k_o\rho \leq 10$, the results agreed at least upto the fourth decimal place. Increasing the number of terms in the summation did not improve the agreement. For Y = 1, the derivatives of $h_1(x)$ were also calculated and substituted into the differential equation (3.24). The value was less than 10^{-7} for all angles and $k_o\rho \leq 8$, for $m \leq 16$. For $k_o\rho = 8.0$ the result was 10^{-6} for θ = 0 - 25° but again converged to less than 10^{-7} for higher values of θ. For arguments $k_o\rho$ upto 10 the equation was satisfied at least upto the

fourth decimal place. Taking the sum over a very large number of terms also did not make any improvement in the results.

ii) Effect of Inhomogeneous Density Profile

The influence of the shape of the inhomogeneous density profile on the antenna characteristics is studied in two ways: (a) by keeping the on-axis plasma density constant and changing the shape of the density profile by varying the profile index Y, and (b) by keeping the average plasma density constant as the profile index Y is varied. All the other parameters are kept constant at $k_o a = 5.0$, $k_o b = 7.5$, $k_o c = 1.15\ k_o b$ and $\epsilon_d = 5.0$. The numerical results for the above two cases are discussed below.

a) Antenna System Characteristics for Constant Axial Plasma Density:

The axial plasma density is fixed by keeping the relative axial plasma frequency constant at $\omega_{po}/\omega = 0.5$. All other parameters are fixed at the values given above. A set of values of the profile index Y = 0.0 (homogeneous case), 0.4, 0.6, 0.8 and 1.0 is chosen for numerical calculations. The shape of the density profile for these values of Y is shown in fig.(3.1). The results for the antenna system characteristics are illustrated in fig.(3.2) and table (3.1). The radiation pattern etc. for Y = 0 were compared with those obtained for the inhomogeneous

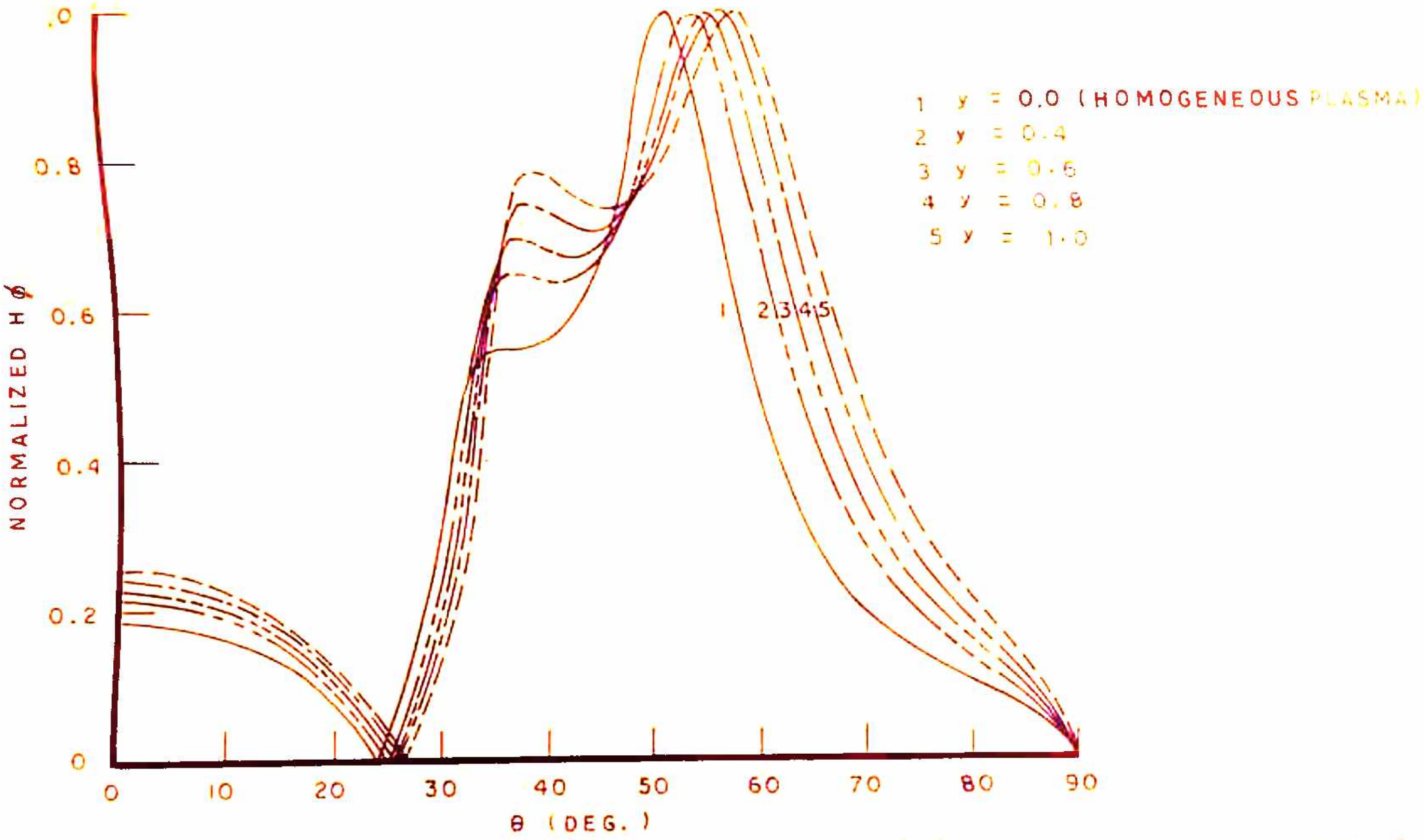

IG. 3.2 RADIATION PATTERNS FOR CONSTANT AXIAL PLASMA DENSITY (MAGNETIC RING SOURCE)
$K_0 a = 5.0$, $K_0 b = 7.5$, $K_0 C = 8.625$, $\epsilon_d = 5.0$ and $\omega_{po}/\omega = 0.5$

TABLE 3.1 EFFECT OF INHOMOGENEITY PROFILE ON THE RADIATION CHARACTERISTICS FOR CONSTANT AXIAL PLASMA DENSITY (MAGNETIC RING SOURCE)

Y	Peak Position θ_m^o	HPBW	Peak Amplitude (rel. units)	Radiation Resistance (rel. units)	Directivity (dB)
0.0 (homogeneous plasma)	53.0	10.5	6.1360	7.0494	10.182
0.4	55.5	13.5	5.8635	7.5257	9.510
0.6	57.0	16.0	5.7653	7.7783	8.960
0.8	58.5	27.0	5.6845	8.0419	8.960
1.0	59.5	29.0	5.6312	8.3173	8.732

$k_o a = 5.0$, $k_o b = 7.5$, $k_o c = 8.625$, $\varepsilon_d = 5.0$ and $\omega_p/\omega = 0.5$

TABLE 3.2 EFFECT OF INHOMOGENEITY PROFILE ON THE RADIATION CHARACTERISTICS FOR CONSTANT AVERAGE PLASMA DENSITY (MAGNETIC RING SOURCE)

Y	ω_{po}/ω	Peak Position θ^o	HPBW	Peak Amplitude (rel. units)	Radiation Resistance (rel. units)	Directivity (dB)
0.4	0.53	54.0	13.0	5.6594	7.3507	9.402
0.6	0.56	54.5	16.5	5.3880	7.5664	8.850
0.8	0.59	55.0	30.5	5.0813	7.8621	8.174

$k_o a = 5.0$, $k_o b = 7.5$, $k_o c = 8.625$, $\varepsilon_d = 5.0$ and $(\omega_p/\omega)_{av} = 0.5$

case of chapter 2 and were found to be exactly identical. The fig.(3.2) shows that the major peak shifts towards the end-fire direction by a small angle with the increasing Y. This is in agreement with the geometrical optics. Since the rays will bend toward the axis as they traverse through the inhomogeneous plasma. Similar effect has been observed by Tyras (1967) for the case of a slotted cylinder in inhomogeneous plasma. The HPBW increases significantly with the increasing Y and the peak amplitude shows a very slight decrease with the increasing Y. Consequently, the directivity decreases with the increasing Y. The knee in the pattern around $\theta = 35^{\circ}$ is enhanced and the broadside radiation also increases very slightly with the increasing profile index Y.

b) Antenna System Characteristics for Constant Average Plasma Density:

The average plasma density $(\omega_p/\omega)_{av}$ is kept fixed at 0.5 and the numerical results are obtained for the profile index Y = 0.4, 0.6 and 0.8. The radiation patterns for these profiles along with that for the homogeneous case are shown in Fig.(3.3). The other antenna characteristics and the axial relative plasma frequencies for various values of Y are summarised in table (3.2). It is noticed that the major peak shifts by a very small angle with the increasing profile index (Y) as compared to the previous case. Furthermore, the knee in the radiation pattern around $\theta = 35^{\circ}$ is

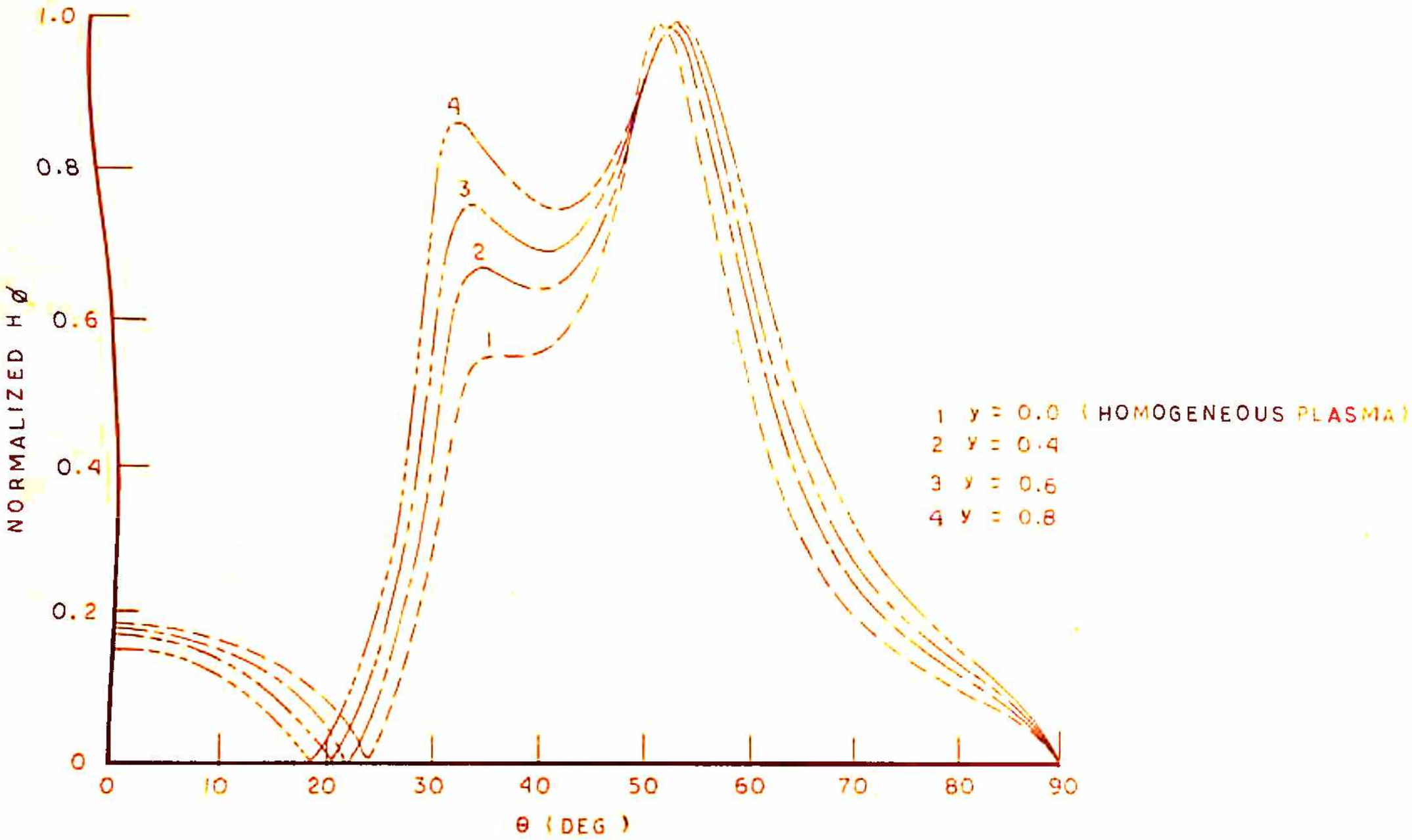

. 3.3 RADIATION PATTERNS FOR CONSTANT AVERAGE PLASMA DENSITY (MAGNETIC RING SOURCE)
$K_0 a = 5.0$, $K_0 b = 7.5$, $K_0 C = 8.625$, $\epsilon_d = 5.0$ and $(\omega_p / \omega)_{av} = 0.5$

more prominent in this case than in the previous one . In the present case the peak amplitude, radiation resistance and the directivity are slightly lower than the previous case. Contrary to the preceding case the broadside radiation shows a decrease with the increasing Y.

3.4 EXCITATION BY ELECTRIC RING SOURCE

3.4.1 Introduction

A situation complementary to the one discussed in the previous section is that of a plasma column excited by an electric ring source. A similar problem for the case of a homogeneous plasma column has been solved in ch.2 and by Gupta and Garg (1971). A similar problem without the dielectric tube has been recently solved by Wong and Cheng (1977). The radiation field of an electric current loop in an inhomogeneous plasma column were obtained. They obtained the closed form solution of the wave equation in the inhomogeneous region, having a parabolic permittivity profile, in terms of the Whitteker's functions. The final expression for the radiation field and the numerical result were presented in a symposium and could not be received from the authors. However, since the arguement of the Whitteker's function is complex in their solution, the numerical computation is difficult. So, we have adopted another simpler approach to obtain the solution. We have solved the wave equation in the inhomogeneous plasma region

by the series solution method (Whitteker's and Watson 1952) used in the previous section.

3.4.2 Formulation of the Problem:

The geometry of the problem is the same as illustrated in fig.(2.1) and analyzed in the section (2.4) with the difference that the plasma column is inhomogeneous in the present case. A wave equation similar to eqn.(2.39) is obtained by combining the two Maxwell's equations, but with $\epsilon(\rho)$ as defined by eqn.(3.12). On taking the Fourier transform of this equation with respect to z we get the following differential equation.

$$\frac{d^2\tilde{E}}{d\rho^2} + \frac{1}{\rho}\frac{d\tilde{E}}{d\rho} + (k_o^2\,\epsilon(\rho) - \eta^2 - \frac{1}{\rho^2})\,\tilde{E} = -j\omega\mu_o I\,\delta(\rho-a) \qquad (3.43)$$

where η is the transformation variable and $\tilde{E}$ is the Fourier transform of E_ϕ by the Kernel $\exp(-j\eta z)$ definied by an equation similar to eqn.(2.9).

3.4.3 Solution of the Problem

Here we proceed to solve the eqn.(3.43) in the various regions of space denoted by I-IV, according to the procedure used in sec.(3.3.3).

In the homogeneous dielectric region ($b < \rho < c$) and in free space ($\rho > c$) the above wave equation takes a form of the Bessel equation. The solutions are obtained as a linear combination of Bessel and Neumann functions in the dielectric region and as a linear combination of Hankel functions in the free space.

In the plasma region ($0 \leq \rho < b$) the above non-homogeneous differential equation becomes homogeneous for all ρ except at $\rho = a$. Thus, the region is divided into two regions $0 \leq \rho < a$ and $a < \rho < b$. To solve the homogeneous wave equation in these regions we make the following substitution.

$$E(\rho) = e(x) \tag{3.44}$$

where x is given by eqn.(3.22a). The resulting equation is then written as :

$$x \frac{d^2e}{dx^2} + \frac{de}{dx} + \frac{1}{4}(t + \beta x - 1/x)\, e = 0 \tag{3.45}$$

where β is defined by eqn.(3.20b) and t is defined by eqn.(3.22b).

This equation has a regular singularity at $x = 0$. Thus the series solution can be obtained by expanding the function e(x) as a power series in x around $x = 0$ in the following form.

$$e(x) = \sum_{m=0}^{\infty} a_m x^{m+n} \tag{3.46}$$

On substituting this solution in eqn.(3.45) the two roots of the indicial equation are obtained to be $n = \pm 1/2$. The root $n = -1/2$ does not give any solution. The root $n = +1/2$ gives the following solution.

$$e_1(x) = \sum_{m=0}^{\infty} a_m x^{m+1/2} \tag{3.47}$$

with

$$a_o = 1 \text{ (arbitrary)} \tag{3.48a}$$

$$a_1 = -ta_o/8 \tag{3.48b}$$

and for $n \geq 2$

$$a_n = -(t\,a_{n-1} + \beta a_{n-2})/4n(n+1) \tag{3.48c}$$

The second series solution is obtained in the following form (Whittker and Watson 1952).

$$e_2(x) = e_1(x)\,\ln(x) + \sum_{j=0}^{\infty} b_j\, x^{j-1/2} \tag{3.49}$$

with

$$b_o = -4a_o/t \tag{3.49a}$$

$$b_1 = 0 \tag{3.49b}$$

$$b_2 = -(12a_1 + tb_1)/8 \tag{3.49c}$$

and for $j \geq 3$

$$b_j = -\{4(2j-1)a_{j-1} + tb_{j-1} + \beta b_{j-2}\}/4j(j-1) \tag{3.49d}$$

The second solution will diverge at the origin ($x = 0$) because of the presence of the logarithmic factor. For this reason, it is not a valid solution in the region I ($0 \leq \rho < a$). The first solution $e_1(x)$ converges at the origin and hence is a valid solution in the region I. In the region II ($a < \rho < b$) a general solution can be writtenn as a linear combination of $e_1(x)$ and $e_2(x)$.

The solution of the wave equation, regular at $\rho = 0$ and $\rho = \infty$ and satisfying the radiation condition are written below alongwith their domain of definition.

$$\tilde{E}_I(\rho,\eta) = A_1 \sum_{m=0}^{\infty} a_m (k_d\rho)^{2m+1} \qquad 0 \leqslant \rho < a \qquad (3.50a)$$

$$\tilde{E}_{II}(\rho,\eta) = A_2 \sum_{m=0}^{\infty} a_m (k_d\rho)^{2m+1} + B_2 \left\{ \sum_{m=0}^{\infty} a_m (k_o\rho)^{2m+1} \ln(k_d\rho)^2 + \sum_{j=0}^{\infty} b_j (k_d\rho)^{2j-1} \right\} \qquad a < \rho < b \qquad (3.50b)$$

$$\tilde{E}_{III}(\rho,\eta) = A_3 J_1(v_d\rho) + B_3 Y_1(v_d\rho) \qquad b < \rho < c \qquad (3.50c)$$

$$\tilde{E}_{IV}(\rho,\eta) = A_4 H_1^{(1)}(v_d\rho) \qquad \rho > c \qquad (3.50d)$$

where, v_o and v_d are the same as defined by eqn.(3.32) in the preceding section. A_1, A_2, B_2 ... A_4 are the unknown coefficients to be determined by applying the boundary conditions on $\tilde{E}$'s. The boundary condition on $\tilde{E}$'s follow from the usual boundary conditions for the tangential field components discussed earlier. Since we are interested in the radiation field ($\rho >> c$) we obtain the expression for A_4, which is then simplified using the recurrence relation between Bessel functions and Neumann functions and the following Wronskian relation between $e_1(x)$ and $e_2(x)$

$$e_1' e_2 - e_2' e_1 = \frac{-4a_o^2}{t} \frac{1}{x} \qquad (3.51)$$

The radiation field is now given by the inverse Fourier transform of $\tilde{E}_{IV}(\rho,\eta)$:

$$E_\rho(\rho,z) = \frac{1}{2\pi} \int_{-\infty}^{+\infty} A_4 H_1^{(1)}(v_d\rho) e^{j\eta z} \, d\eta \qquad (3.52)$$

This integral is evaluated by contour integration and using the method of steepest descents to give the

asymptotic value of the radiation field. The procedure of integration has been discussed in the preceding chapter. The details of the method of steepest descents are available elsewhere (Tyras 1969).

The final expression for the radiation field, in spherical polar coordinate system is found to be

$$E_\beta(r,\theta) = j \frac{I}{\pi}\sqrt{\mu_o/\epsilon_o}\, F(\theta) \frac{e^{j(k_o r-\pi/4)}}{r} \qquad (3.53)$$

where, the pattern function $F(\theta)$ is given by

$$F(\theta) = \frac{2(k_o a)\sum_{m=0}^{\infty} a_m (k_o a)^{2m+1}}{\pi\,(P.R_o + Q.S)} \qquad (3.54)$$

with

$$P = 2J_1(v_d b)\sum_{m=0}^{\infty} a_m (m+1)(k_o b)^{2m+1} - (v_d b)J_o(v_d b)\sum_{m=0}^{\infty} a_m (k_o b)^{2m+1} \qquad (3.55a)$$

$$Q = -2Y_1(v_d b)\sum_{m=0}^{\infty} a_m (m+1)(k_o b)^{2m+1} + (v_d b)Y_o(v_d b)\sum_{m=0}^{\infty} a_m (k_o b)^{2m+1} \qquad (3.55b)$$

$$R = (v_d c)Y_o(v_d c)\, H_1^{(1)}(v_o c) - (v_o c)Y_1(v_d c)H_o^{(1)}(v_o c) \qquad (3.55c)$$

$$S = (v_d c)J_o(v_d c)\, H_1^{(1)}(v_o c) - (v_o c)J_1(v_d c)H_o^{(1)}(v_o c) \qquad (3.55d)$$

where, a_m's are defined by eqns.(3.52), with $\eta = k_o \sin\theta$, which is the saddle point.

It can be easily shown that for the special case of homogeneous plasma ($\gamma = 0$) the series involved in the above equations are related with the Bessel functions according to the relations (3.38) to (3.39). Using these relations

the above pattern function reduces to that for the homogeneous case obtained in the preceding chapter.

3.4.4 Numerical evaluation of Antenna System Characteristics

The influence of the shape of inhomogeneous plasma density profile on the antenna characteristics is studied for the two cases (a) when the axial plasma density is kept constant and the shape of the density profile is changed by varying the profile index Y, and (b) when the average plasma density is kept constant and the profile index Y is varied. The normalized radiation pattern, radiation resistance and the directivity are evaluated as per the procedure outlined in sec. (3.3.4).

The convergence of the series $e_1(x)$ has been tested for various arguments, various values of the angle θ and for Y = 0 and 1 in the same manner as used for $h_1(x)$ in sec. (3.3.4). The series has a more or less similar convergence for $m \leq 17$ as for the series $h_1(x)$.

The numerical results for the antenna characteristics for the above two cases are evaluated for the fixed values of the parameters $k_o a = 5.0$, $k_o b = 7.5$, $k_o c = 8.625$ and $\epsilon_d = 5.0$. These results are discussed in the following paragraphs.

a) Antenna System Characteristics for

Constant Axial Plasma Density :

The axial plasma density is kept constant by keeping the relative axial plasma frequency constant at $\omega_{po}/\omega=0.5$. The radiation characteristics are evaluated for various shapes of plasma density profiles corresponding to the following values of the profile index, Y = 0.0 (homogeneous case), 0.4, 0.6, 0.8 and 1.0. The corresponding shapes of the density profile are given in fig.(3.1). The radiation patterns for Y = 0.0, 0.6 and 1.0 are shown in fig.(3.4). The patterns for Y = 0.4, and 0.8 have not been included to avoid overcrowding of radiation peaks. The other radiation characteristics are given in table (3.3). A comparison of the normalized radiation patterns indicates that the direction of the major peak slightly shifts towards the end-fire direction with each increment in Y. It is also evident from the fig.(3.4) and the table (3.3) that the HPBW does not change with the shape of the density profile. The peak amplitude and the directivity are found to decrease as the plasma density falls more steeply with the radius of the plasma column, i.e. as Y increases. The radiation resistance is found to decrease with the increasing value of Y.

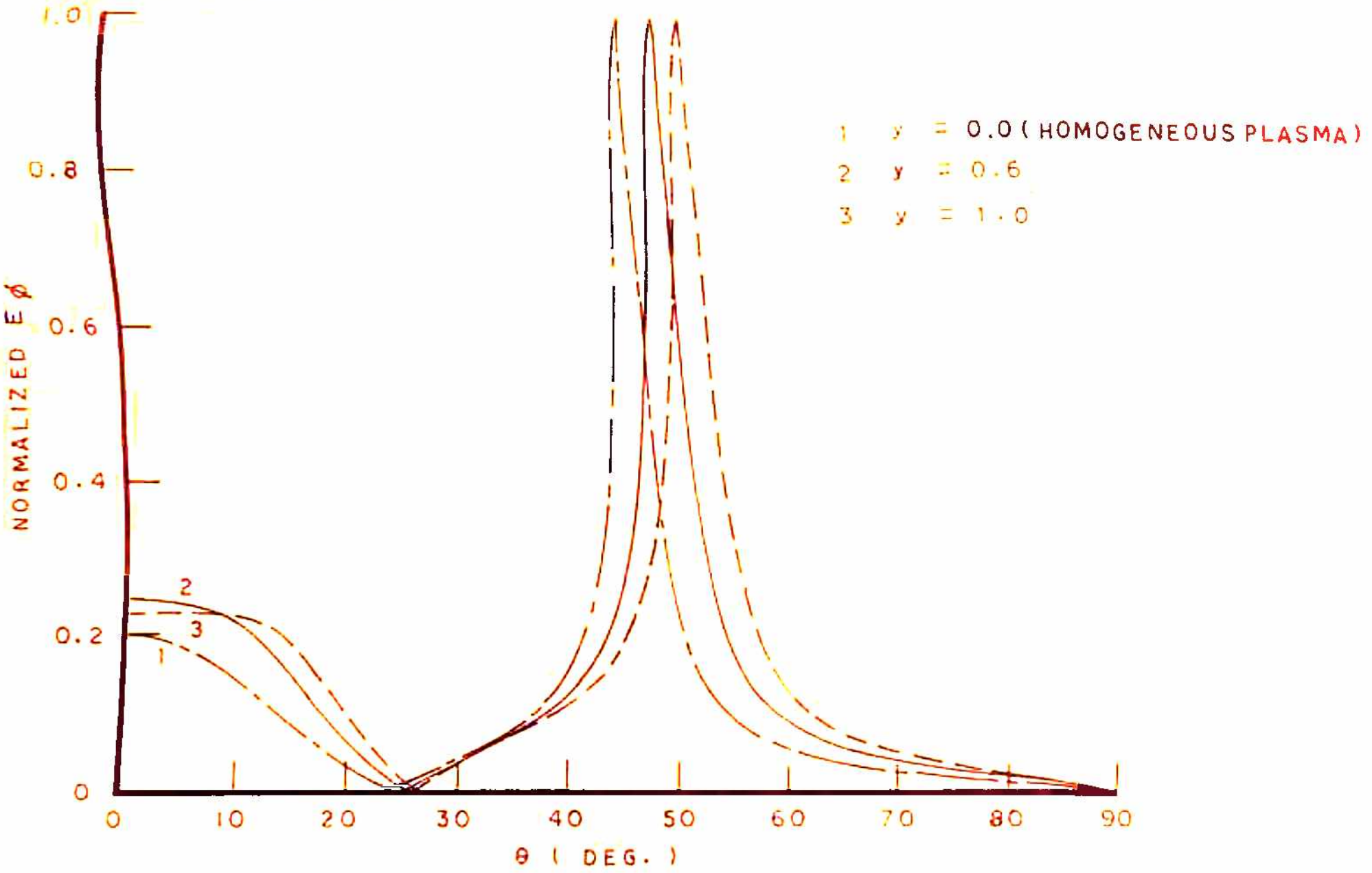

FIG. 3.4 RADIATION PATTERNS FOR CONSTANT AXIAL PLASMA DENSITY (ELECTRIC RING SOURCE)

$K_0 a = 5.0$, $K_0 b = 7.5$, $K_0 C = 8.625$, $\epsilon_d = 5.0$ and $\omega_{po} / \omega = 0.5$

TABLE 3.3 EFFECT OF INHOMOGENEITY PROFILE ON THE RADIATION CHARACTERISTICS FOR CONSTANT AXIAL PLASMA DENSITY (ELECTRIC RING SOURCE)

Y	Peak Position θ°	HPBW	Peak Amplitude (rel. units)	Radiation Resistance (rel. units)	Directivity (dB)
0.0 (homogeneous plasma)	46.0	2.5	17.3940	12.7627	16.7588
0.4	48.0	2.5	16.8675	13.9930	16.0922
0.6	49.0	2.5	16.4143	14.3946	15.7327
0.8	50.5	2.5	16.2217	14.5613	15.5802
1.0	51.5	2.5	16.1639	14.5294	15.5587

$k_o a = 5.0$, $k_o b = 7.5$, $k_o c = 8.625$, $\epsilon_d = 5.0$ and $\omega_{po}/\omega = 0.5$

TABLE 3.4 EFFECT OF INHOMOGENEITY PROFILE ON THE RADIATION CHARACTERISTICS FOR CONSTANT AVERAGE PLASMA DENSITY (ELECTRIC RING SOURCE)

Y	ω_{po}/ω	Peak Position θ°	HPBW	Peak Amplitude (rel. units)	Radiation Resistance (rel. units)	Directivity (dB)
0.4	0.53	46.0	2.5	16.3308	12.5896	16.2703
0.6	0.56	46.0	2.5	15.6015	12.4458	15.8675
0.8	0.59	46.5	3.0	14.9520	12.2806	15.6121
1.0	0.63	46.5	3.5	13.9479	12.1847	15.0423

$k_o a = 5.0$, $k_o b = 7.5$, $k_o c = 8.625$, $\epsilon_d = 5.0$ and $(\omega_p/\omega)_{av} = 0.5$

b) Antenna System Characteristics for

Constant Average Plasma Density:

Here we study the effect of the shape of plasma density profile on the radiation characteristics of the plasma columns having the same average plasma density corresponding to $(\omega_p/\omega)_{av} = 0.5$. The radiation characteristics are evaluated for Y = 0.4, 0.6, 0.8 and 1.0. The normalized radiation patterns for Y = 0.4, 0.8 and 1.0 are shown in fig.(3.5). The other patterns for Y = 0.0 and 0.6 have not been included to avoid overcrowding of radiation peaks. The table (3.4) summarizes the other radiation characteristics and the relative axial plasma frequency corresponding to all the above values of the profile index Y. We find that as Y is increased from 0 to 1 the radiation peak shifts by only 0.5° and the HPBW increases by only 1°. The peak amplitude, radiation resistance and directivity all decrease by a small amount with the increasing Y. In this case the change in the radiation resistance with the increasing Y is opposite to the case (a) where it increases with Y.

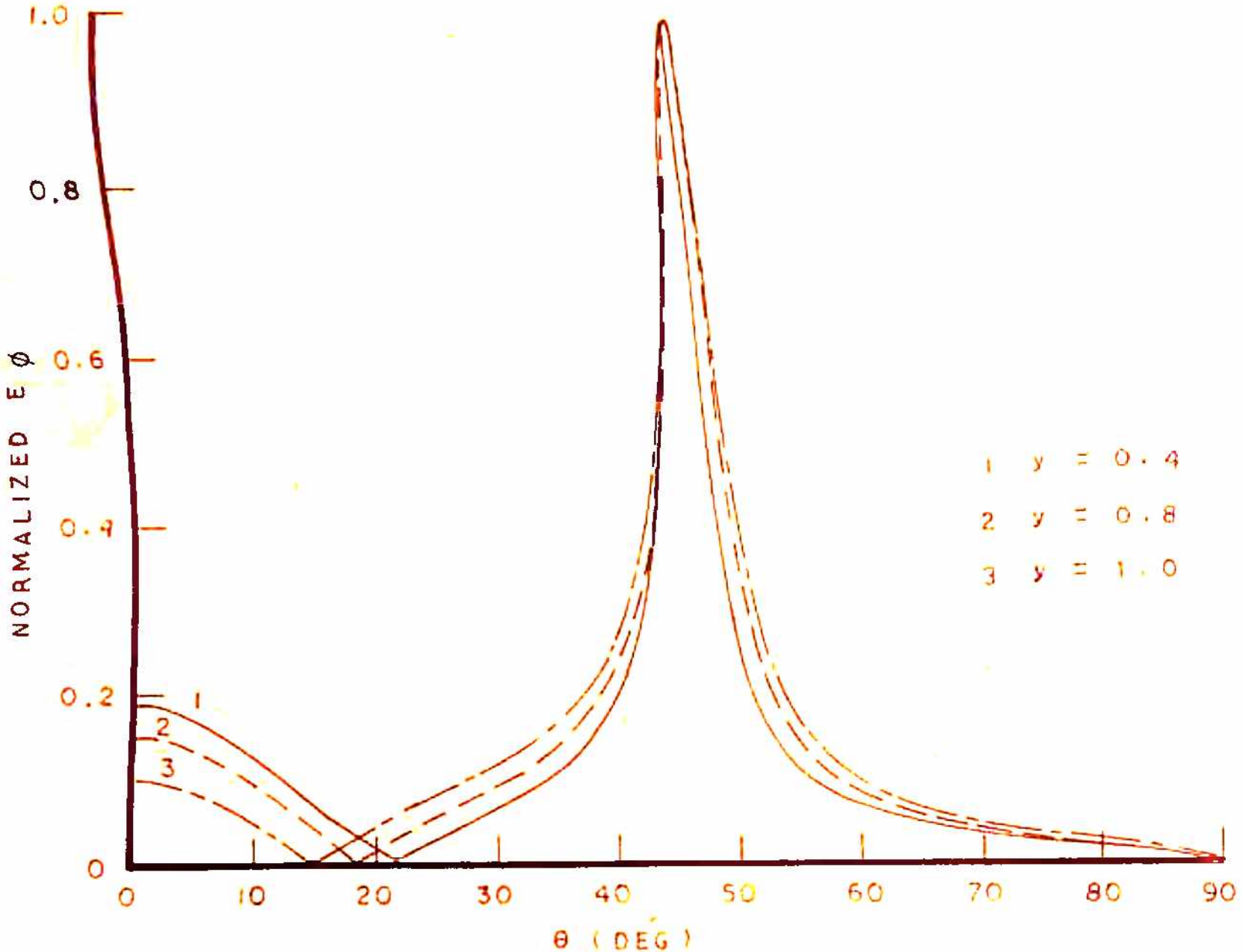

FIG. 3.5 RADIATION PATTERNS FOR CONSTANT AVERAGE PLASMA DENSITY (ELECTRIC RING SOURCE)
$K_0 a = 5.0$, $K_0 b = 7.5$, $K_0 C = 8.625$, $\epsilon_d = 5.0$ and $(\omega_p/\omega)_{av} = 0.5$

3.5 CONCLUSIONS

In the present chapter we have studied the influence of the inhomogeneity of the plasma density on the radiation characteristics of the plasma-antenna system. A parabolic plasma density profile has been assumed. Only the electric and magnetic ring sources of excitation have been considered. The circular waveguide excitation requires the field components of an inhomogeneous plasma filled waveguide. These have been given by Allis et al (1963) for the circularly symmetric TE-mode and the parabolic plasma density profile, in terms of the confluent hypergeometric functions. Now to evaluate the pattern function for the waveguide excitation the evaluation of an integral involving the confluent hypergeometric function is required. Since the evaluation of this integral is a very difficult task, the waveguide excitation has not been considered in the present analysis.

The influence of changing the shape of the plasma density profile on the radiation characteristics has been studied in two ways: by keeping the axial plasma density constant, and by keeping the average plasma density constant. When the axial plasma density is fixed and the profile index is increased the average plasma density decreases and consequently the direction of the radiation peak is found to shift towards the end-fire direction. But for the case of constant average plasma density the direction of the radiation peak remains almost constant showing a maximum shift of 0.50 with

increasing the profile index, Y, from 0 to 1. For the magnetic ring source the HPBW significantly increases as the plasma density falls off more steeply with the radius of the plasma column. But for the electric ring source, it remains constant for the fixed axial plasma density case and increases by a maximum of 1° for the other case as Y increases from 0 to 1. The peak amplitude and the directivity are found to decrease with the increasing value of Y for all the cases.

Thus, we may conclude that as far as the direction of the radiation peak is concerned, an inhomogeneous plasma can be approximated by a homogeneous plasma column having a plasma density equal to the average plasma density of the inhomogeneous column. But the directivity and the radiation resistance etc., will still depend upon the shape of the density profile.

REFERENCES

Allis, W.P., Buchsbaum, S.J. and Bers, A.(1963) Waves in anisotropic plasmas, (M.I.T. Press), Ch 10

Barrar,R.B. and Redheffer, R.M.(1955) On non-uniform/media dielectric IRE Trans. Vol AP-3 No , p 101

Casey,K.F.(1971) Radiation through an inhomogeneous reentry plasma layer, IEEE Trans., Vol AP-19, No 5, p 711

Cobine, J.D.(1958) Gaseous conductors, theory and engineering applications, (Dover Publications), Ch 8.

Daniele, V.G. and Zich, R.S.(1973) Radiation by arbitrary Sources in anisotropic stratified media, Radio Science, Vol 8, No 1, p 63

Engel, A.V. and Steenbeck, M.(1932-34) Electrische gasentladungen, ihre physik und technik, Vol 2,(Julius Springer) p 83

El-Khamy, S.E., El-Kamchouchi, H.A. and Hashist, B.M.(1976) The admittance of a rectangular waveguide radiating in an experimental plasma layer, Int.J.Electron., Vol 40, No 4, p 351

Fante, R.L.(1971) Calculation of admittance, isolation, radiation pattern of slots on an infinite cylinder covered by an inhomogeneous lossy plasma, Radio Science, Vol 6, No 3, p 421

Gupta,K.C. and Garg,R.K.(1971) Antennas using cylindrical columns of isotropic plasma, Res.Rep.I.I.T.K./E.E./71

Harris, J.H.(1963) Radiation through cylindrical plasma sheaths, J.Res.Nat.Bur.Stand. Vol 69D, No 6, p 717

Joshi, N.K. and Verma,J.S.(1975) Radiation field of a magnetic ring source surrounded by an inhomogeneous axially magnetized plasma column, J.Instt.Telecom. Engrs. Vol 21 No 10, p 538

Rusch, W.V.T.(1964) Radiation from an axially slotted cylinder with a radially inhomogeneous plasma coating, Can.J.Phys. Vol 42, No 1, p 26

Samaddar, S.N. (1963) Wave propagation in a cylindrical waveguide containing inhomogeneous plasma involving a turning point, Can.J.Phys. Vol 41, No 1, p 113

Stratton, J.A.(1941) Electromagnetic theory, (McGraw Hill)

Swift, C.T.(1964) Radiation patterns of a slotted cylinder antenna in the presence of an inhomogeneous lossy plasma, IEEE Trans., Vol AP-12, No 6, p 728

Tyras, G.(1967) Field of an axially slotted cylinder clad with an inhomogeneous dielectric, IEEE Trans., Vol AP-15, No 2, p 222.

_____(1969) Radiation and propagation of electromagnetic waves, (Academic Press), Ch 4

Unz, H.(1967) Asymptotic solution of waves in inhomogeneous plasma, IEEE Trans., Vol AP-15, No 3, p 494

Whitteker, E.T. and Watson, G.N.(1952) A course of modern analysis, (Cambridge University Press), Ch 10

Wong, W.C. and Cheng, D.K.(1977) Radiation from a current loop in an inhomogeneous plasma column, IEEE AP-S, International Symposium, Stanford University, Stanford, California

Woo,R.and Ishimaru, A.(1971) Fields excited by an arbitrarily oriented dipole in a cylindrically inhomogeneous plasma, Radio Science, Vol 6, No 5, p 583

Yeh, C. and Rusch, W.V.T.(1967) Radiation through an inhomogeneous magnetized plasma sheath, IEEE Trans., Vol AP-15, No 3, p 627

CHAPTER 6

EXPERIMENTAL PLAN FOR THE STUDY OF PLASMA-ANTENNA SYSTEM

4.1 INTRODUCTION

There is a vast amount of literature available, dealing with the theoretical analysis of a veriety of antennas in plasma. But the experimental studies on antennas in plasma have been comparatively very few. This has been partly due to the difficulty in generating a well-behaved plasma in suitable geometries and partly due to the highly idealized models used in the theory which could be hardly realized in practice. The development of artificial dielectrics using metallic rods in simple geometries, having dielectric properties corresponding to the cold homogeneous plasmas (Rotman 1962, Golden 1965, Gupta 1971, Gupta etal 1974) and wire grids having the conductivity property of the thin overdense plasma sheaths (Smith and Golden 1965a, 1965b) provided a convenient means of simulating the plasma in the laboratory. Another beautiful idea for simulating a plasma sheath with a dielectric constant less than unity was used by Tyras etal (1965). They simulated the air by a dielectric of high dielectric constant and the plasma by a low dielectric constant material, so that the ratio of dielectric constant of the plasma simulation to that of the air simulation remained less than unity.

The above technique was modified by Karas and Antonucci (1968, 1970) to allow for the study of nonplanar geometries of complex shapes. However it can be easily realized that the simulated plasmas have certain limitations, and all the phenomena which might occur in a real plasma can not be demonstrated with the simulated plasmas. Experimental studies on radiation from antennas covered by real plasmas have also been conducted

by several authors. Flock and Elliott (1962) and Cloutier and Bachynski (1963) observed the radiation from horn antennas covered by cylindrical plasma tubes. Jacavanco and Melts (1964) and Jacavanco (1965) generated the plasma in a rectangular glass container to study the radiation from a plasma covered horn antenna. This geometry represented significant improvements over the previous investigations. There have been many other experimental studies on radiation patterns of various antennas using different plasma geometries (e.g. Messiaen and Vandenplas 1967, Kristal et al 1967, Swift et al 1969 and Meyer et al 1974, etc.). Many other experimental studies have been devoted to the impedence properties of the antennas in plasma. Recently a few experimental investigations on impedence of the antennas in plasma have been made by Bhat and Rao (1973) and Nakatani and Kuehl (1976). A good discussion of the experimental aspects of antennas in plasma has been given by Preis et al (1975).

Most of the experimental investigations referred above were performed to understand the re-entry problems. But there have also been a few experimental studies where a plasma column itself has been considered as an antenna. Kaufman and Steier (1963) first used a gas discharge column as a tunable antenna at S-band frequencies. The plasma column was locally excited by a parallel wire transmission line in the dipolar resonance. The observed radiation

characteristics corresponded to those of a line of parallel dipoles oriented perpendicular to the column. The plasma antenna could be electronically tuned by varying the discharge current through the plasma. In another experiment (Alday 1962), an ionized gas plasma column was used in a slotted waveguide for electronically sweeping the beam lean angle of radiation from the slotted waveguide by changing the plasma density. Ghose (1967) has proposed the use of a plasma column as a receiving antenna in a nuclear environment. Gupta(1971) and Gupta and Bahl (1974) have proposed that a plasma slab simulated by an artificial dielectric can be used as a narrow beam scanning antenna. Recently Levitskiy and Burykin (1973, 1974) and Burykin et al (1975) performed some remarkable experiments to show that a plasma column can be used as an efficient radiator of electromagnetic waves. They excited surface waves on the positive column of the discharge in thin, straight as well as bent tubes and showed that the radiation characteristics of the plasma waveguide can be controlled by changing the discharge current. In the present work we are mainly concerned with the excitation of leaky waves on the cylindrical plasma columns. A leaky wave continuously radiates energy as it propagates along the guiding structure. This is in contrast with the radiation from surface waves which radiate only at the discontinuities along the guiding structure. The theoretical analysee have predicted that a sharp radiation peak appears near the critical optical angle.

This radiation peak can be scanned through large angles by varying the plasma density or the signal frequency. The number and level of the side lobes and beamwidth etc. can be controlled by suitably choosing the geometrical parameters of the antenna system.

A simple model of the plasma antenna system consisting of a long cylindrical column of plasma excited by circularly symmetric sources such as an electric or magnetic ring source or an open-ended circular waveguide carrying a circularly symmetric mode has been chosen for experimental investigations. The X-band has been chosen as the working frequency range since the required plasma density and the plasma column dimensions are more easily manageable for a plasma -antenna system in this frequency range. Moreover, the set-up is compact and has a lower cost. The cold as well as hot cathode d.c. discharges in a gas at low pressure have been used to generate the plasma column. A cylindrical Langmuir probe and an X-band microwave interferometer have been used for plasma diagnostics. The experiments for measuring the input impedance and radiation pattern have been set up. The details of various parts of the experimental setup are discussed in the following sections.

4.2 PLASMA GENERATION

In order to carry out some useful investigations on a plasma-antenna system it is necessary to produce a suitable

plasma column. The plasma column should be sufficiently long to approximate an infinite length considered in the theoretical analysis. A plasma column more than a few wavelengths long will be sufficient to approximate an infinite length. This is because a leaky wave continuously radiates energy as it propagates and an insignificant amount of power will be left by the time the wave reaches at the end of the plasma column. Even if reflected, this small amount of power will not cause any serious effect. The plasma density is desired to be variable in the range 10^{9} - 10^{11} cm^{-3}, to obtain a significant change in the plasma permittivity. The plasma should preferably have small losses. Moreover, it should be stable and reproducible.

There are various methods of producing a plasma in the laboratory, such as the electrical discharge, thermal ionization and shock wave ionization etc. Out of these methods an electrical discharge is a convenient source of plasma which gives a sufficient plasma density. An electrical discharge may be of a d.c. or an r.f. type. A d.c. discharge is produced by applying a high d.c. potential across two electrodes in a gas at low pressure. The more usual type of the d.c. discharge, the glow discharge, has been discussed in a great detail by Francis (1956). If the current in a glow discharge is increased beyond the abnormal glow region an arc discharge takes place. The arc discharges

are characterized by low operating voltages coupled with the high current densities. The arc discharges may be of the field emission type or of the thermionic type. For thermionic arcs the cathode is made of a refractory material, for example, C, W or Mo.

The most important region of a d.c. discharge for plasma generation is the positive column. This region occupies most of the volume in a discharge extending from the anode upto very near to the cathode. It is a fairly uniform column of plasma having a very small electric field and almost equal densities of electrons and ions.

A novel technique for creating a quiet, well behaved, and high density plasma was demonstrated by Prescon (1965). Using a brush shaped cathode, the cathode fall of about an order of magnitude larger than for the corresponding normal cold cathode was obtained. The brush cathode generates a uniform high energy electron beam and a corresponding negative glow with a longitudinal dimension upto two orders of magnitude larger than that for the normal cathode glow. The discharge tube with a brush cathode can be operated far into the abnormal glow region without making the discharge unstable. The electron density in the He plasma in the range: 10^{10} - 10^{14} cm^{-3} were achieved.

An r.f. plasma is produced by a capacitive or an inductive coupling of energy to the gas atoms without the necessity of any internal electrodes. The power required for

the breakdown and maintenance of the discharge is significantly lower because the electron and ion losses from the discharge are minimized. Its major disadvantage is the high noise level which is unsuitable for the antenna applications.

The three types of d.c. discharges namely the cold cathode discharge, the hot cathode discharge and the brush cathode discharge have been considered suitable for the plasma antenna studies. Although, the brush cathode discharge is best among the above, it could not be set up due to the lack of facilities. The other two types of discharge were created in the laboratory and their densities were measured with a Langmuir probe and the microwave interferometer. Three different plasma tubes were constructed. The first one is a versatile demountable tube suitable for the study of discharge under different conditions with a Langmuir probe and microwave interferometer. The second tube is a cold cathode discharge tube for the study of plasma-antenna system. The third one is used to create a hot cathode discharge for the study of plasma-antenna system.

The first plasma tube is 50 cm long Pyrex glass cylinder having an i.d. = 7.5 cm and open at both the ends (fig. 4.1a). It has two big side arms opposite to each other to accomodate the small horn antennas for plasma diagnostics, and a small side tube near one end for connecting it to the vacuum system. The ends of the tube are closed by flat circular aluminium discs held by the annular flanges worn on the

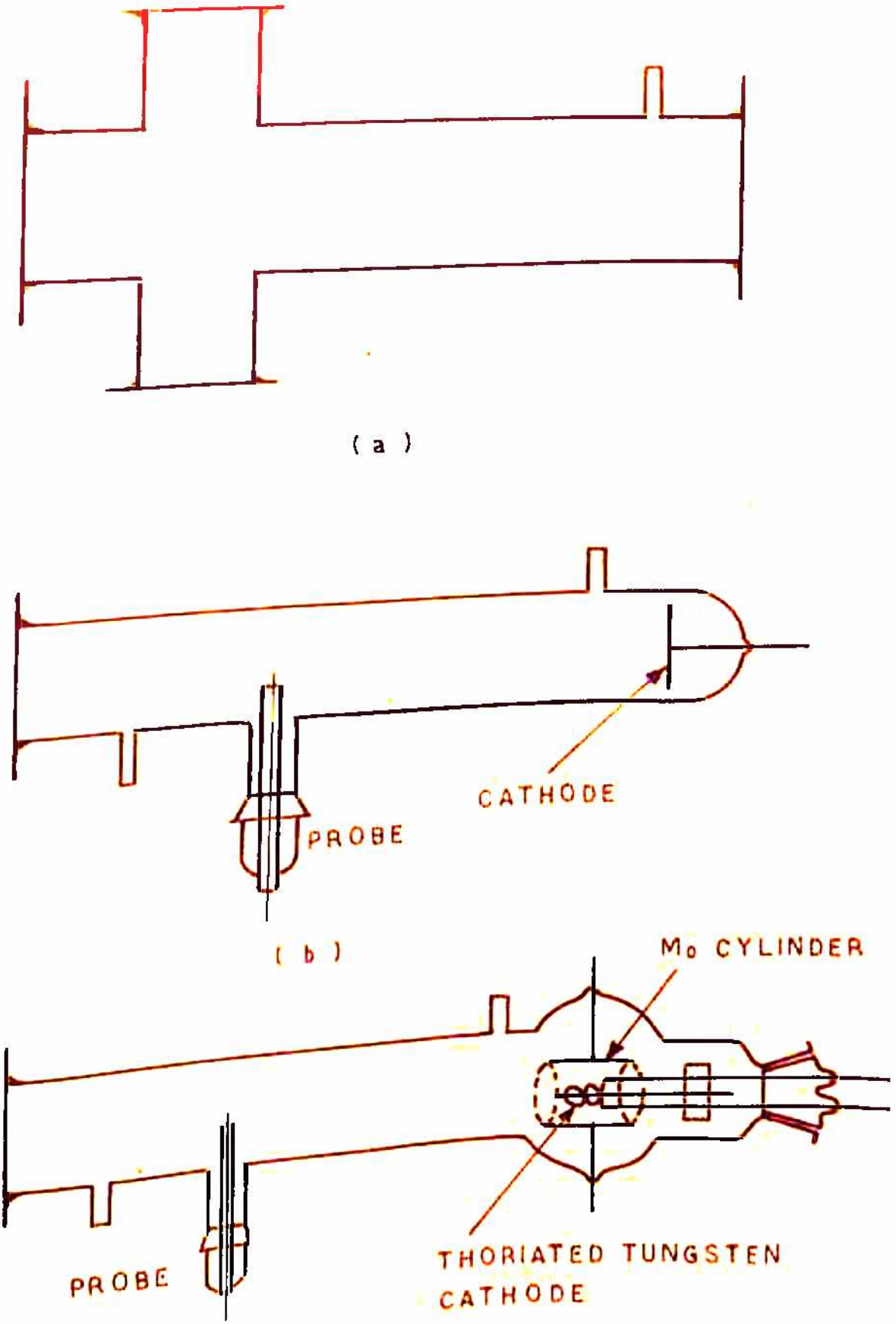

FIG. 4.1 DISCHARGE TUBES FOR PLASMA GENERATION

glass tube. These aluminium discs are also used as the electrodes for the electrical discharge. Aluminium has been chosen as the cathode material due to its low work function, low sputtering and good machineability. A cylindrical Langmuir probe coaxial to the tube is introduced through a vacuum seal in one of the discs. The tube is connected to a high vacuum system through the side tube and evacuated to a pressure of less than 10^{-4} torr. The ultra high purity (UHP) argon gas is introduced through another vacuum seal in the aluminium disc. The flow of the gas is finely controlled by means of a needle valve to maintain the tube pressure at the desired level. The pressure in the tube is monitored with a Pirani gauge connected through a T-arm in the side tube. The plasma is created by connecting the electrodes to a high voltage (1 KV) stabilised power supply through a variable resistance. The discharge current can be controlled by changing the variable resistance.

The second discharge tube is a 50 cm long straight cylindrical Pyrex glass tube having 5.0 cm i.d. and 5.5 cm o.d. (fig. 4.1b). A flat aluminium disc supported by a 1 mm diameter Tungsten wire sealed through the end of the glass tube acts as the cathode. The other end of the glasstube is open and terminates in a grounded flange. The exciting e.m. source is mounted on a metallic end-plate which covers the open end of the glass tube. It is held in proper

position by clamping with a perspex annular flange worn on the glass tube. Two thin side tubes are provided near each of the ends for connecting the tube with the vacuum system and the gas line. A cylindrical Langmuir probe is introduced perpendicular to the tube axis through a grounded glass conical joint in another side tube. The plasma was created by evacuating the tube and applying a high voltage (1 KV) across the cathode and the metallic end-plate which was grounded.

The third discharge tube (fig.4.1c) is similar to the second one except for the cathode which is directly heated thoriated Tungsten filament. The cathode is made in the shape of a helix and arc-welded with thick Tungsten leads running out of the glass tube. It is surrounded by a molybdenum cylinder maintained at a slightly negative potential. The glass tube is made in the shape of a big bulb around the cathode to protect it from the high temperature of the cathode. The dimensions and rest of the details of this tube are similar to the second tube described in the above paragraph. To generate the plasma the tube is evacuated to 10^{-4} torr. and then filled with UHP argon at a pressure in the range 0.1 to 1.0 torr. The filament is heated by supplying it 23 Amp current at 12 volts and applying a high voltage across the cathode and the grounded end-plate.

range is found to be suitable. The microwave interferometer gives an averaged plasma density and collision frequency over the entire cross-section of the plasma column.

A detailed account of Langmuir probe theories has been given by Swift and Schwar (1970) and a detailed description of microwave diagnostics has been given by Heald and Wharton (1965). Both of these methods, of course, have some inherent inaccuracies. The sources of error in the probe method have been discussed by Medicus and Wehner (1952), Nicoll and Basu (1962), and others. The inaccuracies in microwave method arise because of reflection, diffraction and other effects from the plasma and the glass tube, and due to the limitations of theoretical models (Warder et al 1962). Both of these methods have been simultaneously used to study a glow discharge at different pressures (0.1 - 1.0 torr) and different discharge currents (100 - 400 mA), in the discharge tube shown in fig. (4.1a) and described in the previous section. The microwave interferometer gives an average plasma density whereas the probe gives the on-axis plasma density. The probe results are averaged over the tube radius assuming a parabolic density profile and compared with the interferometer results. The theoretical results for the on-axis plasma density are also obtained by using the drift velocity data from Brown (1967) and averaged over the tube radius for comparison with the experimental results. For the plasma columns in the other two discharge tubes (fig. 4.1 b,c) the diameter is small as compared

The high vacuum system consists of a large three stage oil diffusion pump backed by an oil rotary pump. The system is fitted with moisture trap, cold trap, and air admittance-cum-isolation solenoid valve. Two pirani and a penning gauges are also fitted at proper locations to read the pressure in the system and the backing-line. The same rotary pump is used for roughing the system through a roughing-line. The system is capable of giving an ultimate vacuum of the order of 10^{-5} torr, without the liquid N_2 trap and a vacuum of the order of 10^{-6} torr. with the liquid N_2 trap.

4.3 PLASMA DIAGNOSTICS

The plasma diagnostics, particularly the measurements of plasma density and collision frequency, are very much essential for characterizing a plasma. The technique to be used for plasma diagnostic is decided by the range of the plasma density and the simplicity of operation. We decided to use a simple Langmuir probe and a microwave interferometer for this purpose. The Langmuir probe offers the advantages of simple hardware, a localized measurement and almost an unlimited range of measurable plasma densities. The microwave interferometer can be used to probe, steady as well as transient plasmas and gives a direct measurement of plasma density and collision frequency. The range of measurable, densities is, however, limited by the signal frequency and the sensitivity of the detector. For the range of plasma density of our interest the X-band frequency

to the incident wavelength and the interferometer can not be used. A novel method for the measurement of phase shift by plasma columns with a diameter comparable to the wavelength, has recently been presented by Kuwahara et al.(1974) but it requires the measurements at the cutoff plasma density. Since we do not attain the cutoff plasma density for the X-band frequencies and for the lower frequencies the plasma column diameter may be smaller than the wavelength, this method is not useful in our case. Hence, we used the Langmuir probe for the small diameter plasma columns.

1) Theory

Consider a small electrical probe immersed in a low pressure equilibrium, Maxwellian plasma, and having a radius much larger than the Debye length and much smaller than the electron mean free path. The electron current drawn by the probe is given by (Swift and Schwar 1970)

$$I_e = A\, n\, e\, \frac{\bar{C}_e}{4}\, e^{-(eV/k_\beta T_e)} \qquad (4.1)$$

Where A = Surface area of the probe

n = the undisturbed electron density

$\bar{C}_e$ = average random electron speed

$V = V_p$ (probe potential) - V_a (applied potential)

k_β = Boltzmann constant

T_e = the electron temperature

Thus, the electron temperature can be obtained by the slope of the $\ln(I_e)$ vs V_a curve. A similar expression for the ion current can be written as (Swift and Schwar 1970):

$$I_i = 0.6 \, A \, n \, e \, (k_\beta T_e / m_i)^{1/2} \qquad (4.2)$$

where m_i is the ionic mass.

It has been shown in the preceding chapter (eq.3.7) that the electron density in the positive column of a d.c. discharge $n(\rho)$, at a radial distance ρ is written as :

$$n(\rho) = n_o \{1 - (\rho/R)^2\} \qquad (4.3)$$

where R is the radius of the plasma column and n_o is the electron density at the axis of the tube (at $\rho = 0$). It is related to the discharge current, by the following relation:

$$n_o = I/(1.36 \, e v_o R^2) \qquad (4.4)$$

where v_o is the electron drift velocity.

In a microwave interferometer the phase shift due to the plasma is measured by comparing the transmitted signal with a reference signal. The phase shift introduced by a collisionless plasma slab of thickness d in a microwave transmission path, under the adiabatic approximation, is related to the average plasma density $\bar{n}$ by (Heald and Wharton, 1965)

$$\bar{n} = (2.05 \, f \triangle \phi / d) \ cm^{-3} \qquad (4.5)$$

where f is the incident microwave frequency in H_z, $\triangle \phi$ is the phase shift in degrees and d is in cm.

ii) Experimental Set-up

The experimental setup for the simultaneous measurement of plasma density by Langmuir probe and microwave interferometer is schematically shown in fig.(4.2) and photographically in fig.(4.3). The Langmuir probe consists of a 0.5 mm diameter tungsten wire sealed in a glass capillary tube such that about 5 mm length of the wire is exposed. The probe is positioned at the axis of the tube as described in the previous section. The probe is connected to a stabilised power supply capable of giving a variable voltage from - 250 V to + 250 V with respect to the anode which is gounded. An X-Y recorder is connected as shown in the fig.(4.2). The probe voltage is manually swept from the extreme negative to slightly positive value and the I-V characteristics is obtained on the X-Y recorder. At positive bias voltages the plasma is greatly disturbed by the probe and so we omit the electron current saturation part of the I-V characteristics.

A 2K25 reflex klystron is used as a microwave source. The microwave signal is amplitude modulated by a 1 KHz square-wave signal. The input signal is fed into the H-arm of a hybrid tee through a 10 dB multihole directional coupler. A direct reading wave-meter and a crystal detector are connected to the auxiliary arm of the directional coupler. The output of the crystal detector is fed to an oscilloscope. The E-arm of the hybrid tee is terminated by a matched termination. A pair of

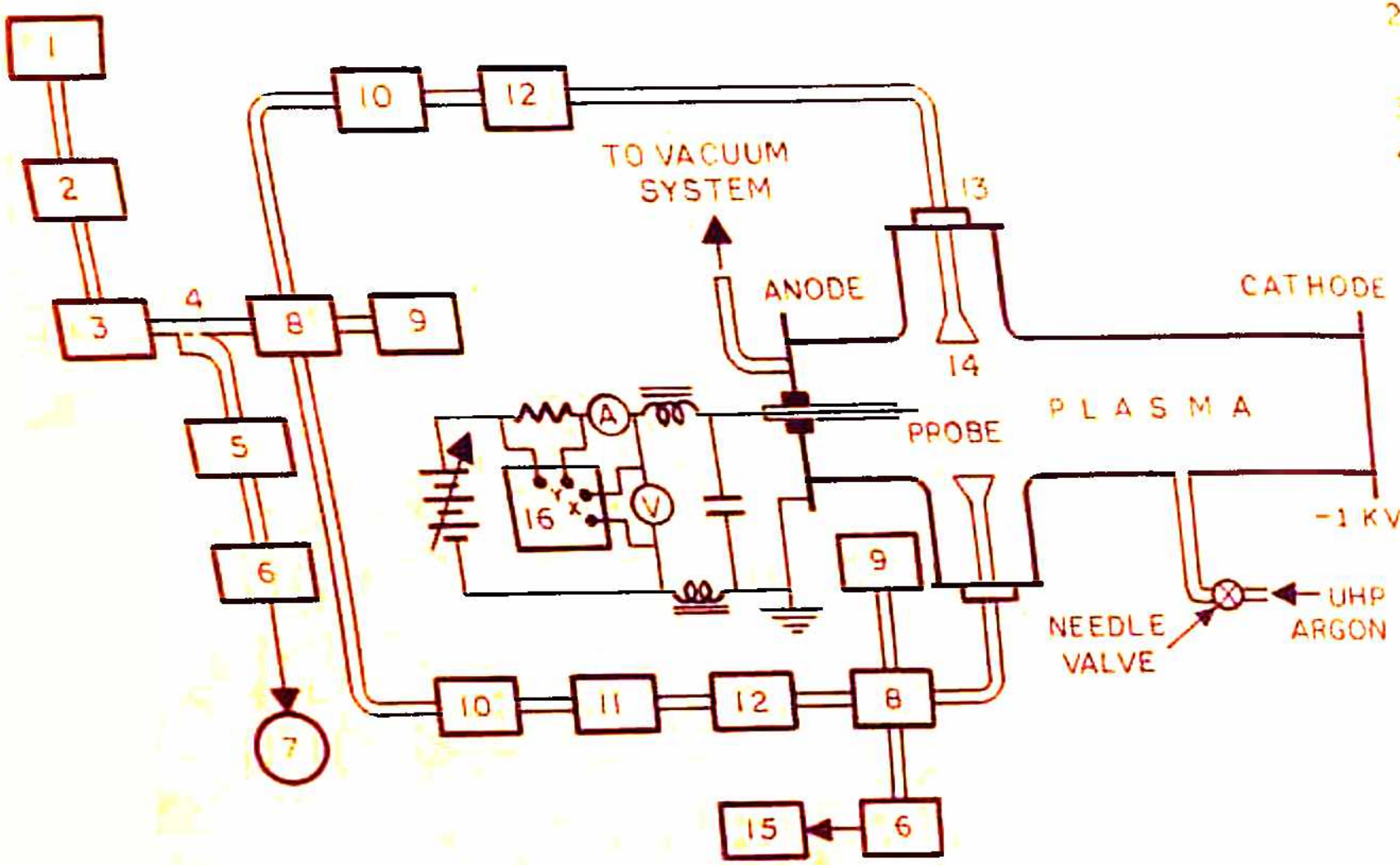

1 MODULATOR
2 KLYSTRON POWER SUPPLY
3 KLYSTRON MOUNT
4 MULTIHOLE DIRECTIONAL COUPLER
5 FREQUENCY METER
6 CRYSTAL DETECTOR
7 OSCILLOSCOPE
8 MAGIC TEE
9 MATCHED TERMINATION
10 VARIABLE ATTENUATOR
11 VARIABLE PHASE-SHIFTER
12 TUNER
13 WAVEGUIDE-VACUUM WINDOW
14 HORN ANTENNA
15 VSWR METER
16 X-Y RECORDER

FIG. 4.2 SET UP FOR PLASMA DENSITY MEASUREMENT BY LAMGMUIR PROBE AND MICROWAVE PHASE – SHIFT INTERFEROMETER.

small nondirective horn antennas (4.0 x 2.5 cms) is introduced into the side arms of the plasma chamber through the waveguide-vacuum windows. The horn aperture is kept very near to the plasma column. The waveguide-vacuum windows are constructed by pressing a thin (0.2 mm) mica sheet against an O-ring between a choke flange and a plane flange. Insulating screws are used to fasten the window which also serve as an insulation between plasma and the ground. The impedance of the antennas is matched to the line by using tuners. The output signals from the reference path and the transmission path are combined in a hybrid tee and the resultant signal is detected in the E-arm, the H-arm being terminated by a matched termination. The electrical lengths of the two paths are kept equal to avoid a phase difference if the klystron frequency drifts. The interferometer is first adjusted for a null in the absence of plasma. The presence of the plasma introduces a phase shift in the transmission path and a net resultant signal appears in the detector arm. This phase shift in the transmission path is nullified by introducing an equal phase shift $\Delta\phi$ in the reference path by means of a direct reading phase shifter. The phase shift is measured at the two different signal frequencies to make sure whether it is $\Delta\phi$ or $\Delta\phi+2m\pi$. The product $f\Delta\phi$ remains the same at the two frequencies when $m = 0$.

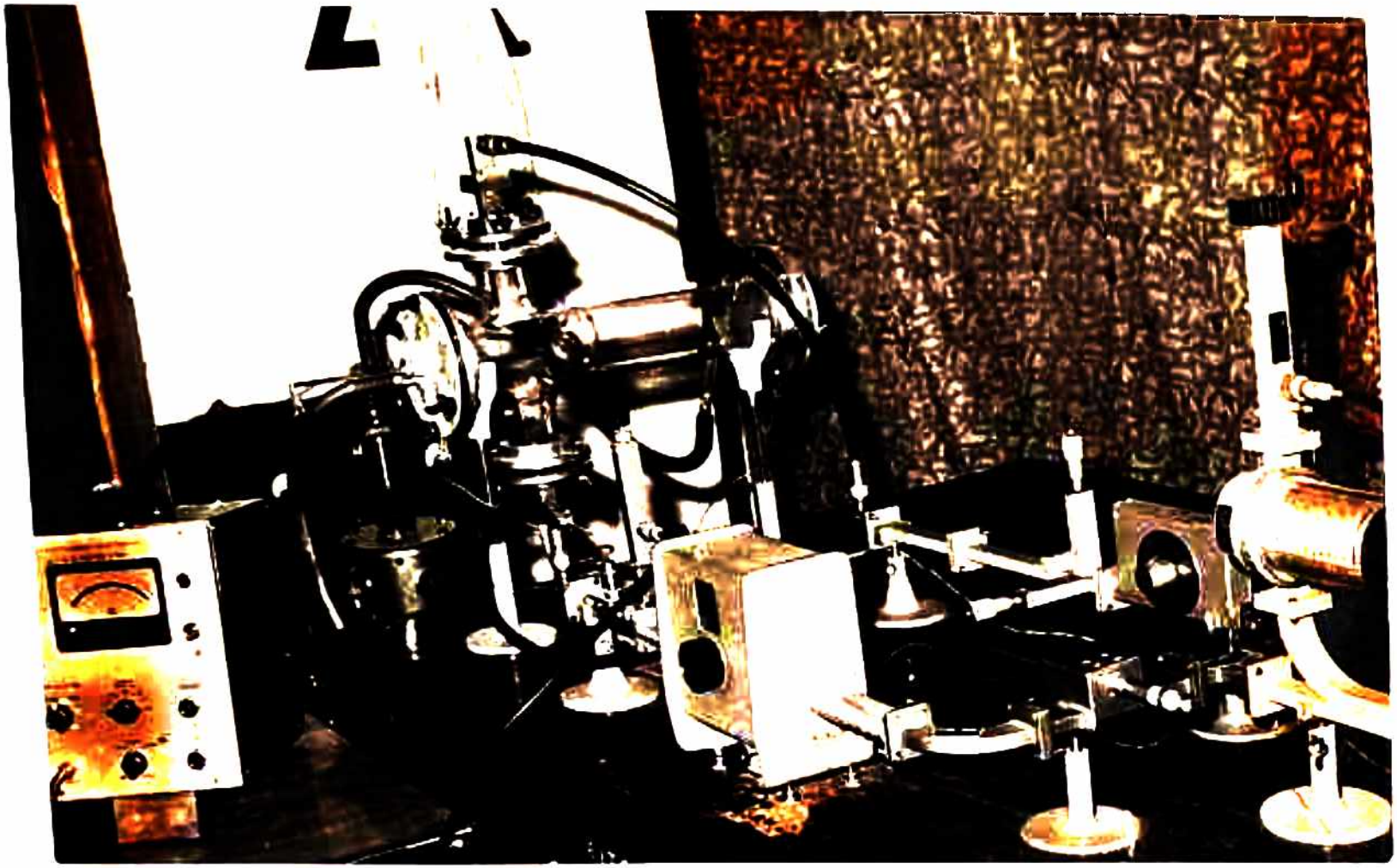

FIG. 4.3 SET-UP FOR PLASMA DIAGNOSTICS BY LANGMUIR PROBE AND MICROWAVE INTERFEROMETER

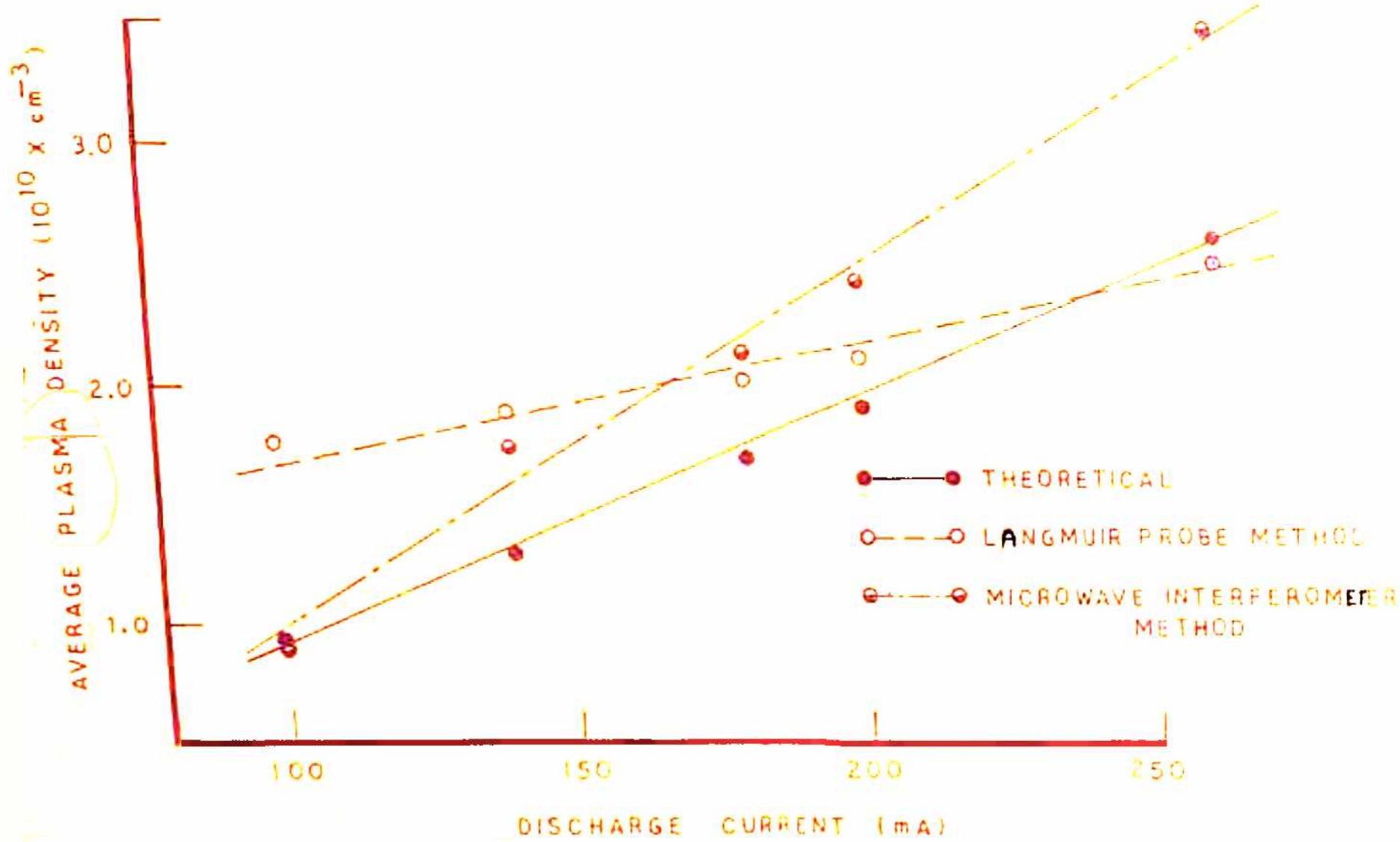

FIG. 4.4 EXPERIMENTAL RESULTS FOR AVERAGE PLASMA DENSITY.

iii) Experimental Results

The on-axis plasma denisty n_o is obtained by two methods, an experimental and a theoretical. The experimental values of n_o are obtained by first evaluating the electron temperature T_e from the slope of $\ln(I_e)$ vs V_a curve and then using this value of T_e in expression (4.2). The ion saturation current is noted at a fairly negative potential ($eV/kT_e >> 1$) where the electron current contribution is almost negligible. The theoretical values of n_o are obtained from the relation (4.4) using the values of drift velocity at various E/P values (E = electric field, P = pressure) taken from Brown (1967). The average plasma densities are now obtained by integrating eqn.(4.3) and using the n_o values obtained by the above two methods. The microwave interferometer directly gives the average plasma denity through equation (4.5). The typical results for average plasma densities obtained by the above three methods, for various discharge currents at 0.1 torr are plotted in fig. (4.4). The results are found to be in a good agreement. The deviation of the Langmuir probe results from the theoretical ones at low dischrage currents may be attributed to the inaccuracy in the measurement of the very small ion current. The disagreement of microwave interferometer results with the theoretical results is considered to be due to the reflection and interference effects since the plasma diameter is only a few wavelengths thick.

Similar density measurements were performed, using the Langmuir probe only, on the plasma in the other discharge tubes described in the previous section. The discharge tube shown in fig.(4.1b) gave a maximum plasma density of the order of 4×10^{10} cm^{-3} at 200 mA current at a pressure of 0.2 torr. At the higher current or pressure the discharge became unstable. The discharge tube with hot cathode (fig.4.1c) was operated around 0.1 torr upto 600 mA discharge current. The Tungsten cathode was heated with 23 amp current at 12 V a.c. A maximum plasma density of the order of $10^{11} cm^{-3}$ was obtained. The tube could be operated only for short intervals due to the problem of overheating.

4.4 EXPERIMENTAL SETUP FOR RADIATION PATTERN AND INPUT IMPEDANCE MEASUREMENT

The complete experimental setup for the radiation pattern and input impedance measurement of a plasma-antenna system is schematically shown in fig.(4.5). The discharge tube shown in fig.(4.1c) and described in section (4.2) is used for plasma generation. The tube is connected to a high vacuum system and a gas-line supplying UHP Argon gas at a controlled rate. The vacuum pumps and the gas supply are continuously run to maintain a minimum impurity level. The pressure in the tube is maintained at a constant level around 0.1 torr. and measured with a Pirani gauge. The plasma is created by heating the Tungsten cathode and applying a high voltage across the cathode and the grounded end-plate. The

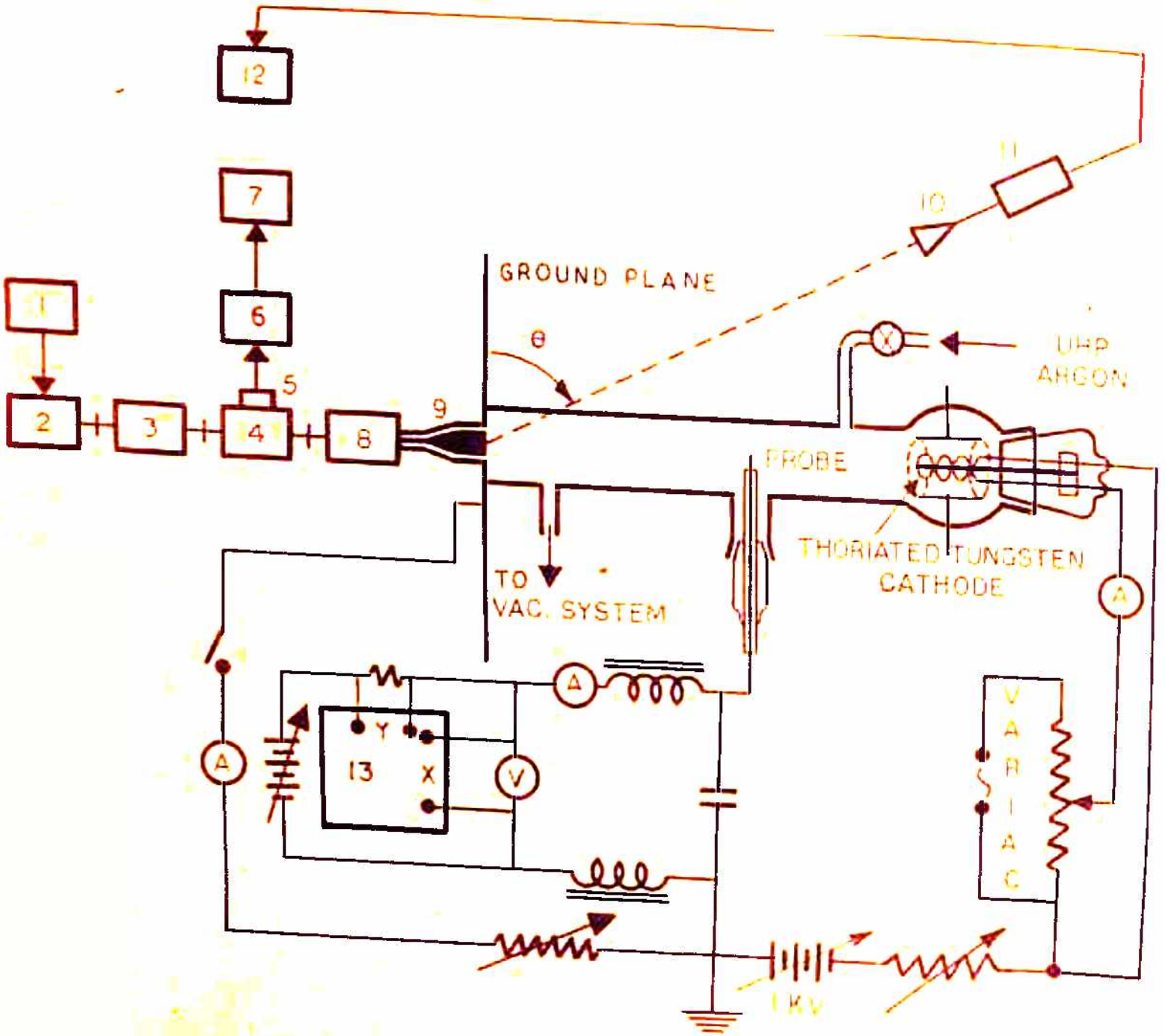

1. SIGNAL GENERATOR
2. ISOLATER
3. ATTENUATOR
4. SLOTTED-LINE SECTION
5. TUNABLE PROBE
6. CRYSTAL DETECTOR
7. INDICATOR
8. COUPLER
9. TAPERED COAXIAL-LINE
10. RECEIVING HORN ANTENNA
11. CRYSTAL DETECTOR
12. SENSITIVE POWER METER
13. X-Y RECORDER

FIG. 4.5 SET UP FOR STUDY OF PLASMA – ANTENNA SYSTEM

plasma density is measured with a cylindrical Langmuir probe method discussed in the preceding section.

The plasma column is excited by means of a magnetic ring source. It has been shown in Chapter 2 that a magnetic ring source can be approximated by a narrow annular slot in a large conducting screen placed at the location of the ring source. It is required that the slot width should be small compared to a wavelength and the electric field in the slot be radial and uniform for the annular slot to be a good approximation of the magnetic ring source. The annular slot may be illuminated by means of a circular waveguide carrying the circular symmetric TM_{01}-mode or by a coaxial line excited in the dominant TEM-mode. A coaxial line is preferred, because its central conductor can be used as support for the circular disc which is a part of the ground plane within the annular slot. Two different annular slots were constructed. The first one has a mean radius 1.02 cm and a slot width 1 mm. The other one has a mean radius 1.92 cm and a slot width 1.5 mm. The first slot correspond to $k_0a = 2.0$ and the second one corresponds to $k_0a = 3.83$ at a frequency around 9.5 GHz. A narrow annular slot with later dimensions gives a single narrow peak in free space (Blass 1961). Since an annular slot of such a narrow width has a very small impedence, an impedence matching transformer is necessary to match the slot impedence to the 50 ohm coaxial line. The continuous tapers were constructed to match

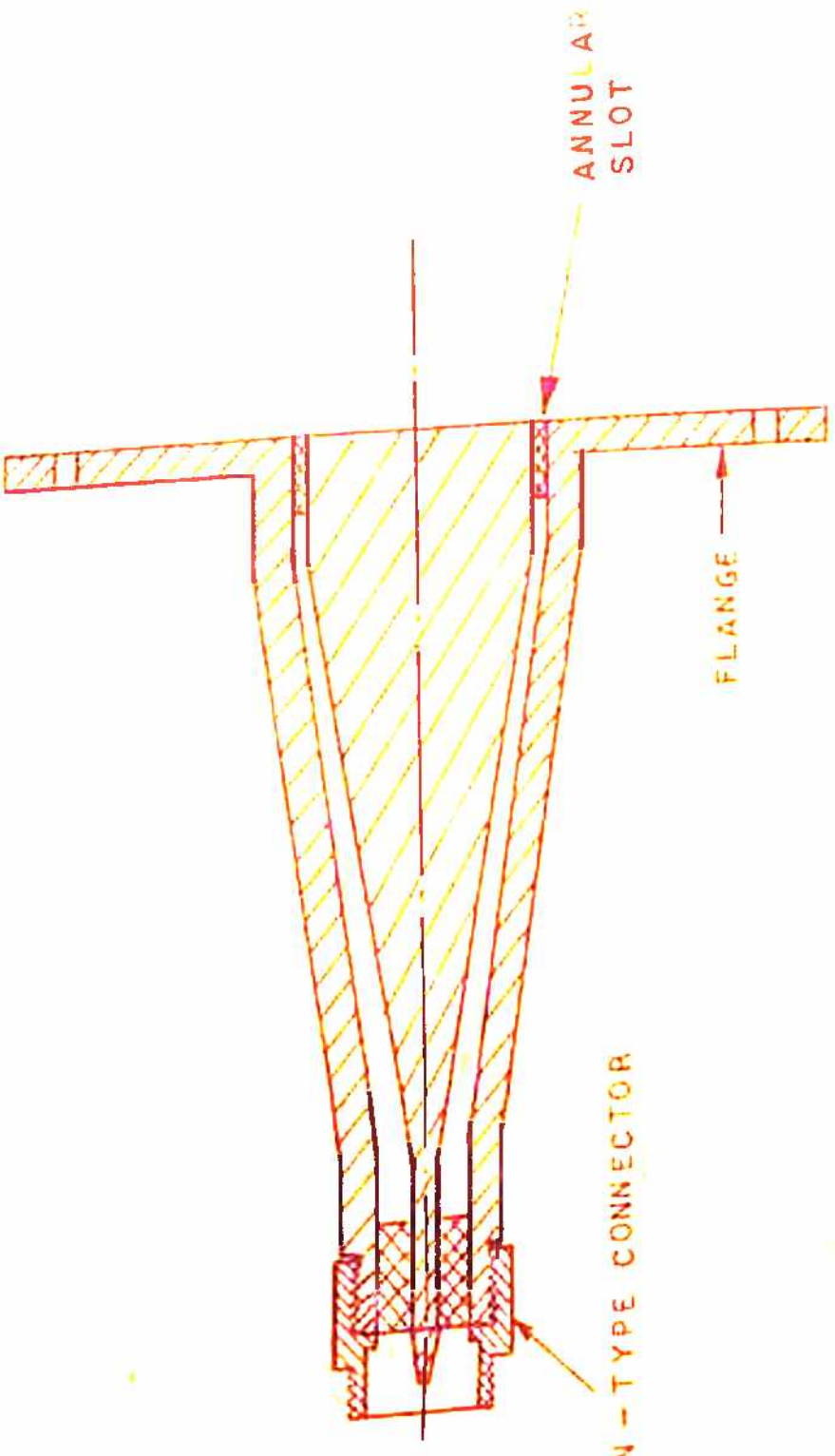

FIG. 4.6 TAPERED COAXIAL LINE AND ANNULAR SLOT

the impedence. The length of the tapered section was taken to be equal to one wavelength for the smaller slot and three wavelengths for the larger slot. The coaxial tapered section was brazed to the circular flange which is to be used as the end plate for the discharge tube (figs. 4.6 and 4.7). The whole thing is vacuum tight and the coaxial taper terminates into an N-type connector. A large square conducting screen was separately attached to the circular disc by means of an overlapping annular ring. The tapered line is connected to the microwave line (fig.4.5). The microwave line consists of a signal generator, an isolater and a slotted line. The microwave signal is amplitude modulated by a 1 KHz square wave signal. A travelling voltage probe is inserted into the slotted line and connected to the crystal detector which is connected to a VSWR meter.

To measure the θ-plane radiation pattern a standard gain (17dB) pyramidal horn antenna is rotated in a horizontal plane containing the axis of the plasma column, around a vertical axis passing diametrically through the centre of the annular slot. The distance between the annular slot and the receiving horn aperture is about 2.5 m. A pointer attached with the rotating arm rotates on a graduated circular arc of 50 cm radius and gives the angular position of the horn. The receiving horn is connected to a crystal detector which in turn is connected to a VSWR meter. The VSWR meter gives the received signal directly in dB.

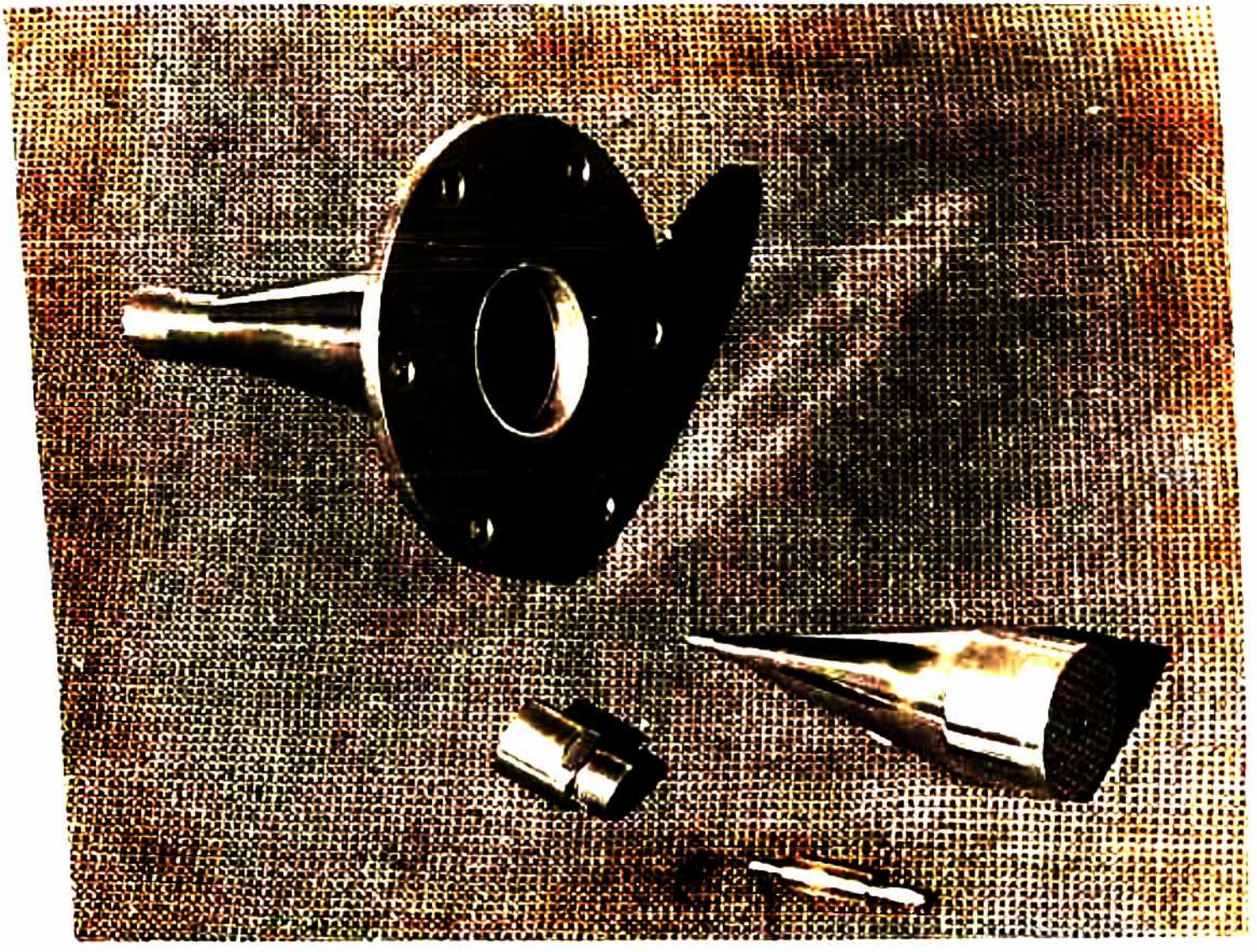

FIG. 4.7 TAPERED COAXIAL LINE WITH FLANGE

To measure the input impedance of the antenna-system the standard slotted-line technique is used. Since it is difficult to measure the impedance at the annular aperture itself, the VSWR and the shift of minimum from the short circuit to the loaded condition are measured at the input of the tapered coaxial section. These two parameters are used to calculate the slot impedance by using a Smith chart or the transmission line equation (Rubia Mol). The calculated value of the impedance at the input of the tapered section could be transferred to any other part on the tapered section if the variation of the characteristics impedance with length was known. In our case of the linear taper this variation is not known and hence the actual slot impedance cannot be measured. However, since the tapered section has small losses the functional dependance of slot impedance with the plasma properties will be approximately given by that at the input of the tapered section.

Some preliminary measurements of radiation pattern of the magnetic ring source in the absence and in the presence of plasma were performed. But due to severe reflections from the walls, floor and table etc. the radiation pattern displayed sharp amplitude variations. Due to the presence of these variations it was not possible to make any reliable measurements. A microwave anechoic chamber is essential for the indoor measurements of the radiation patterns. The microwave absorbing materials used for the anechoic chambers was not available. So

an attempt was also made to make a microwave absorbing material by impregnating the polyurethane foam with the colloidal graphite. But due to many practical difficulties a good absorbing material could not be obtained.

REFERENCES

Alday, J.R. (1962) Microwave plasma beam sweeping array, IRE Trans., Vol AP-10, No 1, p 96

Bhat, B and Rao, B.R.(1973) Experimental investigations of the impedance behaviour of a cylindrical antenna in a collisional magnetoplasma, IEEE Trans., Vol AP-21, No 1, p 70

Blass, J.(1961) Slot antennas, Antenna engineering handbook, ed by H.Jasik, (McGraw Hill)

Brown, S.C.(1967) Basic data of plasma physics, (M.I.T. Press), p 94

Burykin, Y.I., Levitskiy, S.M. and Martyenko, W.G.(1975) The radiation of electromagnetic waves by a variable cross-section cylindrical plasma waveguide, Rad.Eng. and Electron. Phys., Vol 20, No 11, p 86

Cloutier, G.G. and Bachynski, M.P.(1963) Antenna characteristics in the presence of a plasma sheath, Electromagnetic theory and antennas Pt 1, ed by E.C.Jordan, p 557

Flock, W.L. and Elliott, R.S.(1962) The radiation pattern of a microwave horn and a plasma layer, IRE Trans., Vol AP-10, No 1, p 65

Francis, G.(1956) The glow discharge at low pressure, Handbuch der physik, Vol 22, ed by S.Flügge, (Springer-Verlag)

Ghose, R.N. (1967) Plasma antenna in a nuclear environment IEEE Trans., Vol AP-15, No 5, p 713

Golden, K.E.(1965) Plasma simulation with an artificial dielectric in a horn geometry, IEEE Trans., Vol AP-13, No 4, p 587

Gupta, K.C.(1971) Narrow beam antenna using an artificial dielectric medium with permittivity less than unity. El.Lett., Vol 7, No 1, p 16

Gupta K.C. and Bahl, I.J.(1974) A leaky wave antenna using an artificial dielectric medium, IEEE Trans., Vol AP-22, No 1, p 119

Heald, M.A. and Wharton, C.B.(1965) Plasma diagnostics with Microwaves, (John Wiley & Sons)

Jacavanco, D.J. and Melts, G.(1964) An experimental investigation of antenna pattern distortion due to a plasma layer, IEEE Trans., Vol AP-12, No 3, p 365

Jacavanco, D.J.(1965) Electromagnetic properties of a plasma covered antenna, J.Res.Nat.Bur.Stand.,Vol 69D, No 7, p 965

Karas, N.V. and Antonucci, J.D.(1968) An experimental study of simulated plasma covered slots on cylinders and cones, IEEE Trans., Vol AP-16, No 2, p 242

_____ (1970) Application of plasma simulation to radiators on non-planar surface, IEEE Trans., Vol AP-18, No 2, p 292

Kaufman, I. and Steier, W.H. (1963) A plasma antenna and a wave filter, Electromagnetic theory and antenna Pt 2, ed by E.C. Jordan, (Pergamon Press)

Kristal, R.and Shizume, P.(1967) Antenna plasma interaction in a conical geometry, IEEE Trans., Vol AP-15, No 5, p 710

Kuwahara, C., Matsura, K. and Miyahara, A.(1974) Density measurement of plasma with a small diameter by a microwave interferometer, Jap.J.App.Phys., Vol 13, No 2, p 327

Levitskiy, S.M. and Burykin, Y.P.(1973) Radiation of electromagnetic waves by plasma waveguides, Rad.Eng.Electron., Phys.,Vol 18, No 12, p 1938

Levitskiy, S.M. and Burykin, Y.I.(1974)Radiation of electromagnetic waves from a rectangular plasma waveguide using surface waves, Rad. Eng.Electron.Phys.,Vol 19, No 9, p 57

Medicus, G. and Wehner,G.(1952) Reliability of probe measurements in hot cathode gas diodes, J. App.Phys., Vol 23, No , p 1035

Messiaen, A.M. and Vandenplas, P.E. (1967) Theory and experiments of the enhanced radiation from a plasma coated antenna, El. Lett., Vol 3, No 1, p 26

Meyer, P. Vernet, N. and Lassudrie-Duchesne, P.(1974) Theoretical and experimental study of the effects of the

sheath on an antenna immersed in a warm isotropic plasma, J.App.Phys., Vol 45, No 2, p 700

Nakatani, D.T. and Kuehl, H.H.(1976) Input impedance of a short dipole antenna in a warm magnetoplasma, Radio Science, Vol 11, No 6, p 517

Nicoll, G.R. and Basu, J.(1962) Comparison of microwave and Langmuir probe measurements on a gaseous plasma, J.Electron.Control, Vol 12, No 1, p 23.

Preis, D.H. Ward, M.A.V. and King, R.W.P.(1975) Experimental aspects of antennas in plasma, Int. Conf. Plasma Sci., Ann Arbor, Mich., USA

Rotman, W.(1962) Plasma simulation by artificial dielectrics and parallel plate media, IRE Trans., Vol 10, No 1, p 82

Rubin, R.(1961) Antenna measurements, Antenna engineering handbook, ed by H.Jasik, (McGraw Hill)

Smith,T.M. and Golden,K.E.(1965a) Radiation patterns from a slotted cylinder surrounded by a plasma sheath, IEEE Trans. Vol AP-13, No 5, p 775

_____ (1965b) Radiation patterns of a slot covered by a simulated plasma sheet, IEEE Trans., Vol AP-13, No 2, p 285

Swift, C.T., Gooderum, P.B. and Castellow, S.L.(1969) Experimental investigation of a plasma covered axially slotted cylinder antenna, IEEE Trans., Vol AP-17, No 5, p 598

Swift J.D. and Schwar, M.J.R.(1970) Electrical probes ofor plasma diagnostics,(Iliffe Books Ltd)

Tyras, G., Bargeliotes, P.C.Hamm, J.M. and Schell,R.R.(1965) An experimental study of plasma sheath effects on antennas, J.Res.Nat.Bur.Stand, Vol 69D, No 6, p 839

Warder,R.D., Brodwin, M. and Cambel, A.B.(1962) Sources of efror in microwave diagnostics of plasmas, J.App.Phys. Vol 33, No 9, p 2868

Addendum

Presson, K.B.(1965) Brush cathode plasma - a well behaved plasma, J.App.Phys., Vol 36, No 10, p 3086

CHAPTER 5

RADIATION FROM A RADIAL WAVEGUIDE IN AN ANISOTROPIC PLASMA MEDIUM

6.1 INTRODUCTION

The study of radiation from sources in anisotropic plasma medium has received a great deal of attention due to its relevance to space communication through ionosphere and re-entry plasma sheaths. The detailed theories of radiation from sources in anisotropic media have been given by Bunkin (1957), Kogelnik (1960, 1963), Arbel and Felsen(1963), Clemmow (1963) and others. Wait (1964) has given a good review of sources in anisotropic media. Recently, Daniele and Zich (1973), Akindinov et al (1974) and others have also analysed the problem of radiation from localised sources in anisotropic plasma media. The antennas to be used for re-entry vehicles are required to be suitable for flush-mounting. The externally mounted type of antennas have been considered, but due to the heating caused by the external protrusion, have found limited usage. Moreover, an omni-directional radiation pattern coverage is required for the antenna system to prevent or minimise the fading or loss of signal due to random tumbling or rolling of the re-entry vehicle. For the spin-stabilized vehicles the antenna radiation pattern is required to be omnidirectional at least in the plane orthogonal to the spin axis or a despun type of antenna is used.

In the present chapter we propose that an open-ended radial waveguide can be used as a suitable spacecraft antenna.

A radial waveguide consists of two parallel circular discs separated by a small distance and excited by a circularly symmetric source at or near the axis (Harrington 1961). The geometry of the radial waveguide easily lends itself to flush-mounting in the nose-portion of the space-vehicle. The central post is used to hold the two halves together. The far field radiation patterns of an open-ended radial waveguide in free space have recently been obtained by Holst (1973). The azimuthal plane pattern for the TEM (TM_{00}) mode was found to be isotropic and the axial plane patterns were found to depend upon the waveguide radius. Moreover, the desired pattern shapes can also be obtained, using the radial waveguides, in both the axial and the azimuthal planes. In the axial plane this is achieved by constructing an array of radial waveguides along the axis. The desired pattern in the azimuthal plane can be obtained by combining different modes in the radial waveguide with proper relative amplitudes. Thus from the view point of the radiation pattern also, the open radial waveguide possesses favourable characteristics.

In the following sections we proceed to evaluate the performance of an open-ended waveguide antenna excited in the TM - mode in an unbounded, lossless and anisotropic plasma medium. The radiation patterns are obtained at high frequencies, under the quasi-longitudinal (q.l) approximation (Ratcliffe 1959).

5.2 FORMULATION OF THE PROBLEM

Consider a radial waveguide (fig.5.1) consisting of two parallel circular discs of radius a, separated by a distance b, and excited in the TM-mode by a source situated at its axis (Z-axis). The waveguide is surrounded by an unbounded, lossless, and anisotropic plasma medium characterised by the tensor permittivity

$$\hat{\epsilon} = \begin{bmatrix} \epsilon_1 & -j\epsilon_2 & 0 \\ j\epsilon_2 & \epsilon_1 & 0 \\ 0 & 0 & \epsilon_3 \end{bmatrix} \qquad (5.1)$$

with

$$\epsilon_1 = 1 - X/(1-Y^2) \qquad (5.2a)$$

$$\epsilon_2 = XY/(1- Y^2) \qquad (5.2b)$$

$$\epsilon_3 = 1 - X \qquad (5.2c)$$

where $X = \omega_p^2/\omega^2$ and $Y = \omega_c/\omega$; ω_p and ω have their usual meanings and ω_c is the cyclotron frequency. The anisotropic plasma characterised by the eqn.(5.1) is generally used as a model of the ionosphere with the magnetic field along the Z-axis.

For the TM mode, the field components in a radial waveguide in the cylindrical coordinate system , are given by

$$E_\rho = \frac{1}{j\omega\epsilon} \frac{n\pi}{b} \sin(n\pi z/b) \sin n\phi \, H_n^{(2)}(k_\rho \rho) \qquad (5.3a)$$

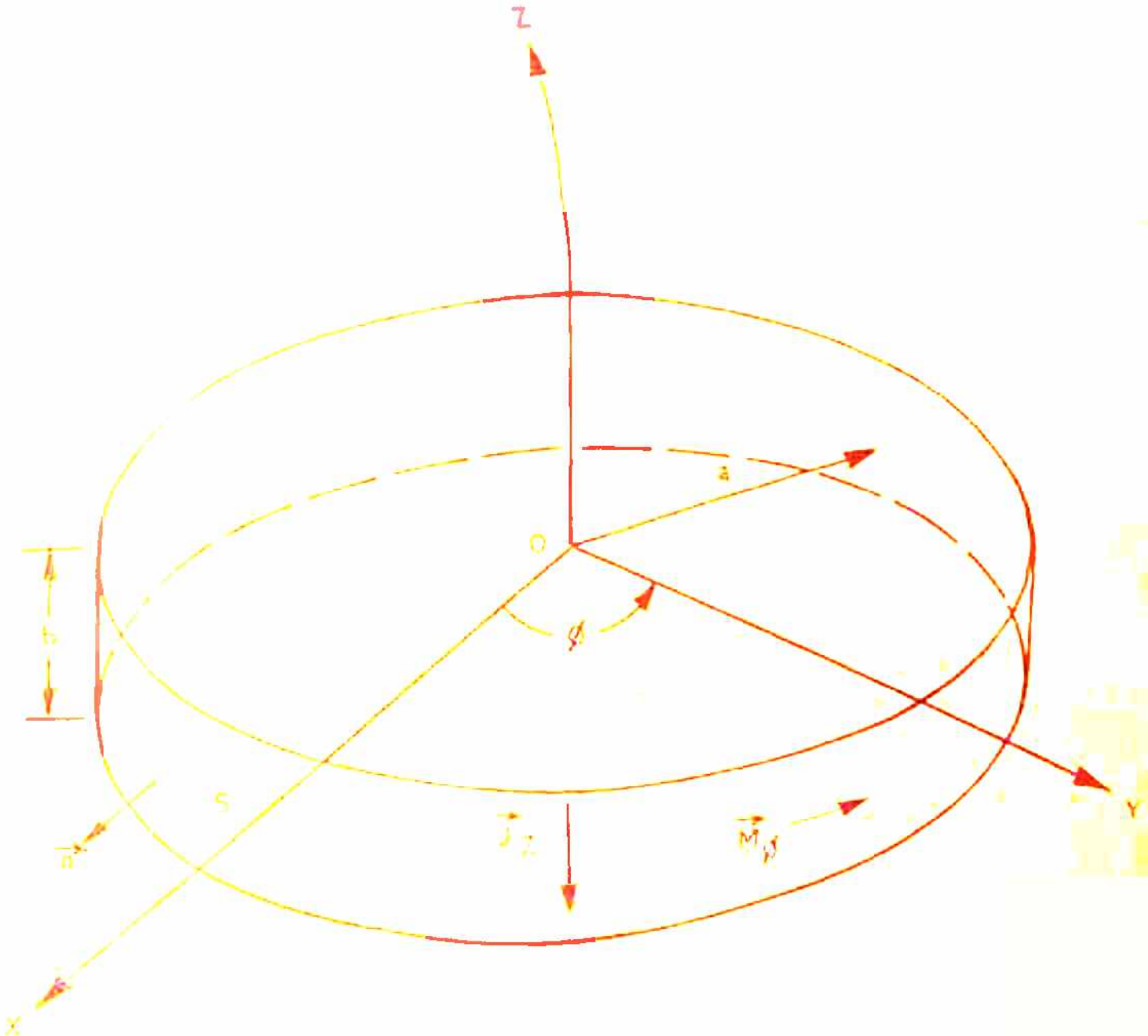

FIG. 5.1 THE GEOMETRY OF THE RADIAL WAVEGUIDE.

$$E_z = \frac{k_\rho^2}{j\omega\epsilon} \cos(n\pi z/b) \cos m\phi \; H_m^{(2)}(k_\rho \rho) \qquad (5.3b)$$

$$H_\phi = -\cos(n\pi z/b) \cos m\phi \; H_m^{(2)\prime}(k_\rho \rho) \qquad (5.3c)$$

where the prime denotes the derivative with respect to ρ ; m and n are integers and k_ρ is the radial propagation constant given by

$$k_\rho^2 = k^2 - (n\pi/b)^2 \qquad (5.4)$$

with k the propagation constant in the medium of the radial waveguide, for free space $k \equiv k_o = \omega\sqrt{\mu_o \epsilon_o}$, where μ_o and ϵ_o have their usual meanings.

Now we restrict ourselves to the case in which there is no Z-variation of the waveguide fields. This is accomplished by putting n = 0 in eqns. (5.3) and making the plate separation b less than half-wavelength to render all the modes with Z-dependence below cut-off. The fields at the waveguide aperture are now replaced by the equivalent fictitious electric and magnetic surface current distributions given by

$$\bar{J} = \hat{n} \times \bar{H} = \hat{a}_z H_{mo} \cos m\phi \qquad (5.5a)$$

and

$$\bar{M} = \bar{E} \times \hat{n} = \hat{a}_\phi E_{mo} \cos m\phi \qquad (5.5b)$$

where $\hat{n}$ is the unit vector normal to the curved surface S and a_z and a_ϕ are the unit vectors.

$$H_{mo} = H_m^{(2)}(k_\rho a) \qquad (5.6a)$$

$$E_{mo} = \frac{k_\rho^2}{j\omega\varepsilon_o} H_m^{(2)}(k_\rho a) \qquad (5.6b)$$

Assuming a harmonic time dependence of the form $\exp(-j\omega t)$, which is suppressed throughout, the source form of the Maxwell's equations for the electric and magnetic fields are written as

$$\nabla \times \bar{E} = j\omega \mu_o \bar{H} - \bar{M} \qquad (5.7a)$$

and

$$\nabla \times \bar{H} = -j\omega\varepsilon_o \hat{\varepsilon}\, \bar{E} + \bar{J} \qquad (5.7b)$$

5.3 SOLUTION OF THE PROBLEM

A formal solution of the problem of radiation from sources in anisotropic media has been given by Bunkin (1957). Kuehl (1962) obtained the complete solution for radiation from a dipole in an anisotropic plasma medium for various special cases. Marini (1963) considered a more general case and obtained the solution for radiation fields in an anisotropic plasma under the assumption that the signal frequency is much higher than the cyclotron frequency ($\omega >> \omega_e$) but only greater than the plasma frequency ($\omega > \omega_p$). The method of solution involves the standard technique of taking the Fourier transform of the Maxwell's eqns.(5.7), solving the resulting system of algebraic equations by matrix methods and evaluating the inverse Fourier transform integral by the method of residues and the method of steepest-descents. The steepest-descents evaluation gives a transcendental equation, which

can be solved only for some special cases. Marini (1963) has solved this equation under the assumption of high frequencies and using the quasi-longitudinal (q.l) approximation. The q.l approximation is used in the Appleton-Hartee equation(Ratcliffe 1959) to obtain the indices of refraction for the ordinary and the extra-ordinary waves. The q.l approximation holds for most of the region surrounding the source except in the vicinity of $\theta = 90^{\circ}$.

The far field radiation pattern are expressed in terms of the electric and magnetic radiation vectors given by

$$\bar{V}_{1,2} = \int_S \int \bar{J} \exp (j k_o \eta' \rho' \cos \pm j k_o \eta' h z') \, d s' \quad (5.8a)$$

and

$$\bar{M}'_{1,2} = \int_s \int \bar{M} \exp (j k_o \eta' \rho' \cos \pm j k_o \eta' h z') \, d s' \quad (5.8b)$$

where

$$\eta'^2 = 1 - X \quad (5.9a)$$

$$h = XY/2\eta'^2 \quad (5.9b)$$

$$\cos = \cos\theta \cos\theta' + \sin\theta \sin\theta' \cos(\phi - \phi') \quad (5.9c)$$

and $$ds' = a d\alpha' \, d\phi' \quad (5.9d)$$

The primed quantities* denote the source coordinates, while the unprimed quantities denote the far field coordinates. In eqn.(5.8) the upper sign is associated with the index '1' and the lower sign with the index '2'. The radiation vectors associated with the index '1' correspond to the ordinary wave

* $(\rho', \theta', \phi', z' \text{ and } s')$

when $\theta < 90^{\circ}$ and to the extra-ordinary wave when $\theta > 90^{\circ}$, and vice-versa for the index '2'.

If we assume the separation b to be very small, we can take $\theta' = 90^{\circ}$ and then the radiation vectors take the following forms

$$\bar{V} = \hat{a}_z \, abH_{mo} \int_0^{2\pi} \text{Cos } m\phi' \exp\left\{ j\alpha \text{ Cos}(\phi - \phi') \right\} d\phi' \qquad (5.10a)$$

$$\bar{M}' = \hat{a}_\phi \, ab \, E_{mo} \int_0^{2\pi} \text{Cos } m\phi' \exp\left\{ j\alpha \text{ Cos}(\phi' - \phi) \right\} d\phi' \qquad (5.10b)$$

with $\alpha = k_o \eta' a \text{ Sin } \theta$. The indices '1' and '2' have been dropped since both the indices give the same radiation vectors. The radiation vector $\bar{M}'$ is evaluated by substituting

$$\hat{a}_\phi = - \text{Sin } \phi \, \hat{a}_x + \text{Cos } \phi \, \hat{a}_y \qquad (5.11)$$

Since we are interested in the circulalrly symmetric TEM (TM_{00}) mode, the radiation vector components for $m = 0$, in spherical coordinates are written as

$$V_\theta = 2\pi \, ab \, H_{mo} \text{Sin } \theta \, J_o(\alpha) \qquad (5.12a)$$

$$M'_\phi = 2j\pi \, ab \, E_{mo} \, J_1(\alpha) \qquad (5.12b)$$

Following the analysis given by Marini (1963) and using the above radiation vector components, the radiation field component for the TEM-mode is given by

$$E_\theta = - j \pi \, ab \, \frac{E_{mo}}{\lambda} \, \frac{e^{-jk_o \eta' r}}{r} \, F(r, \theta) \qquad (5.13)$$

with $F(r,\theta) = P + jQ$

$$P = \cos(k_o r\sqrt{h}\cos\theta)\sin\theta J_o(\alpha) + h\sin(k_o r\sqrt{h}\cos\theta) \qquad (5.14)$$

$$\sin^2\theta J_1(\alpha)/X\cos\theta \qquad (5.15a)$$

$$Q = \cos(k_o r\sqrt{h}\cos\theta)J_1(\alpha) + h\sin(k_o r\sqrt{h}\cos\theta)\left\{\cos\theta - \sin^2\theta/X\cos\theta\right\}$$

$$\sin\theta J_o(\alpha) \qquad (5.15b)$$

The other field components for the TM-modes, $E_\phi = H_\theta = 0$ and H_ϕ can be obtained in a similar manner. The above field expression reduces to that for the case of anisotropic medium for $h = 0$ (Holst, eqn. 10). For the small values of h, if we neglect the terms containing the factor h, the only effect of anisotropy would be the Faraday rotation of fields whichis manifested by the presence of the Cosine factor. The value of h will be very small for the case $\omega >> \omega_e$ and $\omega >> \omega_p$ This case has been analyzed by Kuehl (1962) for an electric dipole. He has also predicted that the field amplitude will be the same as that for the isotropic case but the electric field will suffer a Faraday rotation.

5.4 NUMERICAL EVALUATION OF THE RADIATION PATTERNS

The expression for the radiation field for the TEM-mode is independent of ϕ and so the azimuthal plane pattern is isotropic. The far field axial plane patterns are obtained by numerically evaluating the pattern function $F(r,\theta)$ given by eqns. (5.14) and (5.15). Before going for the numerical evaluation the validity of the q.l approximation was varified

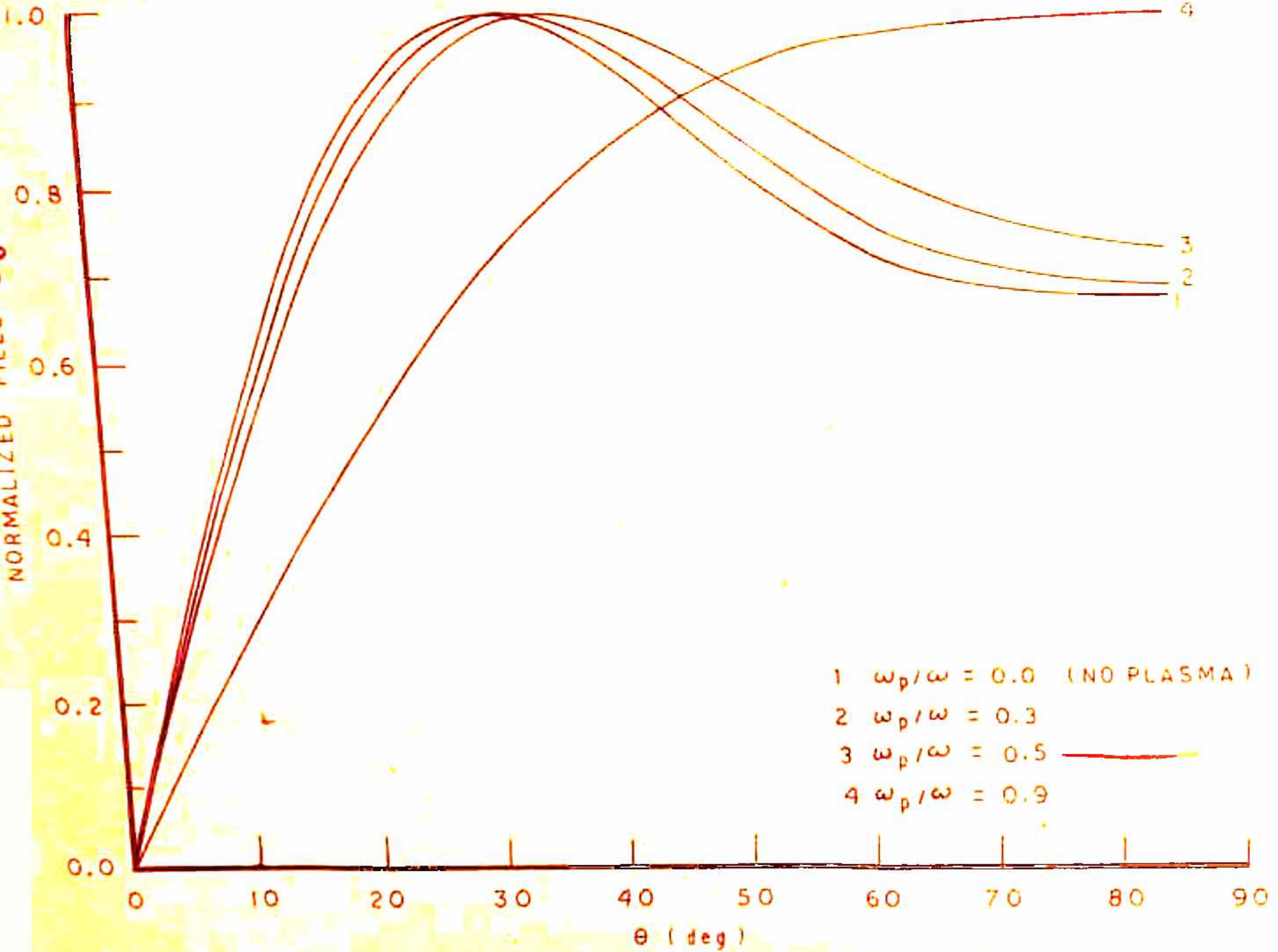

FIG. 5.2 RADIATION PATTERNS OF RADIAL WAVEGUIDE IN ISOTROPIC PLASMA (TEM-MODE)
$a = 0.5\lambda$, $r = 100\lambda$, $\omega_c/\omega = 0$

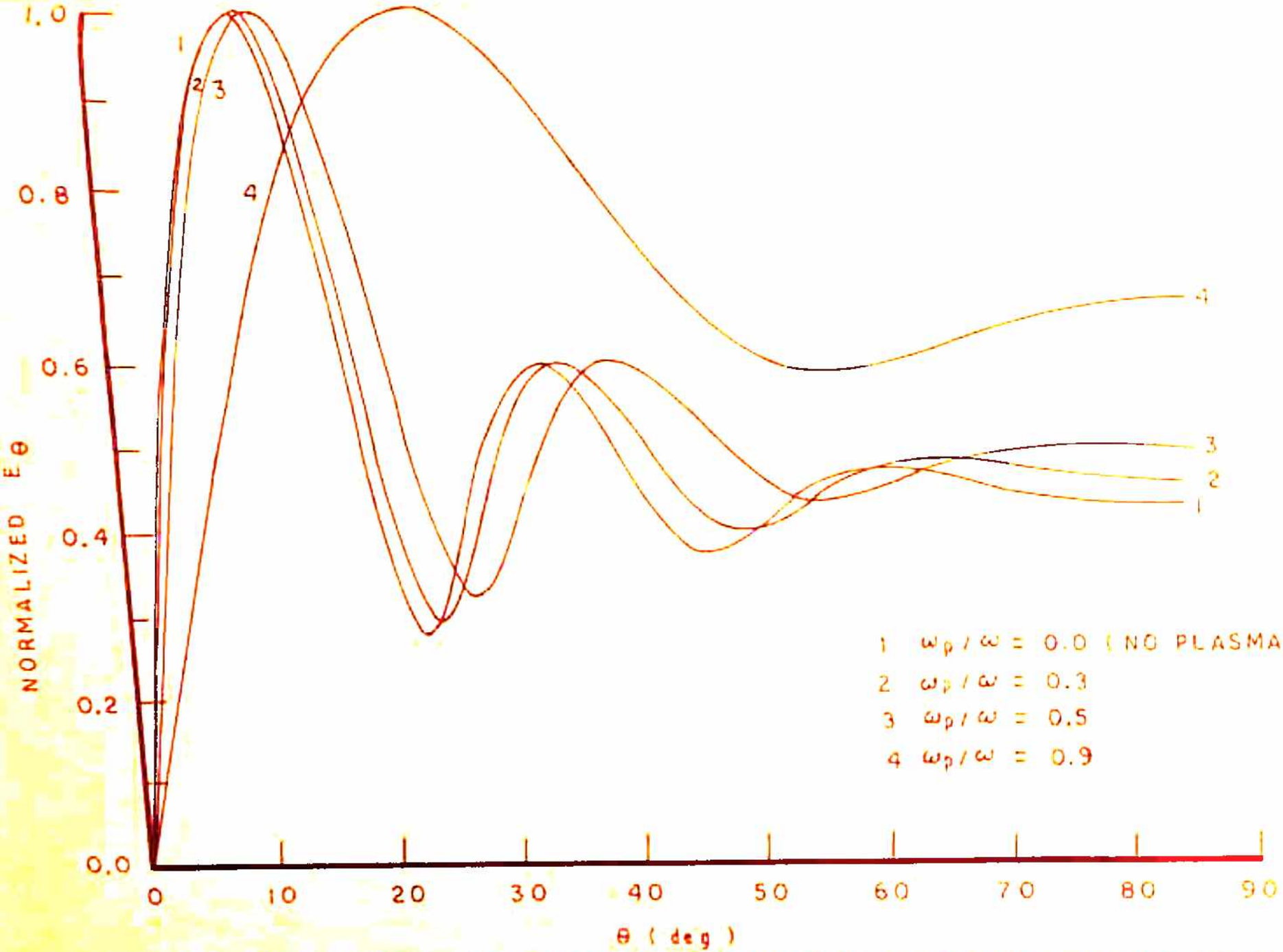

FIG. 5.3 RADIATION PATTERNS OF RADIAL WAVEGUIDE IN ISOTROPIC PLASMA (TEM – MODE)
$a = 1.5\lambda$, $r = 100\lambda$, $\omega_c/\omega = 0$

for $\theta \leq 85^{\circ}$ and for various values of ω_p/ω and ω_c/ω, used for the computations.

The cutoff wavelength for the radial waveguide is given by the condition $ka = n$ (Harrington 1961) and so for the TEM mode ($n = 0$) there is no cutoff wavelength and it will be supported by a radial waveguide of any radius. The axial plane radiation patterns have been obtained for the waveguide radius $a = 0.5\lambda$ and 1.5λ, at a distance sufficiently far from the source at $r = 100\ \lambda$. A typical set of values of the normalized cyclotron frequency $\omega_c/\omega = 0.01$, 0.05 and 1.0 is used to calculate the radiation patterns for fixed values of normalized plasma frequency $\omega_p/\omega = 0.3$ and 0.5. The radiation patterns for $\omega_p/\omega = 0.3$ are found to be identical for all the above values of ω_c/ω and so those patterns are not given here. The radiation patterns are also obtained for the case of isotropic plasma ($\omega_c/\omega = 0$) and for the no plasma case ($\omega_p/\omega = \omega_c/\omega = 0$). Each radiation pattern is normalized with respect to its maximum, for the sake of comparison of various pattern shapes. The normalized radiation patterns in the isotropic plasma ($\omega_c = 0$), for a typical set of normalized plasma frequencies $\omega_p/\omega = 0.0$ (free space), 0.3, 0.5 and 0.9, are shown in fig.(5.2) for $a/\lambda = 0.5$ and in fig.(5.3) for $a/\lambda = 1.5$. The radiation peaks are found to shift away from the waveguide axis with the increasing plasma frequency (ω_p/ω). Moreover, the beamwidth and the peak amplitudes (Table 5.1) tend to

TABLE 5.1 EFFECT OF PLASMA FREQUENCY ON THE RADIATION PATTERN OF RADIAL WAVEGUIDE (TEM-MODE) IN ISOTROPIC PLASMA

	a = 0.5 λ		a = 1.5 λ	
ω_p/ω	Peak Position θ_m^o	Peak Amplitude (rel. units)	Peak Position θ_m^o	Peak Amplitude (rel. units)
0.0 (no plasma)	32.5	6.1669	11.0	5.8511
			34.0	3.4883
0.3	33.5	6.2057	11.5	5.8541
			35.5	3.4924
0.5	37.0	6.3002	13.0	5.8626
			39.5	3.5031
0.9	85.0	7.9212	25.0	6.0030

$\omega_c/\omega = 0$ and $r = 100\ \lambda$

TABLE 5.2 EFFECT OF CYCLOTRON FREQUENCY (ANISOTROPY) ON RADIATION PATTERN OF RADIAL WAVEGUIDE (TEM-MODE)

	a = 0.5 λ		a = 1.5 λ	
ω_c/ω	Peak Position θ_m^o	Peak Amplitude (rel. units)	Peak Position θ_m^o	Peak Amplitude (rel. units)
0.01	37.0	6.3000	13.0	5.8624
			39.5	3.5030
0.05	37.5	6.1977	13.0	5.7202
			39.5	3.4497
0.10	47.0	4.9003	13.0	3.7197
			41.0	2.6968

$\omega_p/\omega = 0.5$ and $r = 100\ \lambda$

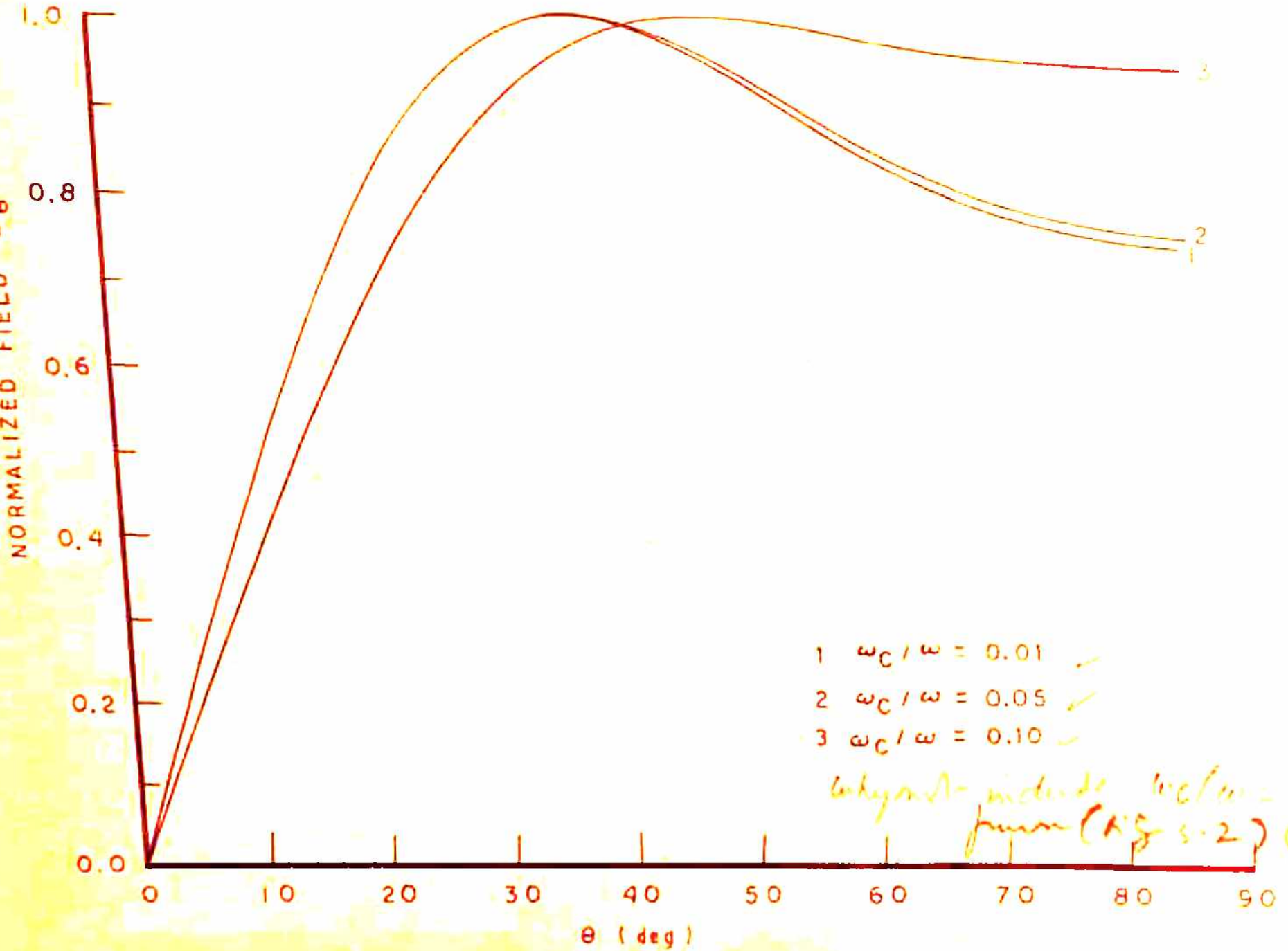

FIG. 5.4 RADIATION PATTERNS OF RADIAL WAVEGUIDE IN ANISOTROPIC PLASMA (TEM-MODE)
$a = 0.5\lambda$, $r = 100\lambda$, $\omega_p / \omega = 0.5$

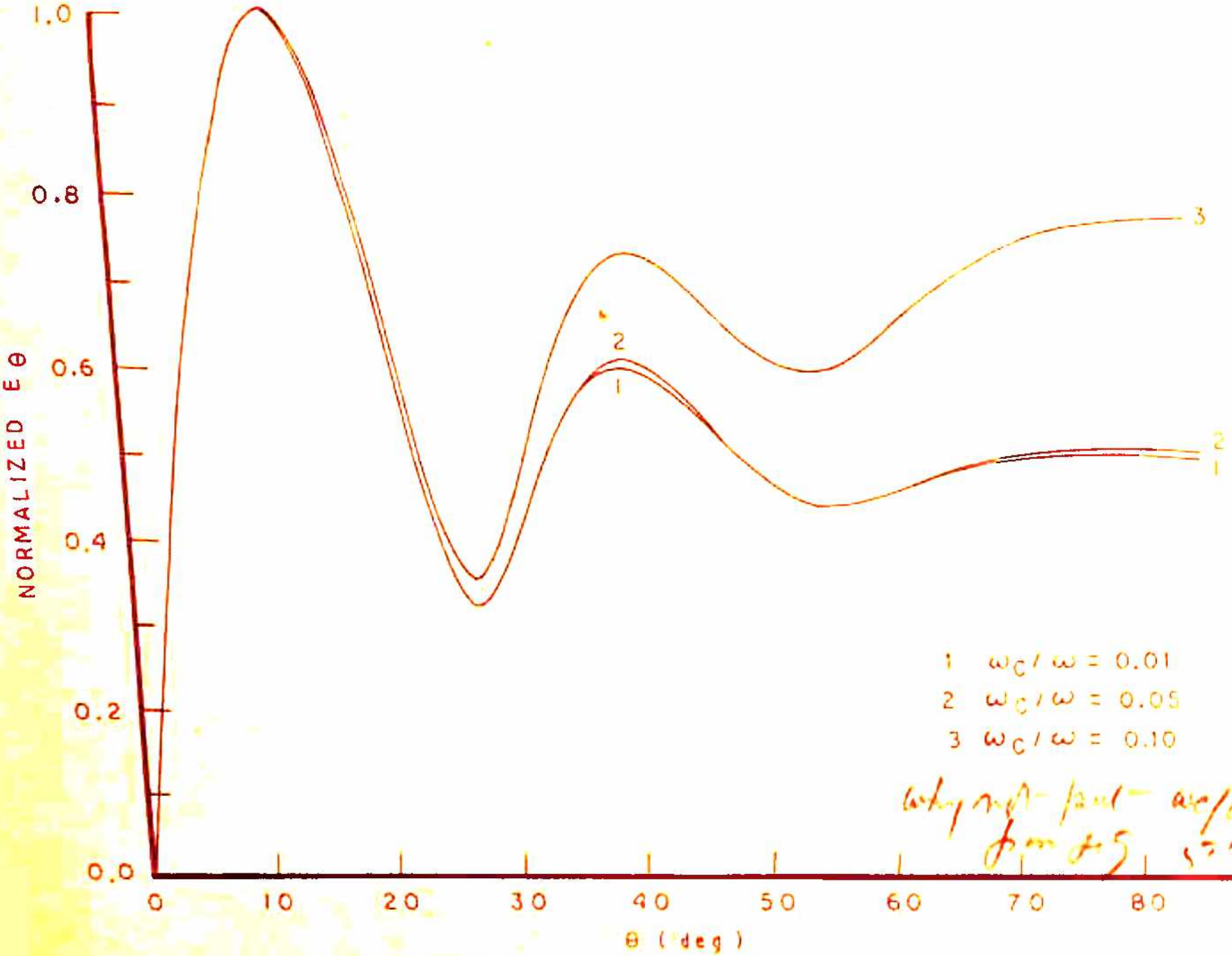

FIG. 5.5 RADIATION PATTERNS OF RADIAL WAVEGUIDE IN ANISOTROPIC PLASMA (TEM-MODE)
a = 1.5λ, r = 100λ, $\omega_p/\omega = 0.5$

increase with the increasing plasma frequency. The beamwidth becomes very large for the sufficiently high value of plasma frequency ($\omega_p/\omega = 0.9$). A comparison of figs.(5.2) and (5.3) indicates that a smaller waveguide radius gives a broader radiation peak. The effect of anisotropy of the plasma on the radiation pattern is shown in figs.(5.4) and (5.5). The radiation pattern suffers only a negligible change for the smaller values of cyclotron frequency. This is because the quantity h is small for these values of ω_c/ω and only the Faraday rotation is present which is resulting in a slight decrease in the peak amplitude (table 5.2). The radiation pattern shape and the peak amplitude are significantly affected for the higher cyclotron frequencies.

5.5 CONCLUSIONS

We have found that the radiation pattern of the open-ended radial waveguide antenna does not suffer significant changes for the moderate values of the normalised plasma frequency and the normalized cyclotron frequency. We have also noted that a radial waveguide can be easily used as a flush-mounted antenna. Moreover, it gives an isotropic radiation pattern in the azimuthal plane for the TEM-mode. A desired radiation pattern in axial plane can be obtained by a proper choice of the waveguide radius and by using an array of radial waveguides. The resultant radiation pattern of the array can be obtained by using the principle of pattern multiplication for

an array of sources in an anisotropic plasma given by Marini (1963). Thus, a radial waveguide seems to be a promising spacecraft antenna.

REFERENCES

Akindinov, V.V., Eremin, S.M., Lishin, I.V.(1974) Radiation field from an elementary magnetic dipole in an uniaxial anisotropic medium, Rad. Eng. and Electron. Phys. Vol 19, No 10, p 121

Arbel, E. and Felsen, L.B.(1963) Theory of radiation from sources in anisotropic media Pt I and II, Electromagnetic theory and antennas, ed by E.C.Jordan (Pergamon Press), p 391

Bunkin,F.V.(1957), On radiation in anisotropic media, Soviet Phys. JETP, Vol 32, No 2, p 338

Clemmow, D.C.(1963) On the theory of radiation from a source in a magneto-ionic medium, Electromagnetic theory and antennas, ed by E.C. Jordan (Pergamon Press) p 461

Daniele, V.G. and Zich,R.S.(1973) Radiation by arbitrary sources in anisotropic stratified media, Radio Sci. Vol 8, No 1, p63

Harrington,R.F.(1961) Time-harmonic electromagnetic fields, (McGraw Hill) Ch 5

Holst, M.W.(1973) Radiation patterns of radial waveguides with TM mode excitation, IEEE Trans. Vol AP-21, No 2, p 238

Kogelnik, H.(1960) On electromagnetic radiation in magneto-ionic media, J.Res.Nat.Bur.Stand, Vol 64D, No 5, p 515

Kogelnik, H. and Metz,H.(1963) Electromagnetic radiation from sources embedded in an infinite anisotropic medium and the significance of the Poynting vector, Electromagnetic theory and antennas, ed by E.C.Jordan,(Pergamon Press), p 477

Kuehl, H.H.(1962) Electromagnetic radiation from an electric dipole in a cold anisotropic plasma, Phys.Fluids, Vol 5, No 9, p 1095

Marini, J.W.(1963)Radiation in a lossless magneto-ionic medium at frequencies high relative to the electron gyrofrequency J.Res.Nat.Bur.Stand Vol 67D, No 6, p 707

Ratcliffe, J.A.(1959) The magneto-ionic theory and its application to the ionosphere, (Cambridge Univ.Press)

Wait,J.R.(1964) Theory of sources immersed in anisotropic media, J.Res.Nat.Bur.Stand, Vol 68B, No 3, p 119

CHAPTER 6

SUMMARY

Several authors have predicted the feasibility of using an electromagnetic source-excited plasma column as an electronically scanning antenna. In most of the theoretical studies on the plasma-antennas, the plasma column has been assumed to be infinitely long, isotropic, homogeneous, collisionless and incompressible. The anisotropy and the incompressibility of the plasma has also been included in the analysis of some authors. In the present study, a simple laboratory model of the plasma-antenna system has been chosen for the theoretical and experimental studies. It consists of a long plasma column generated by a dc discharge in a gas, filled in a glass tube at a low pressure, and a suitable electromagnetic source for excitation of the column. Such a laboratory plasma, in the absence of an external magnetic field is isotropic, inhomogeneous, collisional and incompressible. The circularly symmetric electric and magnetic ring sources and open-ended circular waveguide carrying a TM_{01}-or TE_{01}-mode have been considered for excitation of the plasma column. Similar models have already been studied by several authors neglecting the collision frequency, the inhomogeneity of the plasma and the glass tube. Some of the authors have included the effect of the inhomogeneity also, but their analysis is either incomplete or the complete results have not been published. Furthermore only the radiation patterns were obtained and the other antenna characteristics such as the radiation resistance, the directivity

and the input impedance were not evaluated. The present study has taken into account the collision frequency, the inhomogeneity of the plasma and the dielectric tube containing the plasma to make a more realistic analysis of the plasma-antenna system. A parabolic plasma density profile which represents the actual density profile in a discharge tube has been considered. The numerical results have been obtained for the radiation pattern, the radiation resistance and the directivity. The mathematical approach used for the theoretical analysis is fairly standard. It involves the use of Fourier transform technique and contour integration using the method of steepest descents to solve the Maxwell's equations to obtain the radiation field. To obtain the radiation field for the waveguide excitation, first an equivalent fictitious surface current distribution due to the undisturbed fields at the waveguide aperture is obtained. It is divided into a large number of elementary current rings having different radii ranging from zero to the waveguide radius. A vector sum of the radiation fields due to all these elementary current rings then gives the radiation field for the waveguide excitation.

To study the influence of the collision frequency and the dielectric tube the plasma has been assumed to be homogeneous to simplify the mathematics. To obtain the numerical results for the various values of the collision frequency and the dielectric tube thickness the fixed parameters, are kept in the dimensionless form and are

and the input impedance were not evaluated. The present study has taken into account the collision frequency, the inhomogeneity of the plasma and the dielectric tube containing the plasma to make a more realistic analysis of the plasma-antenna system. A parabolic plasma density profile which represents the actual density profile in a discharge tube has been considered. The numerical results have been obtained for the radiation pattern, the radiation resistance and the directivity. The mathematical approach used for the theoretical analysis is fairly standard. It involves the use of Fourier transform technique and contour integration using the method of steepest descents to solve the Maxwell's equations to obtain the radiation field. To obtain the radiation field for the waveguide excitation, first an equivalent fictitious surface current distribution due to the undisturbed fields at the waveguide aperture is obtained. It is divided into a large number of elementary current rings having different radii ranging from zero to the waveguide radius. A vector sum of the radiation fields due to all these elementary current rings then gives the radiation field for the waveguide excitation.

To study the influence of the collision frequency and the dielectric tube the plasma has been assumed to be homogeneous to simplify the mathematics. To obtain the numerical results for the various values of the collision frequency and the dielectric tube thickness the fixed parameters, are kept in the dimensionless form and are

so chosen that they can be easily realized for the proposed model at X-band frequencies. The dielectric is chosen to be a borosilicate glass to represent actual glass tube. It has been found that the radiation pattern is distorted by the presence of the glass tube. The radiation resistance and the directivity also change with changing the glass tube thickness. It has been found that the radiation pattern for a quarter wavelength thick glass tube lies very close to the radiation pattern for the no glass tube case. This result is consistent for all the cases considered. A glass tube thickness equal to the integral multiples of the quarter wavelength also shows a similar effect. The peak amplitude, the radiation resistance and the directivity for the quarter-wave thick glass tube, all differ very slightly from those in the absence of the glass tube. Thus a quarter-wave thick glass tube behaves as if it were not present there. This result may be used in choosing a proper glass tube thickness for the plasma-antenna system. The major influence of the collisions in all the cases considered is a decrease in the radiated power. It has been found that a relative collision frequency of the order of 0.01 does not have a very serious effect on the radiation characteristics. The direction of the radiation peak is very slightly affected by the inclusion of the collision frequency, except in the TM_{01}-mode waveguide excitation where the change is rather drastic.

The influence of the inhomogeneity of the plasma has been studied by neglecting the collision frequency for the sake of mathematical simplicity. The solution of the wave equation in the inhomogeneous plasma has been obtained by the series solution method. Only the electric and magnetic ring sources have been considered for the excitation. The analysis of the waveguide excitation is highly complicated since it involves the evaluation of an integral having the confluent hypergeometric function in its integrand. The influence of the shape of the inhomogeneity profile has been analysed for a constant axial plasma density and for a constant average plasma density.

It is found that for the case of a fixed axial plasma density the radiation peak shifts towards the end-fire direction. The direction of the radiation peak for the inhomogeneous plasma is found to be almost the same as that of the radiation peak for the homogeneous plasma column having a uniform plasma density equal to the average plasma density of the inhomogeneous plasma column. But the shape of the radiation pattern, the radiation resistance and the directivity are different for these cases. Thus, the assumption of a homogeneous plasma with a plasma density equal to the average density of the inhomogeneous plasma may be valid as far as the direction of the radiation peak is concerned.

An attempt has been made to pursue an experimental study on the plasma-antenna model described above. An experimental plan and the facilities used for the plasma generation, plasma diagnostics, and measurement of the radiation pattern and the input impedance have been discussed. Since the experimental setup is very bulky the indoor radiation pattern measurements were tried. But due to the lack of availability of a microwave anechoic chamber, the radiation patterns have shown very sharp fluctuations due to reflections from the surroundings and it could not be possible to make any useful inferences.

The radiation patterns of a radial waveguide antenna in an unbounded anisotropic plasma have been studied at high frequencies under the quasi-longitudinal approximations. It has been found to have suitable radiation pattern characteristics for a space-vehicle antenna. It has been proposed that the open-ended radial waveguide may be used as a flush-mounted space-vehicle antenna.

In the present work only the circularly symmetric mode of the ring sources and the circular waveguide have been considered, but in practice it is very difficult to excite only these modes without exciting the higher order modes. For the case of ring sources unless the circumference of the ring is smaller than the wavelength the higher order modes are excited. For the case of a circular waveguide when we excite the TM_{01}-mode the TE_{11}-mode is also excited and similarly when we excite the TE_{01}-mode both the TM_{01}- and the TE_{11}-modes are

excited. The multimode excitation may be desirable if a directional pattern is required in the azimuthal plane. Furthermore, a careful design of the source may eliminate these unwanted modes by using the mode-filters or the mode suppressers. In our analysis the glass has been considered to be lossless but in reality the glass is quite lossy at high frequencies. These losses may also be included in the theoretical analysis. The excitation of an inhomogeneous plasma column by a circular waveguide should also be analyzed for the circularly symmetric modes as well as for the multimode excitation. The experimental study on the plasma-antenna system should be thoroughly carried out and the results should be compared with the theoretical predictions.

List of Publications

1. Radiation from a plasma column contained in a glass tube and excited by a waveguide, Lalit Kumar and J.S.Verma, Ind.J.Radio & Space Physics, Vol 7, No 1, p 51, Feb.1978, also presented at Plasma Physics and MHD Symposium, BARC, Bombay Feb.21-23, 1977

2. Radiation from a radial waveguide in a magnetoplasma, Lalit Kumar and J.S.Verma, Electronics Letters, Vol 14, No 3, p 57, Feb. 1978

3. Plasma column as an electronically scannable narrow beam antenna system, Lalit Kumar and J.S. Verma, Presented at Plasma Physics and MHD Symposium, BARC, Bombay, Feb.21-23, 1977

4. A radial waveguide antenna for space vehicles, Lalit Kumar and J.S.Verma, presented at Space Sciences Symposium, Andhra University, Waltair, Jan. 9-12, 1978

5. Measurement of plasma density in argon discharge by Langmuir probe and microwave interferometer, Himanshu Kumar, Lalit Kumar and J.S.Verma, Communicated to Ind.J.Pure App. Physics.